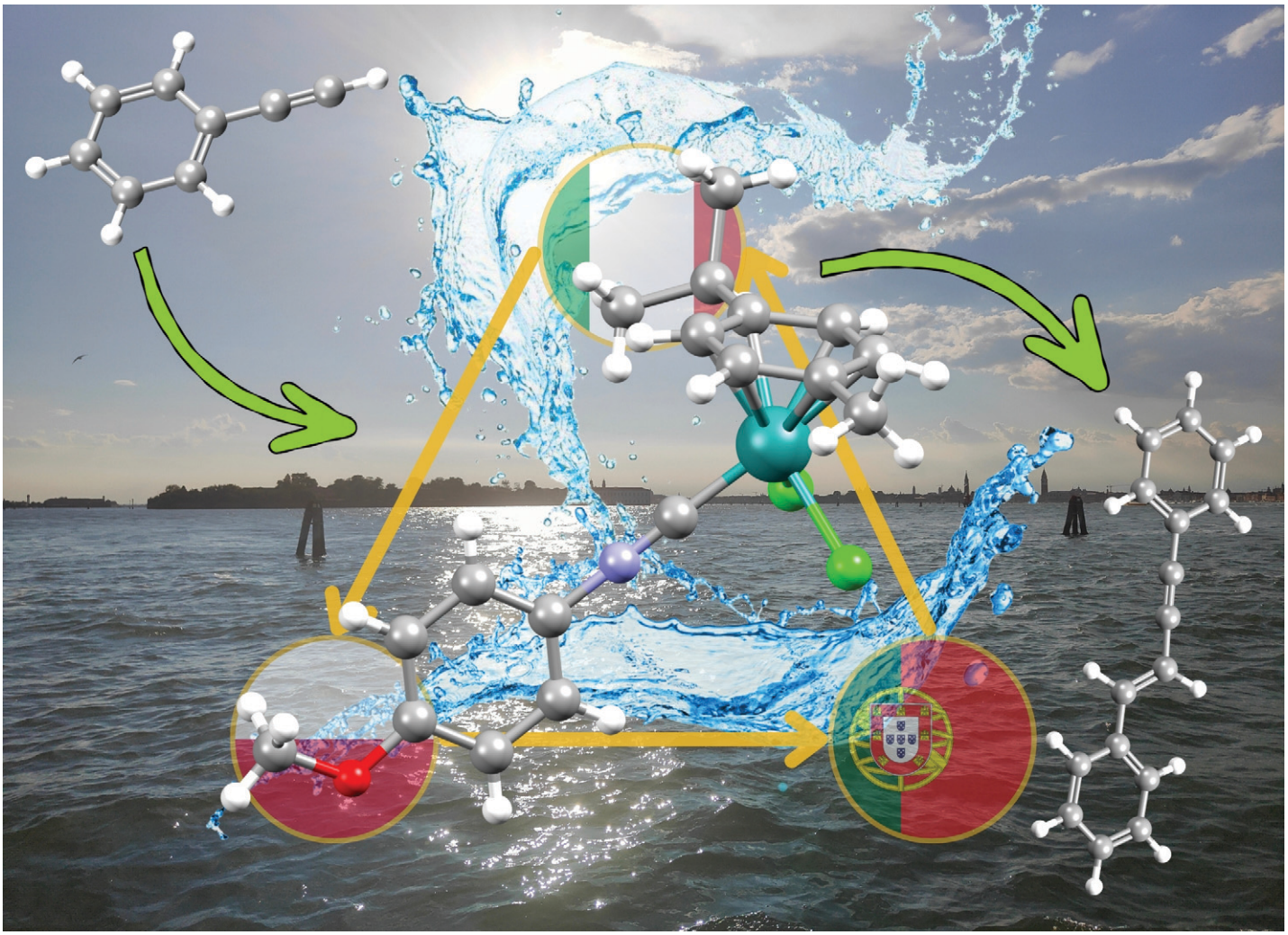

Showcasing the fruitful collaboration between the research groups of Prof. Marchetti and Dr. Biancalana (University of Pisa, Italy), Prof. Martins (University of Lisbon, Portugal), Prof. Zacchini (University of Bologna, Italy) and Prof. Trzeciak (University of Wrocław, Poland).

Controlling alkyne dimerization and trimerization with ruthenium(II) arene isocyanide catalysts

Ruthenium(II) η^6-arene isocyanide complexes offer structural variability, a straightforward synthesis, air-stability and a peculiar reactivity. These complexes are effective catalytic precursors for the dimerization / trimerization of terminal alkynes using water as solvent, a low catalyst loading and Na_2CO_3 as a base, providing a step forward in the sustainability of this process.

Image reproduced by permission of Hugo Lapa from *Catal. Sci. Technol.*, 2026, **16**, 1622.

As featured in:

See Luísa M. D. R. S. Martins, Lorenzo Biancalana *et al.*, *Catal. Sci. Technol.*, 2026, **16**, 1622.

ROYAL SOCIETY OF CHEMISTRY

rsc.li/catalysis

Registered charity number: 207890

Catalysis Science & Technology

ROYAL SOCIETY OF CHEMISTRY

PAPER

View Article Online
View Journal | View Issue

Cite this: *Catal. Sci. Technol.*, 2026, **16**, 1622

Controlling alkyne dimerization and trimerization with ruthenium(II) arene isocyanide catalysts

Hugo M. Lapa, [abc] Mattia del Rosso,[d] Stefano Zacchini, [e] Greta Giarola, †[d] Elisabete C. B. A. Alegria, [ac] Anna M. Trzeciak, [f] Fabio Marchetti, [d] Luísa M. D. R. S. Martins *[ab] and Lorenzo Biancalana *[d]

Ruthenium(II) arene complexes represent a renowned platform to develop effective catalysts for a variety of organic transformations, including C–C bonding processes. On the other hand, isocyanides are overlooked ligands in the design of transition metal catalysts. Herein a panel of ruthenium(II) arene isocyanide complexes were found to be versatile catalytic precursors for the dimerization/trimerization of aryl alkynes in aqueous medium. Fifteen compounds of general formula $[RuX_2(CNR)(\eta^6\text{-arene})]$ (X = Cl, I; R = alkyl or aryl; arene = C_6H_6, *p*-cymene, C_6Me_6) were prepared from the corresponding halido-bridged Ru dimers and the selected isocyanide according to optimized procedures, including examples with the simplest alkyl isocyanide (MeNC) and arene (C_6H_6). Next, two acetylide complexes of the type $[RuCl(CCPh)(CNR)(\eta^6\text{-}C_6Me_6)]$ were obtained by reaction of the corresponding dichlorido complexes with phenylacetylene and NaOH. In addition, a protocol for the thermally promoted *p*-cymene/MeCN substitution was optimized, giving access to hexacoordinate complexes with isocyanide and acetonitrile ligands, $[RuCl_2(MeCN)_3(CNR)]$ (two examples). The Ru(II) compounds, fourteen of which are unprecedented, were characterized by CHNS analyses, IR and NMR spectroscopy and X-ray diffraction in eight cases. The catalytic activity of the complexes was assessed, highlighting the role of the solvent, base, Ru loading, energy source and, more importantly, isocyanide/arene ligands to control the selectivity between dimerization and trimerization of phenylacetylene. Pointing to a sustainable process, a catalytic protocol involving Na_2CO_3 as a base, water as a solvent and a low Ru loading (1%) was applied for the dimerization/trimerization of a range of terminal alkynes, with $[RuCl_2(CNCy)(\eta^6\text{-}p\text{-cymene})]$ emerging as the best performing pre-catalyst. Combined IR, NMR and MS data were instrumental in the elucidation of the reactivity of the isocyanide–arene complexes with $PhCCH/Na_2CO_3$ and the formulation of a possible mechanism of pre-catalyst activation.

Received 8th December 2025,
Accepted 28th January 2026

DOI: 10.1039/d5cy01493j

rsc.li/catalysis

1. Introduction

Ruthenium occupies a prominent role in catalysis, both on academic and industrial levels. Over the past 20 years, remarkable catalytic performances of several classes of ruthenium complexes have been highlighted.[1] Among them, half-sandwich ruthenium(II) arene complexes rose to prominence for (asymmetric) transfer hydrogenation reactions (Noyori–Ikariya catalysts)[2] and have found widespread use in terms of substrates[3] and H_2-donors,[4] as well as commercial availability.[5] Meanwhile, this class of compounds has been extensively investigated for their catalytic properties in dehydrogenation/hydrogen borrowing processes,[6,7] nitrile hydration[8] and C–C bond formation reactions such as arylation of $C(sp^2)$–H bonds[9] and alkene metathesis.[10] In terms of synthetic design, the $\{Ru(\eta^6\text{-arene})\}^{2+}$ moiety allows to coordinate a wide range of ligands that can be introduced by substitution reactions under mild

[a] *Centro de Química Estrutural, Institute of Molecular Sciences, Instituto Superior Técnico, Universidade de Lisboa, Av. Rovisco Pais 1, 1049-001 Lisboa, Portugal. E-mail: luisammartins@tecnico.ulisboa.pt*
[b] *Chemical Engineering Department of Instituto Superior Técnico, Universidade de Lisboa, Av. Rovisco Pais, 1049-001 Lisboa, Portugal*
[c] *Chemical Engineering Department of Instituto Superior de Engenharia de Lisboa, Instituto Politécnico de Lisboa, R. Conselheiro Emídio Navarro 1, 1959-007 Lisboa, Portugal*
[d] *Dipartimento di Chimica e Chimica Industriale, Università di Pisa, Via Giuseppe Moruzzi 13, I-56124 Pisa, Italy. E-mail: lorenzo.biancalana@unipi.it*
[e] *Dipartimento di Chimica Industriale "Toso Montanari", Università di Bologna, Via Piero Gobetti 85, 40129 Bologna, Italy*
[f] *Faculty of Chemistry, University of Wrocław, 14 F. Joliot-Curie, 50-383 Wroclaw, Poland*
† Current address: Department of Energy Conversion and Storage, Technical University of Denmark, Fysikvej, 2800, Kgs. Lyngby, Denmark.

conditions from the halide-bridged dimers $[RuX_2(\eta^6\text{-arene})]_2$ (X = halide).[11] These benchmark diruthenium precursors can be prepared on a multigram scale and almost quantitative yield from commercial $RuCl_3$ hydrate.[7,12,13] Interestingly, only a few among thousands half-sandwich complexes of the general formula $[RuX_2(L)(\eta^6\text{-arene})]$ (L = monodentate ligand)[11] contain isocyanides (L = CNR).[14,15] For instance, the simplest alkyl isocyanide (MeNC) has not been coordinated to the ruthenium(η^6-arene) scaffold and only one isocyanide complex featuring η^6-benzene has been reported. Isocyanides (CNR) represent valuable and versatile ligands for transition metal complexes.[16] A large number of isocyanides are commercially available or can be prepared from the corresponding primary amine by established methodologies.[17] Their σ-donor and π-acceptor character may provide a robust metal–carbon bond, adapting to diverse metal centers. The organic substituent (R) regulates the steric and electronic properties of isocyanides and may also allow for introduction of additional functional groups. The intense IR absorption for the C≡N stretching is diagnostic of the M–C–N bonding and the electron density at the metal center. Isocyanide coordination to metal centers may promote subsequent reactivity giving access to various, functionalized organometallic fragments.[18] Despite these useful features and their cost-effectiveness, isocyanides have been overlooked in catalyst development with respect to more popular monodentate ligands (*e.g.* NHC carbenes).[19,20] In this respect, we recently reported the optimized synthesis of six $[RuX_2(CNR)(\eta^6\text{-}p\text{-cymene})]$ derivatives [X = Cl, R = m-xylyl (Xyl), 2-naphthyl, benzyl, cyclohexyl (Cy), ^{t}Bu; X = I, R = ^{t}Bu] and their catalytic activity in the transfer hydrogenation of ethyl levulinate to γ-valerolactone.[21]

Creating new carbon–carbon bonds is essential in several industries, including those responsible for producing polymeric materials, pharmaceuticals, agricultural chemicals, and natural products.[22,23,24]

Terminal alkynes are valuable building blocks, which can engage in a variety of C–C bond forming processes among which homocoupling, dimerization and trimerization (Scheme 1). The homocoupling is a dehydrogenation reaction affording a 1,3-diyne, the dimerization involves a formal addition of a C–H group of an alkyne across a C≡C bond of another alkyne, affording a conjugated enyne (sp–sp^2), while the trimerization is a [2 + 2 + 2] cycloaddition reaction providing a benzene ring (sp^2–sp^2). Controlling the selectivity between these processes is essential.

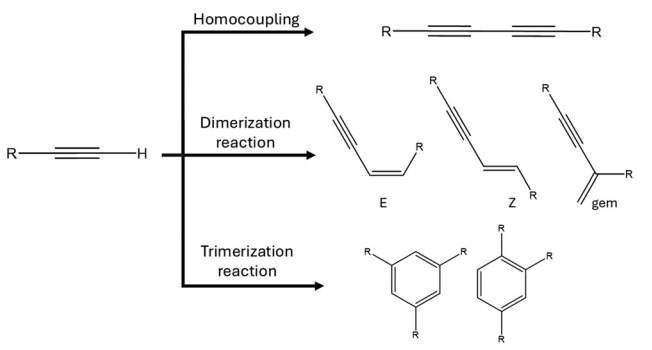

Scheme 1 General scheme for the homocoupling, dimerization and trimerization of terminal alkynes.

Although successful, several transition metal-based systems for dimerization, trimerization and coupling of terminal alkynes suffer from the same problems.[25] To achieve high conversion and selectivity, non-environmentally friendly protocols are usually required, including organic solvents (toluene, DMA and DMF, for example) and organic bases (usually in high concentration), and a relatively high catalyst loading (>5 mol%).

Given our interest in the development of sustainable catalytic systems based on ruthenium(II) η^6-arene complexes employing simple, easily available ligands,[6f,7] in this work we extended the family of $[RuX_2(CNR)(\eta^6\text{-arene})]$ (X = Cl, I) derivatives, starting from seven isocyanides featuring various (hetero)alkyl or (hetero)aryl substituents. These compounds were screened as pre-catalysts for the dimerization or trimerization of terminal alkynes. The reaction conditions (solvent, base, Ru loading, temperature/time), including the energy source, were optimized with phenylacetylene as a model substrate, and then a range of aryl alkynes were tested using $[RuCl_2(CNCy)(\eta^6\text{-}p\text{-cymene})]$ as the best catalyst. The role of isocyanide and arene ligands in the catalytic process was investigated also taking advantage of the synthesis of the derivatives $[RuCl(CCPh)(CNR)(\eta^6\text{-arene})]$ and $[RuCl_2(MeCN)_3(CNR)]$.

2. Results and discussion

2.1. Synthesis and characterization of Ru compounds

2.1.1. Bis-halide arene isocyanide complexes. The reaction of $[RuCl_2(\eta^6\text{-arene})]_2$ (arene = *p*-cymene, C_6Me_6) with a stoichiometric amount of the selected isocyanide (CNR), in CH_2Cl_2 or MeCN at room temperature, gave the corresponding $[RuCl_2(CNR)(\eta^6\text{-arene})]$ complex (arene = *p*-cymene, R = CH_3, **1a**; R = Cy, **1b**; (*S*)-CHMePh, **1c**; $CH_2PO(OEt)_2$, **1d**; $CHCO_2Et$, **1e**; Xyl, **1f**; 4-C_6H_4OMe, **1g**; arene = C_6Me_6, R = CH_3, **2a**; Cy, **2b**; (*S*)-CHMePh, **2c**; $CH_2PO(OEt)_2$, **2d**; Xyl, **2f**) (Scheme 2a). $[RuI_2(CNCy)(\eta^6\text{-}p\text{-cymene})]$, **1b-I**, was prepared from $[RuI_2(\eta^6\text{-}p\text{-cymene})]_2$ and CyNC in refluxing CH_2Cl_2 (Scheme 2b). The isocyanide coordination is generally complete within 1 hour, as checked by IR spectroscopy. All the reactions are straightforward except that of methyl isocyanide and $[RuCl_2(\eta^6\text{-}p\text{-cymene})]_2$. In this case, a slight excess of isocyanide led to an inseparable mixture of **1a** and *trans*-$[RuCl_2(MeNC)_4]$ (*ca.* 6%) while a sub-stoichiometric amount of isocyanide resulted in the formation of unidentified quinoline complexes in small quantity (quinoline is an impurity of freshly prepared methyl isocyanide). Purification *via* silica chromatography afforded **1a** as an orange powder in 75% yield. In all the other cases, filtration of the final reaction mixture over a celite pad allowed the removal of a brown impurity and the desired

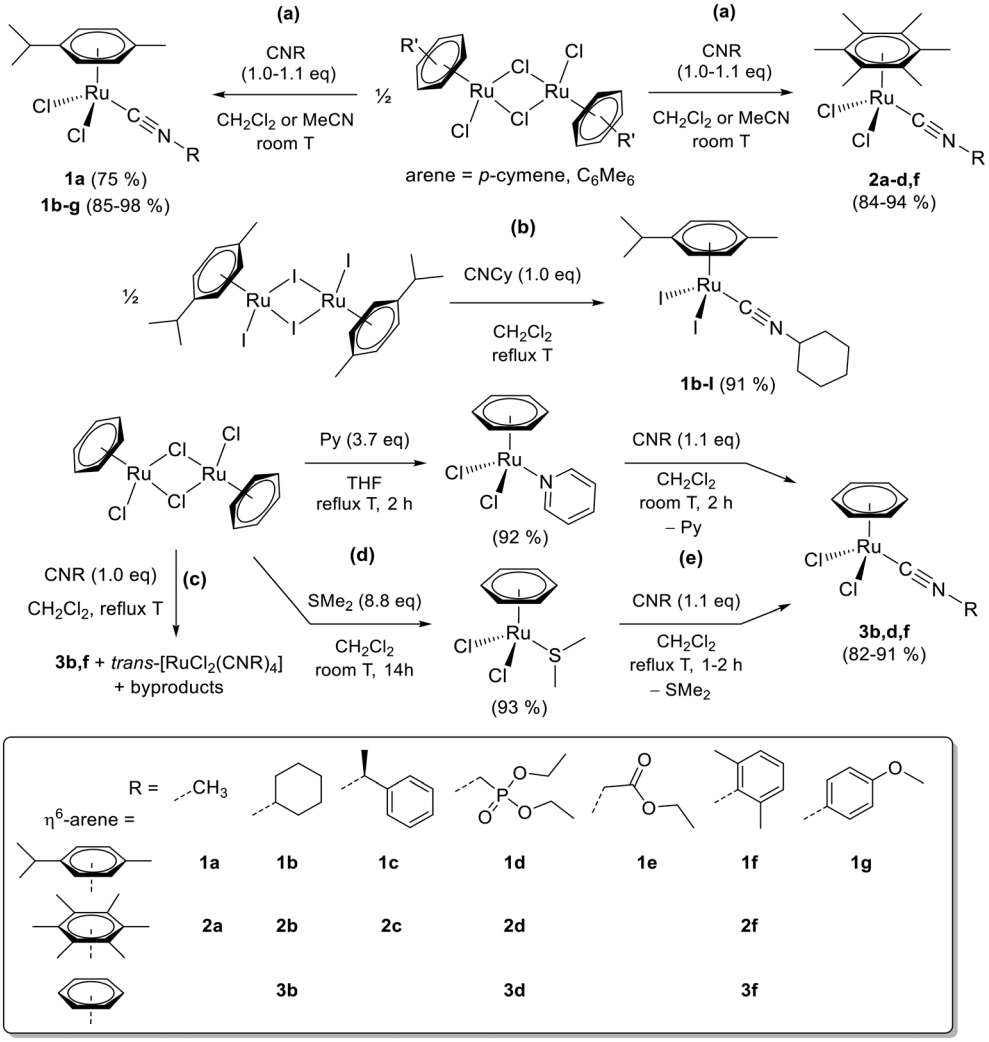

Scheme 2 Synthesis of $[RuX_2(isocyanide)(\eta^6\text{-arene})]$ complexes from the corresponding halide-bridged η^6-arene Ru(II) dimers $[RuX_2(\eta^6\text{-arene})]$ (X = Cl, I; arene = *p*-cymene, C_6Me_6, C_6H_6). All reactions were carried out under N_2; isolated yields in parentheses. The preparation of **1b** and **1f** is described in the literature.[21]

complex was isolated as an orange (**1b–g**, **2a–d**, and **2f**) or violet-red (**1b-I**) powder in 84–98% yield.

The preparation of the benzene analogues, $[RuCl_2(CNR)(\eta^6\text{-}C_6H_6)]_2$ (R = Cy, **3b**; $CH_2PO(OEt)_2$, **3d**; Xyl, **3f**), was challenging. The reaction of $[RuCl_2(\eta^6\text{-}C_6H_6)]_2$ with a stoichiometric amount of cyclohexyl or xylyl isocyanide resulted in the formation of a significant amount of *trans*-$[RuCl_2(RNC)_4]$ (R = Xyl, Cy), together with the desired **3b**, **f** (Scheme 2c). These octahedral complexes, together with the phenyl and tolyl analogues, were previously obtained by the reaction of $[RuCl_2(\eta^6\text{-arene})]_2$ (arene = C_6H_6, *p*-cymene) with excess isocyanide in refluxing benzene or toluene (yields not given).[15a,26] However, the very low solubility of $[RuCl_2(C_6H_6)]_2$ in CH_2Cl_2 results in a large excess of isocyanide in solution even under stoichiometric conditions. These issues were circumvented by adopting a two-step procedure with a more soluble intermediate containing a labile monodentate ligand.[27] We selected $[RuCl_2(Py)(\eta^6\text{-}C_6H_6)]$ and $[RuCl_2(SMe_2)(\eta^6\text{-}C_6H_6)]$ for this purpose, which were isolated in 92–93% yield from $[RuCl_2(C_6H_6)]_2$ (up to 600 mg scale) according to an optimized procedure (Scheme 2d). Next, the substitution of either pyridine or dimethylsulfide with the selected isocyanide in CH_2Cl_2 proceeded with discrete selectivity (Scheme 2e) to give **3b**, **d**, **f**. The impurities (by-products) in the crude reaction mixture were removed by trituration in Et_2O/THF mixtures, affording the desired compounds as orange powders in 82–90% yield.

Compounds **1c**, **1e** and **2b** were previously obtained in lower yield and/or using harsher reaction conditions (*e.g.* a large excess of isocyanide, longer reaction time, higher temperature) and a more complex purification (chromatography and/or re-crystallization), while **3b** was not isolated as a pure compound.[15a,b,g] Instead, **1b**, **f** were prepared according to the same optimized procedure herein described.[21] To the best of our knowledge, **1a**, **1d**, **1g**, **2a**, **2c**, **2d**, **2f**, **3b**, and **3f** are unprecedented. Moreover, **3d**, **f** add to

the very few examples of [RuX_2(C-donor)(C_6H_6)] complexes (X = halide).[28]

All the ruthenium isocyanide complexes **1–3** are air- and moisture-stable in the solid state, except for **3d**. The benzene complexes **3** are generally less soluble in chlorinated solvents than their *p*-cymene or C_6Me_6 counterparts and they are more sensitive to decomposition in solution under air, as shown by the partial release of benzene occurring at room temperature in $CDCl_3$ (6–35% after 14 h).

All compounds were characterized by elemental (CHN) analyses, IR and NMR spectroscopy (Fig. S1–S53). The isocyanide ligand gives rise to a strong IR absorption (CH_2Cl_2 solution) in the 2140–2220 cm^{-1} range and a relatively weak ^{13}C NMR signal ($CDCl_3$ solution) around 135–155 ppm. Minimal differences (≤5 cm^{-1}) in the isocyanide stretching absorption were generally observed between IR spectra of the solids and their CH_2Cl_2 solutions. Table S1 shows IR and ^{13}C NMR data for **1–3**, some previously reported complexes of the same type, and the corresponding isocyanides. The C≡N stretching band in **1–3** is shifted to higher wavenumbers (+20–50 cm^{-1}) with respect to the free isocyanide, indicating a scarce π-backdonation from the Ru(II) center.[15b,g,j] Specifically, the coordination-induced IR shift ($\Delta\nu_{CN}/cm^{-1}$ = $\nu_{Ru\text{-}CNR} - \nu_{CNR}$) reflects the donor/acceptor properties of the isocyanide substituent (aliphatic > aromatic) and the arene and halide co-ligands (C_6H_6/Cl_2 > *p*-cymene/Cl_2 > *p*-cymene/I_2 ≈ C_6Me_6/I_2; Fig. 1). Similarly, the chemical shift of the ^{13}C NMR resonance of isocyanide carbon decreases in the order: CNR > [$RuCl_2$(CNR)(η⁶-C_6Me_6)] > [$RuCl_2$(CNR)(η⁶-*p*-cymene)] > [$RuCl_2$(CNR)(η⁶-C_6H_6)]. The P=O stretching in **1–3d** gives rise to a strong absorption around 1250–1270 cm^{-1} in the solid-state IR spectra.

The crystal structures of **1a**, **1c**, **1e**, **1g**, **2c** and **1b-I** were elucidated by single-crystal X-ray diffraction (Fig. 2, S54–S56 and Table S2). The complexes display a three-legged piano-stool geometry, as found in related compounds where Ru is bonded to an η⁶-arene, two chlorides and one isocyanide ligand.[15f,j,h,21] The C(1)–N(1) [1.209(15), 1.150(8), 1.172(10), 1.156(11), and 1.142(5) Å for **1a**, **1c**, **1e**, **1g**, **2c** and **1b-I**, respectively] and the Ru–C(1) contacts [1.981(10), 1.969(6), 1.960(5), 1.954(8), 1.961(3), and 1.962(4) Å for **1a**, **1c**, **1e**, **1g**, **2c** and **1b-I**, respectively], as well as the Ru1–C1–N1 angle [165.7(12), 178.3(7), 172.7(8), 177.2(8), 176.1(3), and 176.2(4)° for **1a**, **1c**, **1e**, **1g**, **2c** and **1b-I**, respectively], are in agreement with a σ-bonded isocyanide with little π-backdonation from the metal center.[16] With the exception of **1a**, very small differences in Ru–C–N bond distances and angles are observed in this series of compounds, even when changing the arene (*p*-cymene in **1c** *vs.* C_6Me_6 in **2c**) or the halide (chloride in **1b** (ref. 21) *vs.* iodide in **1b-I**) co-ligands, in contrast to the infrared scenario.

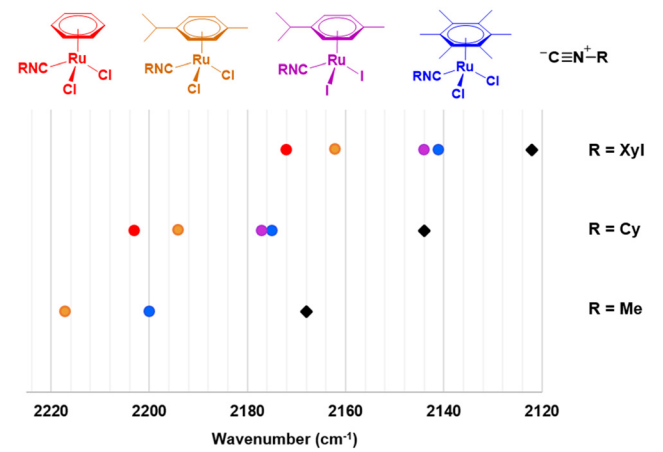

Fig. 1 Wavenumber of the C≡N stretching band for selected isocyanides and their corresponding {RuX_2(η⁶-arene)} adducts (X = Cl, I; arene = *p*-cymene, C_6Me_6, C_6H_6). IR data refer to CH_2Cl_2 solutions except [RuI_2(CNXyl)(η⁶-*p*-cymene)][15j] (solid state).

2.1.2. Acetylide–isocyanide and acetonitrile–isocyanide complexes. The reactivity of [$RuCl_2$(isocyanide)(η⁶-arene)] complexes is almost completely unexplored in the literature.[15b,h] We investigated two processes, namely the activation of terminal alkynes,[29] and the isocyanide-promoted thermal displacement of the arene ligand in coordinating solvents,[21] which could be potentially relevant in view of the catalytic application. Cyclohexyl and xylyl isocyanide, phenylacetylene and acetonitrile were selected as model isocyanides/alkyne/coordinating solvent, respectively.

The acetylide compounds [RuCl(CCPh)(CNR)(η⁶-C_6Me_6)] (R = Cy, **4b**; Xyl, **4f**) were obtained from the reaction of the corresponding bis-chloride complexes **2b**, **f** with a slight excess of phenylacetylene and NaOH as a Brønsted base in MeOH at room temperature (**4b**) or 45 °C (**4f**). A two-step procedure starting from [$RuCl_2$(CNR)(η⁶-C_6Me_6)]$_2$ was optimized (Scheme 3), thus **4b**, **f** were isolated as ochre-yellow solids in 57–64% yields. The synthetic steps and the work-up were carried out under N_2 since both compounds are moderately air-sensitive. Conversely, all reactions of **1b**, **f**, phenylacetylene and various Brønsted bases resulted in mixtures of non-arene ruthenium complexes, some of which probably contain an acetylide ligand (IR data). The expected *p*-cymene derivatives [RuCl(CCPh)(CNR)(η⁶-*p*-cymene)] (R = Cy, Xyl) were never observed.

Complex **4b** is unprecedented while **4f** was previously obtained in lower yield using a large excess of phenylacetylene, and limited spectroscopic characterization was provided.[15c] In general, relatively few Ru(η⁶-arene) acetylide complexes are known[29,30] and Ru(isocyanide)(acetylide) complexes are also comparatively rare.[31]

Compounds **4b**, **f** were characterized by elemental analyses (CHN), IR and NMR spectroscopy (Fig. S57–S64). The Ru–C≡C(Ph) fragment is identified by a strong absorption at 2100 cm^{-1} in the IR spectrum (CH_2Cl_2) and by ^{13}C NMR signals at *ca.* 105 and 110 ppm ($CDCl_3$). By comparison, phenylacetylene shows a weak IR absorption at 2110 cm^{-1} (pure liquid) and ^{13}C NMR signals at 77 and 83 ppm ($CDCl_3$) for the alkynyl carbons.[32] A strong IR absorption in the 2130–2160 cm^{-1} range (CH_2Cl_2) is related to the isocyanide ligand in **4b**, **f**. The formal replacement of

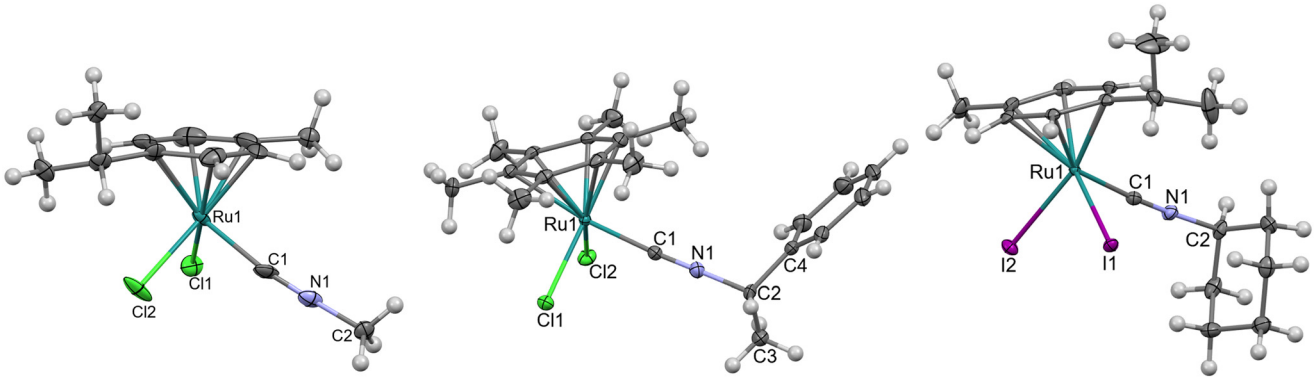

Fig. 2 Molecular structures of **1a** (left), **2c**·H_2O (center) and **1b-I** (right). Displacement ellipsoids are at the 50% probability level.

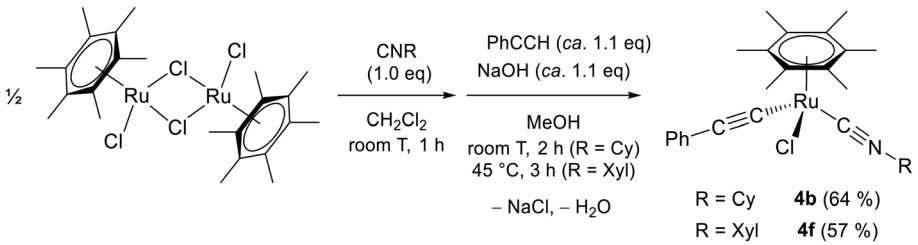

Scheme 3 Two-step synthesis of [RuCl(CCPh)(CNR)(η^6-C_6Me_6)] from [$RuCl_2$(η^6-C_6Me_6)], and the corresponding isocyanide, phenylacetylene and NaOH. Reactions were carried out under N_2; isolated yields in parentheses.

Cl^- with $PhCC^-$ on the $\{RuCl(CNR)(\eta^6\text{-}C_6Me_6)\}^+$ scaffold leads to a decrease of about 15 cm^{-1} in the wavenumber of the isocyanide (C≡N) stretching band (Fig. S58 and S62), reflecting an increased electron density at the metal center.

The crystal structures of **4b** and **4f** were elucidated by single-crystal X-ray diffraction (Fig. 3 and Table S3). The compounds display a three-legged piano-stool geometry as **2c** where one chloride has been replaced by an acetylide. The structures of **4b** and **4f** may be compared to that of the previously reported [$RuCl(CCPh)(PPh_3)(\eta^6\text{-}C_6Me_6)$]:[29] the replacement of PPh_3 with CNR (R = Cy, Xyl) causes a slight elongation of the Ru1–C11 bond [2.020(3) Å in **4b**; 2.025(4) Å in **4f**; compared to 1.952(9) Å for the phosphane derivative]. These bonding parameters are in agreement with a Ru–C(sp) single bond, whereas C11–C12 [1.208(4) Å in **4b**; 1.170(6) Å in **4f**] is a typical triple bond,[29] as also corroborated by the fact that Ru1–C11–C12 [171.1(3)° in **4b**; 176.9(4)° in **4f**] and C11–C12–C13 [172.6(3)° in **4b**; 176.6(5)° in **4f**] are close to linearity.

Heating acetonitrile solutions of **1b**, **f** at reflux resulted in *p*-cymene displacement and acetonitrile coordination. The process takes several hours to reach complete conversion, while the solution progressively changes from red to light yellow. The XylNC complex **1f** is more reactive than the CyNC complex **1f** (14 h *vs.* 24 h as the optimal reaction time, respectively), analogously to what previously observed for a

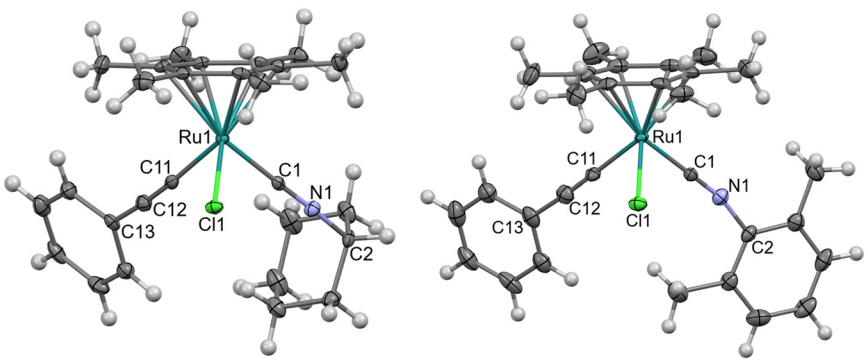

Fig. 3 Molecular structures of **4b** (left) and **4f** (right). Displacement ellipsoids are at the 50% probability level.

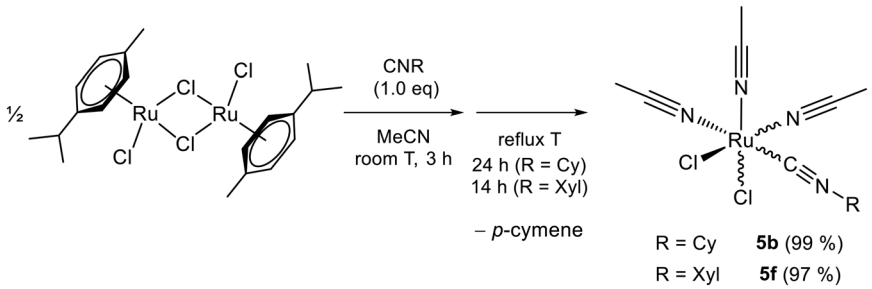

Scheme 4 One-pot, two step synthesis of $[RuCl_2(MeCN)_3(CNR)]$ from $[RuCl_2(\eta^6\text{-}p\text{-cymene})]$ and the corresponding isocyanide in MeCN as a solvent. Reactions were carried out under N_2; isolated yields in parentheses. Wavy bonds denote *fac*/*mer* and *cis*/*trans* isomerism.

related *p*-cymene/DMSO exchange.[21] A one-pot procedure starting from $[RuCl_2(\eta^6\text{-}p\text{-cymene})]_2$ was optimized and the resulting tris-acetonitrile complexes $[RuCl_2(MeCN)_3(CNR)]$ (R = Cy, **5b**; Xyl, **5f**) were isolated as sand yellow powders in almost quantitative yield (Scheme 4). To the best of our knowledge, *trans*,*trans*,*trans*-$[RuCl_2(CNR)_2(NCR')_2]$ (R′ = Me, Ph; R = ^{t}Bu, Cy, Xyl)[33] complexes are the only prior examples of Ru complexes containing an isocyanide, a nitrile and chloride as ligands.

Compounds **5b**, **f** were characterized by elemental analyses (CHN), molar conductivity, IR and NMR spectroscopy (Fig. S65–S74). The IR spectra of **5b**, **f** in CH_2Cl_2 show a strong absorption at 2104 or 2137 cm^{-1}, with a shoulder about 30 cm^{-1} higher, accounting for xylyl and cyclohexyl isocyanide ligands, respectively. The main isocyanide stretching band shows a negative coordination shift (−7 cm^{-1} for CyNC → **5b** and −19 cm^{-1} for XylNC → **5f**; Fig. S66 and S71), indicative of increased backdonation from the Ru(II) center as compared to the *p*-cymene precursors **1b**, **f**. The relative intensity of these bands is reversed in the solid-state IR spectra. A weak absorption around 2290 cm^{-1} (CH_2Cl_2) or 2280 cm^{-1} (solid state) is ascribable to coordinated acetonitrile.[34] The ^{13}C NMR spectra (CD_3CN) of **5b**, **f** show four sets of signals of comparable intensity for isocyanide ligands. Several resonances for acetonitrile ligands are present around 4 and 125 ppm in the ^{13}C NMR spectra and around 2.4 ppm in the ^1H NMR spectra. There is some free MeCN in the ^1H NMR spectra, which, if included in the integrals, returns a MeCN/isocyanide ratio of 3 : 1. Overall, **5b**, **f** are presumably mixtures of *fac*, *mer*,*cis* and *mer*,*trans* isomers of $[RuCl_2(MeCN)_3(CNR)]$, while a fourth species may form in solution by water/acetonitrile replacement.[35] A similar case of lability towards water is documented for the well-known *cis*,*fac*-$[RuCl_2(\kappa S\text{-DMSO})_3(\kappa O\text{-DMSO})]$.[36] The four species are not clearly discernible in the ^1H NMR spectra of **5b**, **f** due to the extensive overlap of signals. Exchange of the coordinated acetonitrile with the solvent (CD_3CN) is minimal over several days at room temperature while it is almost complete after 24 h at 50 °C. The IR spectrum of the solid recovered from these solutions shows a weak band at 2300 cm^{-1} attributed to nitrile stretching (+15 cm^{-1} shift due to H/D exchange; Fig. S65 and S70).[34]

2.2. Catalytic studies

The ruthenium(II) isocyanide complexes reported in this work were screened for dimerization/trimerization of phenylacetylene as a benchmark substrate. The reaction conditions were optimized using **1b** as a model compound, featuring an isocyanide ligand with a simple alkyl substituent, *p*-cymene and chloride ligands. Several parameters were investigated to identify the key factors for designing an efficient and sustainable catalytic system, including temperature and energy source, solvent effects, catalyst concentration and choice of the base. The remaining complexes were screened under the optimized conditions to assess the influence of different isocyanide substituents, arene and halide ligands on the catalytic performances. Additionally, the activation steps of the Ru pre-catalysts were studied to elucidate the mechanism of the reaction.

Overall, the reactions afforded a maximum of five coupling products: three dimers (*cis* and *trans* dimers plus the product of homocoupling) and two trimers (Scheme 5). It was essential to assess the selectivity between dimerization and trimerization, rather than focusing on individual products. However, it was determined from combined GC–MS (Fig. S75) and ^1H NMR data (section 4.7) that the major dimer was the *trans* (*E*) enyne.

2.2.1. Solvent and base screening. The coupling of terminal alkynes requires a base to facilitate proton

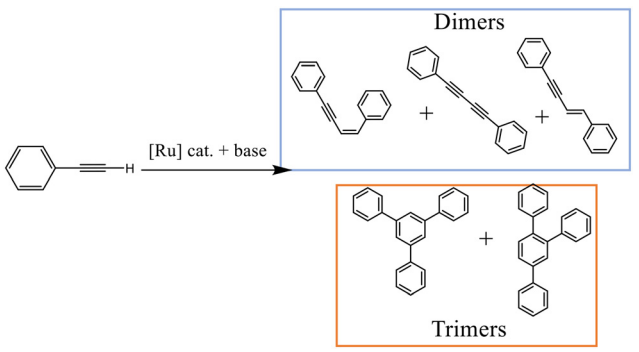

Scheme 5 Phenylacetylene dimerization/cyclotrimerization reaction and products.

Table 1 Catalytic results for the coupling of phenylacetylene with **1b** as a catalytic precursor and Na_2CO_3 as a base in different solvents

Entry[a]	Solvent	Conversion (%)	Dimer selectivity (%)	Trimer selectivity (%)
1	Ethanol	58	38	62
2	Hexane	39	21	79
3	Toluene	63	34	66
4	Acetonitrile	73	66	34
5	Water	85	81	19
6	Acetone	31	81	19
7	DMF	96	85	15
8	THF	45	61	39

[a] Reaction conditions: solvent (3.0 mL), phenylacetylene (1.0 mmol), Na_2CO_3 (100 μmol; 10 mol%), 80 °C, 24 h, **1b** (25 μmol, 2.5 mol%). Conversion and selectivity values were determined by GC–MS after extraction with ethyl acetate (2 mL), using mesitylene as an internal standard.

removal. Organic bases are usually preferred due to their high activity and solubility in organic solvents; however, several of them are environmentally hazardous and pose increased risk in the overall process due to safety concerns such as flammability.[37] We focused our catalytic investigation on Na_2CO_3 as a base, which is cheap, non-toxic and environmentally benign.

In general, the choice of solvent is one of the most critical parameters in homogeneous catalysis, as it may face significant environmental issues and shape the activity of the catalyst.[38] Organic solvents such as DMF and toluene are often used in coupling reactions of terminal alkynes, negatively impacting the environment. The search for greener alternative organic or water systems is highly needed.

Table 1 comprises the results obtained for the coupling reaction of phenylacetylene using **1b** as a catalytic precursor and Na_2CO_3 as a base in various solvents at 80 °C. As expected, the solvent exerted a significant influence on the catalytic activity, from both conversion and selectivity standpoints. Acetonitrile, water and DMF provided the highest conversions of phenylacetylene, with the major products being the dimers. Interestingly, in ethanol, hexane, or toluene the selectivity of the reaction shifted towards the trimers. It is noteworthy that the catalytic system is effective despite the near insolubility of Na_2CO_3 in most of these solvents. Water as a solvent created a biphasic (liquid/liquid) mixture, wherein the organic phase consisted of phenylacetylene, mesitylene and **1b**, while the aqueous phase completely dissolved Na_2CO_3. This system presented the second highest conversion and selectivity. Using water as a solvent allows for a more environmentally friendly process, in which the products can be easily recovered through solvent extraction.

Next, different organic (pyridine, triethylamine and *N*,*N*-diisopropylethylamine (DIPEA)) and inorganic (sodium, potassium and cesium carbonate) bases were tested in water, each one at 10 mol% loading. Fig. 4a and 4b present the conversion of phenylacetylene and dimer/trimer selectivity, respectively. The catalytic performance of **1b** remains high with all these bases except triethylamine,

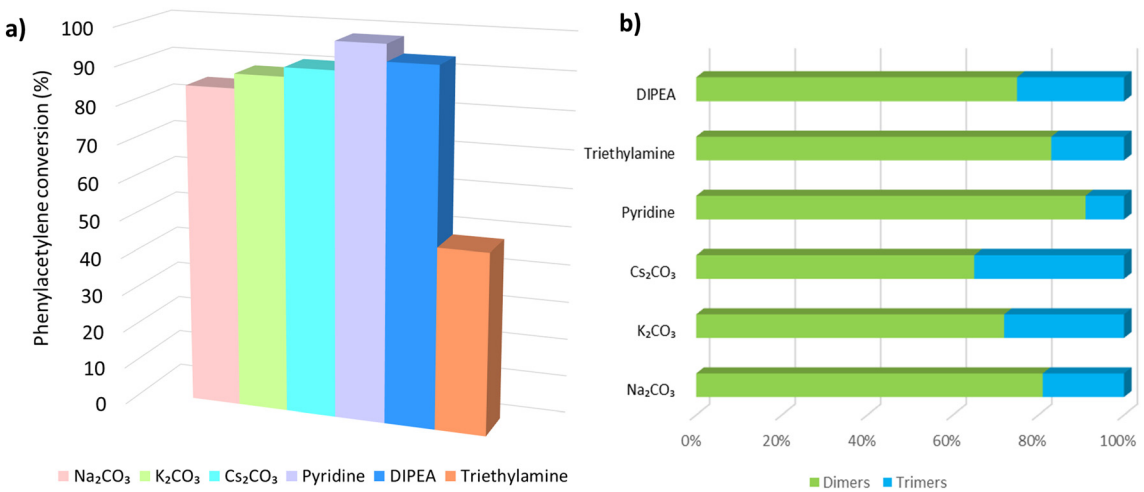

Fig. 4 Catalytic results for the coupling of phenylacetylene with **1b** as a catalytic precursor and different bases in water as solvent: a) phenylacetylene conversion and b) selectivity for phenylacetylene dimers or trimers. Reaction conditions: water (3.0 mL), phenylacetylene (1.0 mmol), base (10 mol%), **1b** (2.5 mol%), 80 °C, 24 h.

determining a substantial decrease in substrate conversion. Pyridine and DIPEA gave a 10–15% increased conversion with respect to Na_2CO_3, with the selectivity to the dimer production remaining high (91 and 75%, respectively). These results do not correlate with the basicity (pK_a of conjugate acids in water: 5.2 for pyridine, 10.3 for carbonate, ≈11 for DIPEA and Et_3N). Despite the slight increase in conversion and selectivity in the case of pyridine, Na_2CO_3 is preferable as a more sustainable reagent. Phenylacetylene conversion tends to increase with the size of the carbonate cation according to the sequence $Na^+ < K^+ < Cs^+$ (85% < 88% < 91%) while the selectivity towards the dimers follows the opposite trend, with a complementary increase in trimer production. Thus Cs_2CO_3 displayed a dimerization selectivity of 65% that contrasts with the value obtained for Na_2CO_3 (81%).

2.2.2. Ru catalyst and Na_2CO_3 loading. The metal catalyst loading represents one of the most significant economic impacts when designing a catalytic system. Several catalytic systems designed for C–C coupling reactions applied high catalytic loadings (up to 10 mol%) and/or precious metals such as palladium and platinum.[39]

Table 2 shows the catalytic results of the coupling of phenylacetylene in water at 80 °C after 24 h using variable loadings of **1b** and Na_2CO_3. A high conversion (85%) was achieved with 2.5 mol% of **1b** and 10 mol% of Na_2CO_3, accompanied by high selectivity towards the dimerization process (81%). When the loading of **1b** was increased to 3 mol%, no variation in the conversion was observed, although a slightly higher selectivity toward dimerization was obtained. In contrast, a decrease in conversion and, more importantly, a decrease in selectivity were observed with a 1 mol% Ru loading. A decline in conversion is anticipated due to the reduction of the ruthenium complex available for the reaction. Still, the change in selectivity represents an important aspect of the system, as it becomes possible to control the product distribution by combining the solvent effect with the catalyst loading.

Next, the amount of Na_2CO_3 was screened to 5 and 15 mol% while keeping **1b** at 2.5 mol%. Decreasing the base resulted in a decreased conversion of phenylacetylene to 60% while also reducing the selectivity toward dimerization to 62%. On the other hand, the increase in base leads to a drop of the conversion to 72% and the selectivity to 69% with respect to the results with 10 mol%.

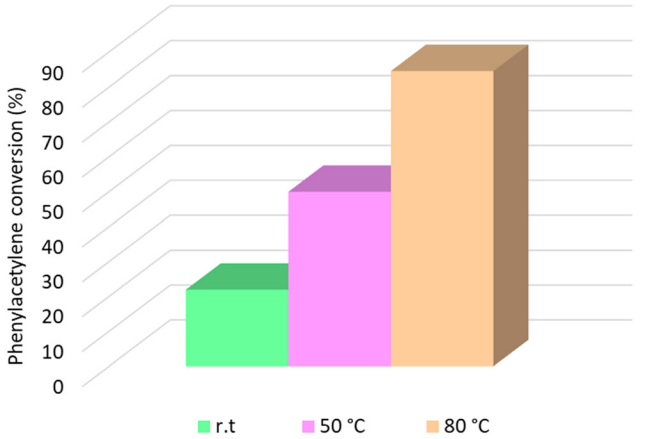

Fig. 5 Conversion of phenylacetylene at different reaction temperatures. Reaction conditions: water (3.0 mL), phenylacetylene (1.0 mmol), Na_2CO_3 (10 mol%), **1b** (2.5 mol%), 24 h.

Blank experiments were also performed, one without the Ru catalyst and one without Na_2CO_3, and in both cases no conversion or product formation was observed.

2.2.3. Temperature screening and time-course conversion/selectivity. Fig. 5 illustrates the variation of conversion with temperature. Compound **1b** showed activity even at room temperature, converting 22% of phenylacetylene. The conversion increased to 50% with a slight rise to 50 °C. The highest conversion was obtained at 80 °C. Importantly, temperature did not significantly affect the product distribution, with only a slight increase in selectivity from 73 to 81%.

To better understand the evolution of the reaction, experiments were carried out at different times, and the results are summarized in Table 3. The reaction follows a very fast initial rate, reaching 21% conversion after one hour, although with low selectivity toward dimerization. As time progresses, phenylacetylene conversion continues to increase, with the most significant rise occurring between 4 and 8 h, and continuing up to 24 h. The gradual increase in yield is accompanied by an increase in dimerization selectivity, reaching its maximum after 24 h.

2.2.4. Isocyanide and arene effect. Complexes **1–3** were tested under the optimized conditions (2.5 mol% Ru, 10

Table 2 Catalytic results obtained for the coupling of phenylacetylene with different loadings of **1b** and Na_2CO_3 in water using different catalyst loads

Entry[a]	**1b** (mol%)	Na_2CO_3 (mol%)	Conversion (%)	Dimer selectivity (%)	Total TON
1	1.0	10	46	65	46
2	2.5	10	85	81	33
3	3.0	10	84	85	28
4	2.5	5	60	62	24
5	2.5	15	72	69	26
6	0	10	0	—	—
7	2.5	0	0	—	—

[a] Reaction conditions: water (3.0 mL), phenylacetylene (1.0 mmol), Na_2CO_3, 80 °C, 24 h. Conversion and selectivity values were determined by GC–MS after extraction with ethyl acetate (2 mL), using mesitylene as an internal standard.

Table 3 Catalytic results for the coupling of phenylacetylene mediated by **1b** at different reaction times

Entry[a]	Time (hours)	Conversion (%)	Dimers selectivity (%)	Total TOF (h^{-1})
1	1	21	60	8.4
2	2	25	63	5.0
3	4	30	68	3.0
4	8	61	76	3.1
5	24	85	81	1.4

[a] Reaction conditions: water (3.0 mL), phenylacetylene (1.0 mmol), Na_2CO_3 (10 mol%), **1b** (2.5 mol%), 80 °C. Conversion and selectivity values were determined by GC–MS after extraction with ethyl acetate (2 mL) using mesitylene as an internal standard.

mol% Na_2CO_3, water, 80 °C, 24 h) to investigate the influence of the different isocyanide and arene ligands on the catalytic performances. During optimization, it was found that the loading of **1b** could switch the reaction's selectivity. Therefore, each Ru pre-catalyst was tested at 1.0 and 2.5 mol%. Results are compiled in Table 4. The change

Table 4 Catalytic results for the coupling of phenylacetylene with different ruthenium(II) arene complexes of general formula $[RuX_2(L)(\eta^6\text{-arene})]$ (X = Cl except for **1b-I**; L = isocyanide or CO), $[RuCl(OAc)(\eta^6\text{-}p\text{-cymene})]$ and their halide-bridged precursors $[RuCl_2(\eta^6\text{-arene})]_2$

Isocyanide or other ligand	η^6-arene ligand 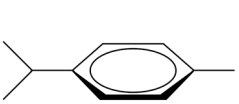	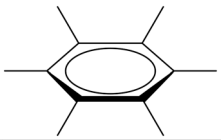	
CN–	**1a** 50% (44%)[a] 67% (47%)[b]	**2a** 54% (69%)[a] 70% (74%)[b]	—
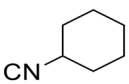	**1b** 46% (65%)[a] 85% (81%)[b] **1b-I** (X = I) 40% (72%)[a] 76% (66%)[b]	**2b** 45% (66%)[a] 65% (67%)[b]	**3b** 56% (64%)[a] 71% (69%)[b]
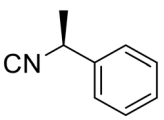	**1c** 62% (28%)[a] 61% (57%)[b]	**2c** 45% (70%)[a] 65% (75%)[b]	—
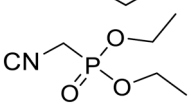	**1d** 54% (53%)[a] 59% (68%)[b]	**2d** 55% (38%)[a] 51% (64%)[b]	**3d** 69% (23%)[a] 57% (18%)[b]
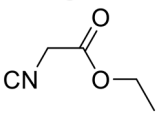	**1e** 62% (48%)[a] 58% (44%)[b]	—	—
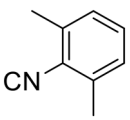	**1f** 55% (45%)[a] 71% (52%)[b]	**2f** 62% (60%)[a] 62% (54%)[b]	**3f** 67% (42%)[a] 66% (43%)[b]
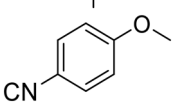	**1g** 65% (34%)[a] 77% (58%)[b]	—	—
CO	27% (31%)[a] 66% (35%)[b]	19% (27%)[a] 68% (36%)[b]	—
$CH_3CO_2^-$	**[RuCl(OAc)(η⁶-*p*-cymene)]** 29% (33%)[a] 46% (35%)[b]	—	—
—	**$[RuCl_2(\eta^6\text{-}p\text{-cymene})]_2$** 66% (41%)[b]	**$[RuCl_2(\eta^6\text{-}C_6Me_6)]_2$** 55% (62%)[b]	**$[RuCl_2(\eta^6\text{-}C_6H_6)]_2$** 48% (43%)[b]

[a] Reaction conditions: water (3.0 mL), phenylacetylene (1.0 mmol), Na_2CO_3 (10 mol%), Ru pre-catalyst (1.0 mol%), 80 °C, 24 h. Conversion values (selectivity to dimer in parentheses) were determined by GC–MS after extraction with ethyl acetate (2 mL), using mesitylene as an internal standard. [b] Reaction performed with 2.5 mol% of catalyst, corresponding to 5% Ru loading for $[RuCl_2(\eta^6\text{-arene})]_2$.

in Ru loading has mixed effects on the conversion and selectivity of the catalytic process that depend on the specific arene/isocyanide combination. Overall, **1b** stands out among the investigated complexes with an 85% phenylacetylene conversion and 81% selectivity for dimer formation at 2.5 mol% loading. In the other cases, phenylacetylene conversion varies in relatively limited ranges, 45–69% and 51–76% with 1.0 and 2.5 mol% Ru, respectively. Increasing the amount of Ru pre-catalyst results in a marked increase in conversion with **1–2a**, **1–3b**, **1b-I**, **2c**, **1f**, and **1g** (+15% to + 40%) while negligible changes or a slight decrease (down to −5%) are observed with **1c**, **1–2d**, **1e**, and **2–3f**.

The catalytic activity of the Ru complexes is more discriminated by the selectivity for dimer or trimer formation. All cyclohexyl isocyanide complexes (**1–3b** and **1b-I**) as well as **1d**, **2a**, and **2c** show a net preference (selectivity values 64–75%; excluding **1b**, 81%) for dimer formation at both catalytic loadings. Instead, the xylyl isocyanide complexes **1–3f** as well as **1a**, **e** equally promote dimerization and trimerization processes (dimer selectivity 44–54% except **2f** at 1 mol%) at both catalytic loadings.

In most cases, it is possible to observe a shift in selectivity with increasing Ru loading, favoring the formation of dimers over trimers. The selectivity increase is moderate (+3–5%) with **1–2a**, **3b**, **2c**, and **1f** while being more pronounced (+15–25%) with **1b**, **1c**, **1g**, and **2b–d**. Compounds **1c**, **1g** and **2d** are remarkable as they tend to favor trimer formation at low catalyst concentration (dimer selectivity 28–38%), whereas dimerization becomes the dominant pathway at the higher concentration (57–64%). Negligible changes (**2b** and **3f**) or a slight decrease (−4–6%; **1b-I**, **3d**, **1e**, and **2f**) in selectivity for dimer formation are observed with the remaining compound. The benzene complex **3d** shows the highest tendency for trimer formation among the investigated complexes, further increasing at higher catalyst amount (dimer selectivity 18–23%) while the conversion decreases substantially (−12%). A slight decrease in conversion was observed on comparing **1b** with the bis-iodide analogue **1b-I** at 1 mol%, with minor changes in selectivity. A more pronounced decrease in conversion (−9%) and selectivity (−15%) occurred at 2.5 mol%. On considering the greater lability of Ru–Cl bonds compared to Ru–I bonds,[40] these results indicate that halide dissociation is relevant for the catalytic mechanism.

Overall, the different arene, isocyanide and halide ligands have variable effects on the conversion and selectivity and respond differently to changes in the catalytic loading. This flexibility, combined with the factors discussed above, demonstrates the versatility of these ruthenium(II) isocyanide complexes.

Next, reference ruthenium(II) complexes were tested for comparative purposes (Table 4). The chloride-bridged precursors $[RuCl_2(\eta^6\text{-arene})]_2$ (arene = C_6H_6, *p*-cymene, C_6Me_6) performed worse in terms of both conversion and selectivity compared to most of their piano-stool isocyanide derivatives. It should also be considered that a 2.5 mol% loading corresponds to 5 mol% of Ru in these cases.

Complexes $[RuCl_2(CO)(\eta^6\text{-arene})]$ (arene = *p*-cymene, C_6Me_6) provide an interesting comparison of isoelectronic carbonyl *versus* isocyanide ligands.[19] The carbonyl complexes performed poorly in terms of both phenylacetylene conversion (20–30%) and dimerization selectivity (≈30%), using 1% Ru loading. At 2.5% loading, the conversion approached a level comparable to some isocyanide analogues but dimer selectivity only marginally increased (≈35%).

The acetate derivative $[RuCl(OAc)(\eta^6\text{-}p\text{-cymene})]$, known to catalyze alkyne dimerization in acetic acid (see section 2.4),[41] showed significantly lower conversion and selectivity compared to the *p*-cymene isocyanide complexes investigated in this work at both catalytic loadings (1 and 2.5%). Overall, these results highlight the beneficial effects of introducing isocyanide ligands in the design of ruthenium(II) arene catalysts.

2.2.5. Scope of substituted terminal alkynes. Table 5 illustrates the conversion and dimer selectivity for the various terminal alkynes studied under optimized conditions (2.5 mol% of Ru, 10% of Na_2CO_3 in water, 80 °C, 24 h) with the best catalytic precursor **1b**. Overall, reactions with substituted terminal alkynes achieved lower conversions compared to phenylacetylene. This can be attributed to several factors, including solubility (some substrates were solid and poorly soluble in water), steric hindrance that may interfere with coordination to ruthenium and electronic effects of the substituents determining activation or deactivation of the alkyne. Nevertheless, some interesting trends were observed. For instance, the three ethynylanisoles showed differences in both conversion and selectivity. *ortho*- and *para*-Ethynylanisoles strongly favored dimerization over trimerization, while *meta*-ethynylanisole gave a less selective outcome, with only 57% dimer formation. Ethynyltoluenes revealed a similar behavior. However, in this case the least selective toward dimerization was the *ortho* substituted derivative (58% dimer). Notably, changing the methyl group to an ethyl (1-ethyl-4-ethynylbenzene) resulted in a 50% decrease in conversion relative to *para*-ethynyltoluene, while maintaining similar dimer selectivity. As expected, an electronegative substituent deactivates the alkyne, leading to lower conversion, as observed for 1-chloro-4-ethynylbenzene. Finally, the combination of the methyl group in the *ortho* position and a methoxy group in the *para* position exhibited a mixed effect: conversion decreased relative to *para*-ethynylanisole (similar to *ortho*-ethynyltoluene), but dimer selectivity increased slightly (by 4%).

2.2.6. Alternative energy sources. Metal complexes can respond differently to various energy sources, and this characteristic can be exploited in the design of a catalytic system. Fig. 6a shows phenylacetylene conversion promoted by **1b** and Na_2CO_3 (2.5 and 10 mol%, respectively) under different energy sources, while Fig. 6b presents the corresponding dimer selectivities.

Table 5 Catalytic results for different substituted terminal alkynes using **1b** as a pre-catalyst

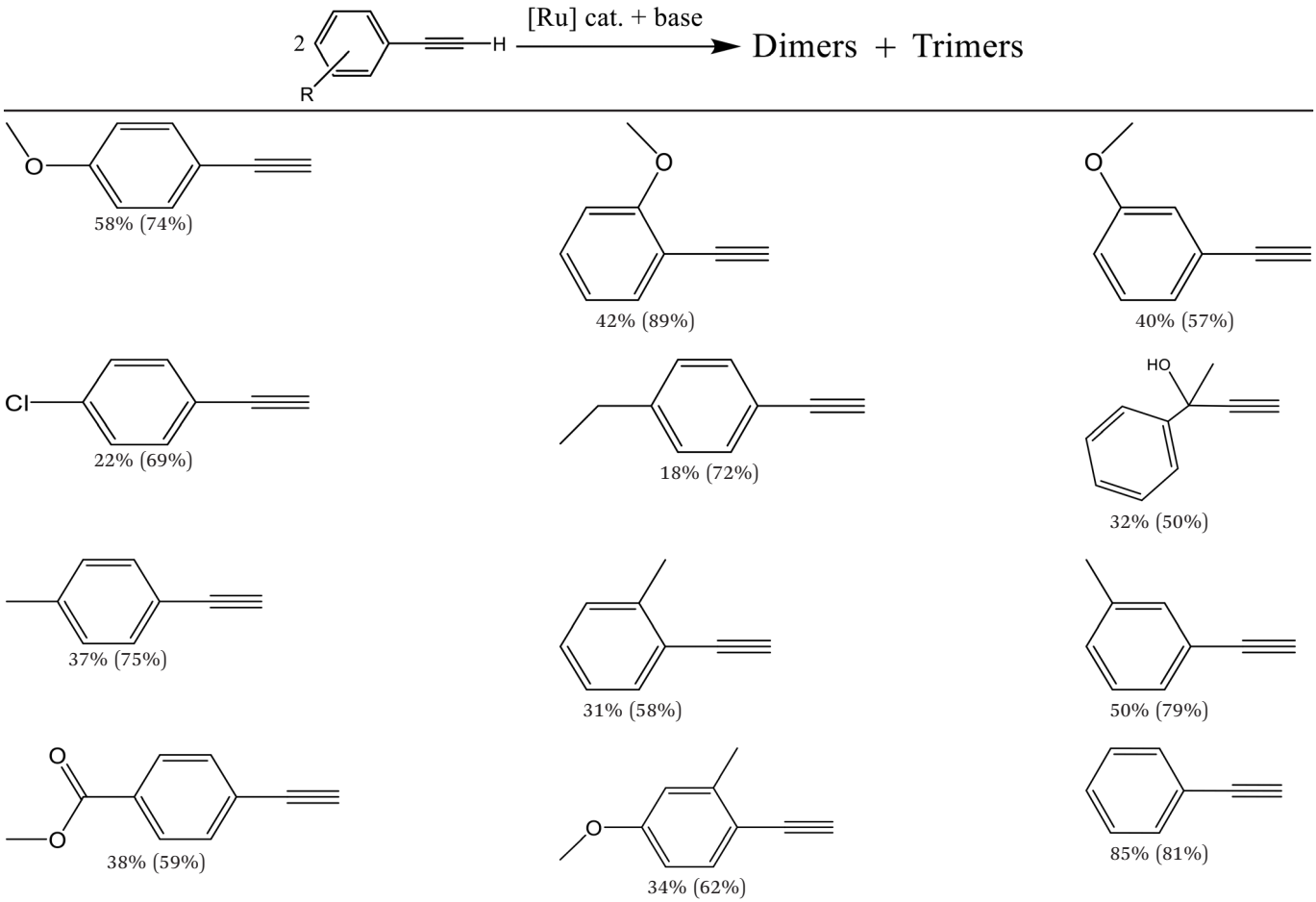

Reaction conditions: water (3.0 mL), terminal alkyne (1.0 mmol), Na_2CO_3 (10 mol%), **1b** (2.5 mol%), 80 °C, 24 h. Conversion and selectivity toward dimerization (in parentheses) values determined by GC–MS after extraction with ethyl acetate (2 mL), using mesitylene as an internal standard.

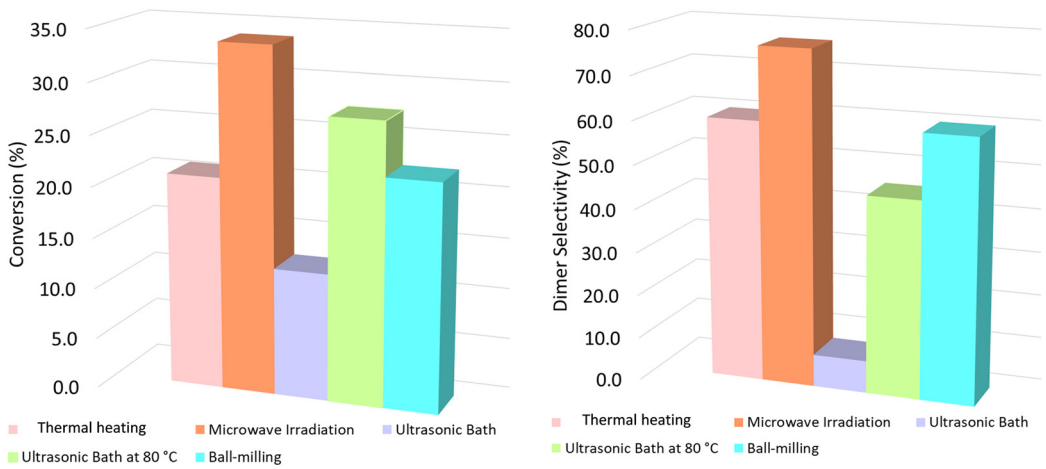

(a) (b)

Fig. 6 Conversion of phenylacetylene (a) and dimerization selectivity (b) under different energy sources. Reaction conditions: water (3.0 mL) except ball milling (solventless), phenylacetylene (1.0 mmol), Na_2CO_3 (10 mol%), **1b** (2.5 mol%), 80 °C, 1 h.

After 1 h of reaction, the catalytic system is more responsive to alternative energy sources than to thermal heating. The highest conversion (34%) was obtained under microwave irradiation, likely due to the high dielectric constant of water, which efficiently absorbs microwave energy and leads to greater system activation. The performance of the ultrasonic bath strongly depends on the reaction temperature. At room temperature (purple color), the conversion was very low (12.5%). When the reaction was performed at 80 °C, the synergistic effect between ultrasonic waves and thermal activation enhanced the conversion of phenylacetylene (21% under thermal heating *vs.* 28% under ultrasound at 80 °C). Ball-milling also proved to be an interesting method, as it enables the reaction to be performed without solvent and provided a conversion similar to thermal heating.

Regarding selectivity, Fig. 6b shows that ultrasonic irradiation favors trimer formation. Even at 80 °C, the reaction predominantly produced trimers, demonstrating another parameter that can modulate the flexibility of the system. Thermal heating and ball-milling catalysis yielded similar selectivities for dimer formation, while the microwave reaction provided the highest dimer selectivity (77%).

2.3. Reactivity and mechanistic studies

To gain insights into the catalytic mechanism, the reactivity of ruthenium(II) arene isocyanide complexes with phenylacetylene and sodium carbonate was investigated. Compounds **1–3b** and **1–3f**, combining an aliphatic (cyclohexyl) or aromatic (xylyl) isocyanide with the three investigated arene ligands (benzene, *p*-cymene, hexamethylbenzene), were selected. Acetonitrile as a solvent is convenient for this purpose due to complete solubilization of both the Ru precursors and phenylacetylene, its coordinative ability and the possibility of monitoring the reaction by IR. A first set of experiments was carried out with each Ru compound, Na_2CO_3 and PhCCH in 1 : 1 : 10 molar ratio. After 2 h at 80 °C, the solutions were analyzed by IR and ^{1}H NMR (Table S4 and Fig. S76–S81). Two reactivity trends emerged based on the consumption of the starting material, which increased in the order C_6Me_6 < *p*-cymene < C_6H_6 and XylNC < CyNC. The displacement of the η^6-arene ligand is minor for **2b**, **f** (≈10%, C_6Me_6), substantial for **1b**, **f** (50–60%, *p*-cymene) and quantitative for **3b**, **f** (C_6H_6). In parallel, both hexamethylbenzene complexes **2b**, **f** partially converted into the corresponding phenylacetylide derivatives **4b**, **f**. In detail, **4b** was the predominant species in the final solution, while the conversion of **2f** into **4f** was much lower. Compound **1f** partially transformed in a chiral *p*-cymene species, while **1b** was the only *p*-cymene complex identified in the final reaction mixture. On the other hand, no traces of **3b**, **3f** or any other benzene complex were detected. The Ru compounds resulting from the release of *p*-cymene and benzene ligands are probably associated with the intense bands appearing in the 2140–2150, 2120–2100, and 1950–1960 cm^{-1} regions of the IR spectra, attributed to CyNC, XylNC and CO ligands, respectively.

Additional experiments were carried out with **1b**, **2b** and **2f** in MeCN under more catalytically relevant conditions, involving a lower Ru concentration and a 1 : 10 : 100 mol ratio with Na_2CO_3 and PhCCH, respectively. Both 80 °C and lower temperatures were tested to better follow the transformations. Aliquots of each reaction mixture were analyzed by IR at different times, allowing to trace a qualitative profile of Ru speciation (see Tables S5–S9 and Fig. S82–S86). In addition, at specified times, volatiles were removed under vacuum; the residue was washed with Et_2O to remove organic compounds, and was then analyzed by IR (CH_2Cl_2), ^{1}H and ^{1}H–^{13}C HMBC ($CDCl_3$) and ESI-MS (MeOH). In agreement with previous results, the new tests confirmed the overall reactivity trend **1b** ≫ **2b** > **2f**. Both hexamethylbenzene complexes **2b**, **f** initially converted into the corresponding phenylacetylide derivatives **4b**, **f**. This reaction was relatively rapid and straightforward for **2b**, which was no longer present after 1.5 h at 80 °C or after 4 h at 60 °C, while **4b** became the main species in solution (IR). The less reactive **2f** required 3 h at 80 °C for its complete consumption, while **4f** already appeared after 1.5 h (Fig. 7). Afterwards, the intensity of the IR bands of **4b**, **f** decreased over time while new IR absorptions appeared around 2137–2120, 2110 and 2100–2080 cm^{-1}, due to CyNC, XylNC and PhCC$^-$ ligands, respectively (Fig. S85–S86). Moreover, IR bands in the 2180–2200 cm^{-1} region were assigned to the C≡C stretching of an (ethynyl)alkenyl ligand derived from the coupling of phenylacetylide and an alkyne or vinylidene ligand.[41,42] The associated processes required several hours to reach high conversion for both **4b** and **4f** at 80 °C and were almost completely inhibited for **4b** at 60 °C over 12 h. NMR analyses indicated the formation of a mixture of Ru complexes with some (**2f**/XylNC) or all (**2b**/CyNC) lacking the C_6Me_6 ligand.

The *p*-cymene compound **1b** confirmed to be more reactive than the related hexamethylbenzene complexes **2b**, **f**. After 1 h at 80 °C, the isocyanide stretching band of **1b** completely disappeared and new isocyanide (2165, 2144 cm^{-1}) and acetylide (2080 cm^{-1}) bands emerged. The conversion of **1b** slowed down at 55 °C, being about 50% after 4.5 h, and was accompanied by the growth of a similar profile of IR bands. The formation of these isocyanide/acetylide complexes is likely associated with the loss of the *p*-cymene ligand since **1b** is the only piano-stool species observed in the ^{1}H NMR spectrum. The putative [RuCl(CCPh)(CyNC)(*p*-cymene)] (expected C≡N stretching ≈2180 cm^{-1}) is bypassed or is short-lived.

For each compound (**1b**, **2b**, and **2f**) two IR bands around 1970 and 1955 cm^{-1} slowly increased over time at 80 °C, reaching a comparable intensity to that of isocyanide stretchings after 3–4 h for **1b**, 7.5 h for **2b** and 22 h for **4f**.

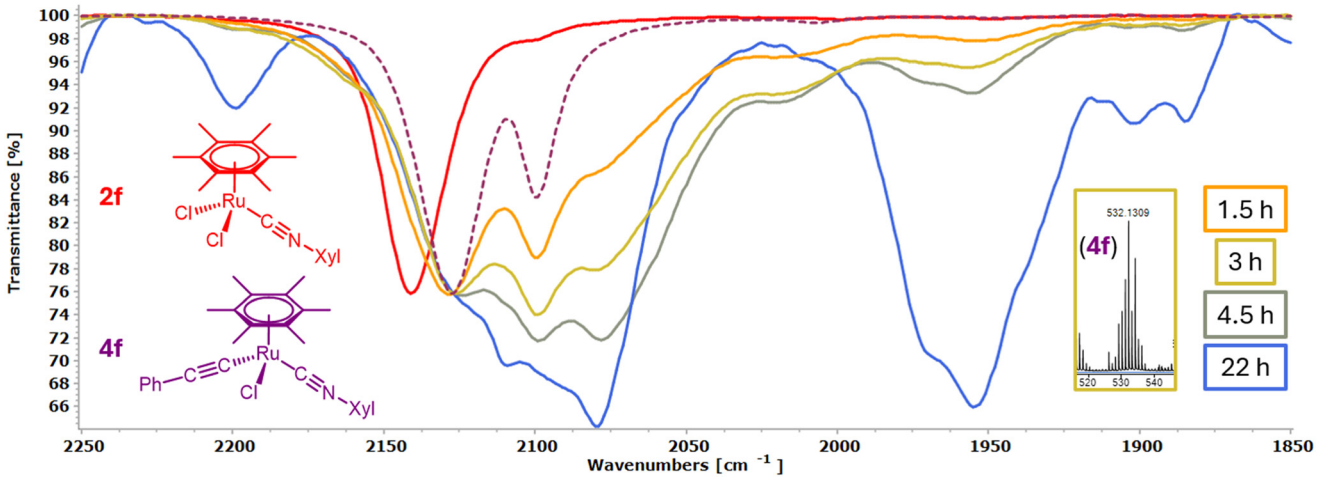

Fig. 7 Solvent-subtracted IR spectra (CH_2Cl_2, 1850–2250 cm^{-1}) of aliquots of the mixture of **2f**, Na_2CO_3 and PhCCH (1 : 10 : 100 molar ratio) in MeCN heated at 80 °C at different times, normalized for the intensity at 2127 cm^{-1} (isocyanide stretching band of **4f**). The red spectrum is the initial spectrum, corresponding to **2f**, while the dashed purple line shows the spectrum of **4f**. Inset shows the MS profile of **4f** observed after 3 h of reaction.

These absorptions were assigned to non-arene carbonyl complexes,[43] which may arise from the hydrolysis or oxidative cleavage of phenylacetylide or related ligands (vinylidene, carbene, and vinyl).[29,44]

Control experiments indicated that **1b**, **2b**, and **2f** are fairly inert in MeCN with Na_2CO_3 and without PhCCH (Fig. S87–S89). Complex **2f** was practically unchanged after 3 h at 80 °C while **1b** and **2b** probably underwent a partial chloride/carbonate exchange after 2 h at 55 °C or 2.5 h at 80 °C, respectively, as suggested by a broad IR absorption emerging at 1450 cm^{-1}.[45] IR bands related to the tris-acetonitrile isocyanide complexes **5b** and **f** were not observed, confirming that the interaction of **1b**, **2b**, and **2f** with PhCCH/Na_2CO_3 is much more rapid than arene/acetonitrile substitution. In fact, **1b**, **f** required 14–24 h in refluxing acetonitrile to fully convert into **5b**, **f** (Scheme 4) and is foreseeable that the displacement of C_6Me_6 from **2b**, **f** would be even more difficult.[12,13] This outcome confirms that acetylide coordination (formal Cl^-/$PhCC^-$ exchange in **2** → **4**) occurs first and likely facilitates the subsequent displacement of the arene ligand (Scheme 6).

Related experiments carried with **1b**/PhCCH/Na_2CO_3 in ethanol (80 °C) or water/mesitylene (55 °C) showed the rapid (1–2 h) formation of new isocyanide–acetylide species, as occurred in MeCN (Fig. S90–S91, Table S10). A reaction carried out with **2f** in water/mesitylene at 80 °C pointed out the initial formation of **4f**, with a similar kinetics to that in acetonitrile as a solvent (comparing Table S11/Fig. S92 *vs.* Table S9/Fig. S86). At variance to MeCN, the scenario in both EtOH and water/mesitylene is complicated by an enhanced tendency to carbonyl formation. In this regard, the higher solubility of Na_2CO_3 probably accelerates the hydrolysis of Ru–C bonds.

To confirm the mechanistic hypotheses, catalytic tests were carried out with **1**, **2**, **4**, **5b** and **1**, **2**, **4**, **5f** in acetonitrile

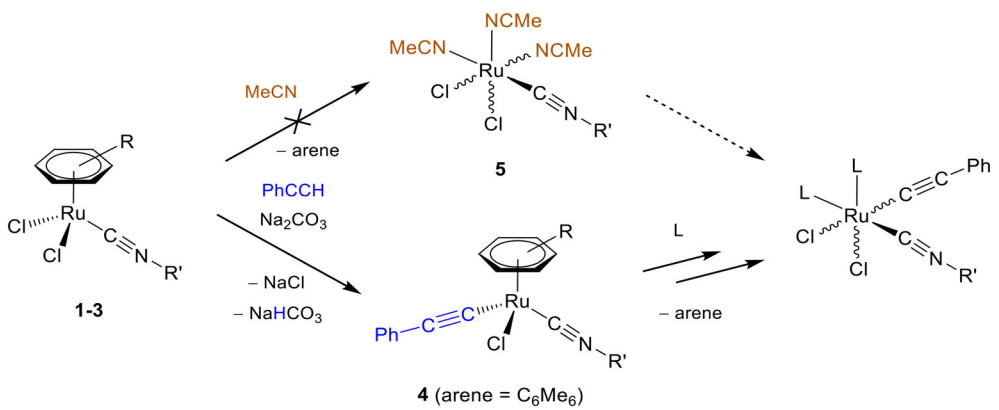

Scheme 6 Overview of the investigated reactivity of ruthenium(II) arene isocyanide complexes with excess PhCCH and Na_2CO_3 in MeCN (L = Cl^-, solvent or other ligands).

Table 6 Results obtained for the coupling of phenylacetylene with **1b**, **1f**, **2b**, **2f**, **4b**, **4f** and **5b**, and **5f** as pre-catalysts

Entry[a]	Catalyst	Time (hours)	Solvent	Conversion (%)	Dimer selectivity (%)
1	**1b**	1	MeCN	20	53
2	**1b**	24	MeCN	73	65
3	**5b**	1	MeCN	8	65
4	**5b**	24	MeCN	73	74
5	**1f**	1	MeCN	13	95
6	**1f**	24	MeCN	63	80
7	**5f**	1	MeCN	8	62
8	**5f**	24	MeCN	82	81
9	**2b**	1	MeCN	17	68
10	**2b**	24	MeCN	75	74
11	**4b**	1	MeCN	15	54
12	**4b**	24	MeCN	64	72
13	**2f**	1	MeCN	21	64
14	**2f**	24	MeCN	63	71
15	**4f**	1	MeCN	14	56
16	**4f**	24	MeCN	63	69
17	**1b**	1	Water	21	60
18	**1b**	24	Water	85	81
19	**1f**	1	Water	38	52
20	**1f**	24	Water	71	52
21	**2b**	1	Water	18	86
22	**2b**	24	Water	65	68
23	**4b**	1	Water	12	82
24	**4b**	24	Water	72	72
25	**2f**	1	Water	14	65
26	**2f**	24	Water	62	54
27	**4f**	1	Water	12	60
28	**4f**	24	Water	62	69

[a] Reaction conditions: solvent (3.0 mL), phenylacetylene (1.0 mmol), Na_2CO_3 (10 mol%), Ru pre-catalyst (2.5 mol%), 80 °C. Percentage of conversion and selectivity values determined by GC–MS after extraction with ethyl acetate (2 mL), using mesitylene as an internal standard.

or water at 80 °C at different reaction times (1 or 24 h). Results are collected in Table 6. First, the catalytic activity of the tris-acetonitrile complexes **5b**, **f** was compared with the *p*-cymene precursors **1b**, **f** (entries 1–8). The significant differences in conversion and selectivity both at 1 h and 24 h support the hypothesis that **5b**, **f** are not formed *in situ* from **1b**, **f** under catalytic conditions. A similar comparison of catalytic activity involved **2b** and **2f**, and **4b** and **4f**, in both water and acetonitrile (entries 9–16 and 21–28). The catalytic activity was similar at both short (1 h) and long (24 h) reaction times, suggesting that the first step of the activation of the dichloride pre-catalysts **2** involved the formation of their acetylide derivatives **4**. The catalytic performances of each Ru compound in water *vs.* in MeCN are not remarkably different at both reaction times (1 h and 24 h), with a few exceptions (namely, **4b** at 1 h; **1f** at 1 h and 24 h), despite the enhanced tendency for carbonyl formation in the aqueous medium.

In conclusion, key steps of the activation of the arene–isocyanide pre-catalysts **1–3** with $PhCCH/Na_2CO_3$ are phenylacetylide coordination and arene displacement, leading to octahedral Ru(II) isocyanide/acetylide species (Scheme 6). This is a multi-step process for hexamethylbenzene complexes **2** that begins with the formation of $[RuCl(CCPh)(CNR)(C_6Me_6)]$, **4**, *via* formal $Cl^-/PhCC^-$ exchange. The release of C_6Me_6 from **4** or related complexes becomes significant after several hours, while *p*-cymene and benzene dissociation from **1** and **3** presumably occurs concerted with phenylacetylene activation. The thermally-induced displacement of the η^6-arene (often *p*-cymene) from ruthenium(II) complexes has been invoked in several cases as a key step to generate catalytically-active species.[7,9c,10,46] Based on literature findings,[47] a generic catalytic cycle for terminal alkyne dimerization may involve the stepwise coordination of two alkyne molecules as acetylide and vinylidene ligands. Nucleophilic (intramolecular) attack of the acetylide on the electrophilic vinylidene carbon followed by protonation of the resulting η^3-butenynyl or η^1-(ethynyl)alkenyl complex by another alkyne molecule liberates the enyne product and regenerates the initial species (Scheme 7). In principle, both piano-stool and octahedral Ru(II) complexes may participate in such a catalytic cycle. However, based on collected evidence, η^6-arene species are short-lived for **1** and **3** while they might become important in the early stages of the process mediated by **2**. Moreover, the selectivity for the dimerization process increases over time with **1b** as a pre-catalyst (Table 3). Therefore, it could be hypothesized that the observed switch in selectivity (dimerization *vs.* trimerization) reflects a different pathway of activation of the pre-catalyst, which depends on the arene and isocyanide ligands and the solvent.

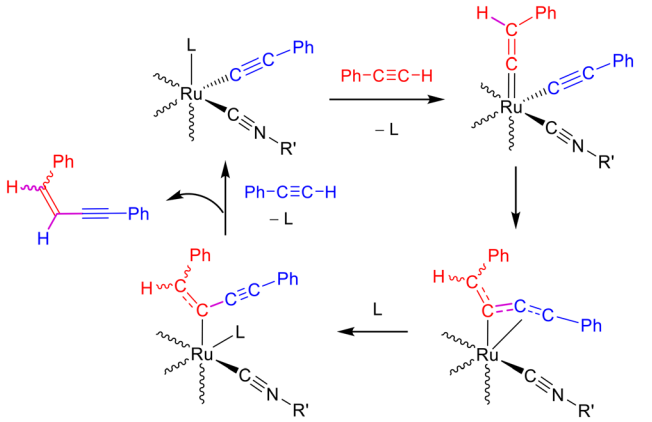

Scheme 7 Proposed general catalytic cycle for phenylacetylene dimerization based on the literature (L = Cl^-, solvent or other ligands).

2.4. Comparison with the literature

There is an extensive catalogue of ruthenium complexes applied as catalysts for the coupling/dimerization/trimerization of phenylacetylene and other terminal alkynes.[25d,48,49] but only a few of these feature an η^6-arene ligand. The halido-bridged dimers $[RuX_2(\eta^6\text{-arene})]_2$ (X = Cl; arene = C_6H_6, *p*-cymene, 1,3,5-$C_6H_3Me_3$, C_6Me_6, X = I, arene = *p*-cymene; Fig. 8a)[50,51] promote the dimerization of terminal aryl alkynes in acetic acid or acetic acid/water 1 : 1 as a solvent at room temperature with 5 mol% of catalyst load, corresponding to 10 mol% Ru. Specifically, $[RuCl_2(\eta^6\text{-arene})]_2$ (arene = *p*-cymene, C_6Me_6) achieved 60–86% yield for the dimerization of phenylacetylene and a range of substituted alkynes after 24 h, and consistently maintained high selectivity (usually > 90%) towards the *E* (*trans*) dimer. The *in situ* formed $[RuCl(\kappa^2O\text{-}O_2CCH_3)(\eta^6\text{-arene})]$[41,51] (arene = *p*-cymene, C_6Me_6; Fig. 8b) were identified as the catalytically active species. Under our conditions (Table 4), $[RuCl_2(p\text{-cymene})]_2$, $[RuCl_2(C_6H_6)]_2$ and $[RuCl(O_2CCH_3)(p\text{-cymene})]$ (2.5 mol%) produced a modest PhCCH conversion and favored phenylacetylene trimerization rather than dimerization. $[RuCl_2(\eta^6\text{-}C_6Me_6)]_2$ was more active and more selective for the dimerization process but still less effective than most of the isocyanide derivatives.

A few piano-stool ruthenium(II) η^6-arene complexes bearing different monodentate ligands such as NHC carbenes,[52,53] phosphanes[54,55] or an imine[56] (Fig. 8c–e) have been investigated for dimerization/trimerization of terminal alkynes. The protocols involved the use of organic solvents (toluene,[52,54,56] acetonitrile,[53] and 1,2-dichloroethane[55]), high (5–10%) Ru loading,[53–55] high amounts (20–25%) of base or other additives (Et_3N,[53,56] NH_4PF_6,[55] and phosphanes[54]) and/or inert atmosphere.[54–56] These conditions represent an increase in the environmental impact, costs and operational aspects compared to the methodology reported here (water, Na_2CO_3 10 mol%, Ru 2.5 mol%, and in air). The N-heterocyclic carbene complexes[53] (one example of which is shown in Fig. 8d) predominantly favored trimer formation (58–81% selectivity) in MeCN at 70 °C with 25 mol% Et_3N, whereas **1b** herein reported preferentially dimerizes phenylacetylene in both acetonitrile as a solvent (Table 1) or in water with triethylamine (Fig. 4). Özgün *et al.* applied $[RuCl_2(p\text{-cymene})]_2$ (4 mol% corresponding to 8 mol% Ru) for the selective cyclotrimerization of a range of terminal alkynes (80–99% yields) in toluene at 80 °C and studied the switchability between dimerization and cyclotrimerization of phenylacetylene using $[RuCl_2(p\text{-cymene})]_2$ by adding PCy_3 or P^iPr_3.[54] By progressively increasing the phosphine to $[RuCl_2(p\text{-cymene})]_2$ ratio up to 40 : 1, the reaction switched from cyclotrimerization to dimerization (90% selectivity). These results were related to the initial formation of $[RuCl_2(PR_3)(p\text{-cymene})]$ (Fig. 8e) followed by *p*-cymene displacement and the formation of the vinylidene derivative $[RuCl_2(PR_3)_2\{{=}C{=}C(H)Ph\}]$.

3. Conclusions

Ruthenium(II) η^6-arene isocyanide complexes are a versatile class of compounds offering structural variability in terms of arene, halide and isocyanide ligands, a simple and straightforward synthesis, air-stability, good solubility in organic solvents and a peculiar reactivity, which makes them effective catalysts for the dimerization/trimerization of terminal alkynes.

Herein, a panel of fifteen $[RuX_2(CNR)(arene)]$ (X = Cl, I) derivatives were prepared in 80–98% yields from the readily available isocyanide and halide-bridged arene precursors.

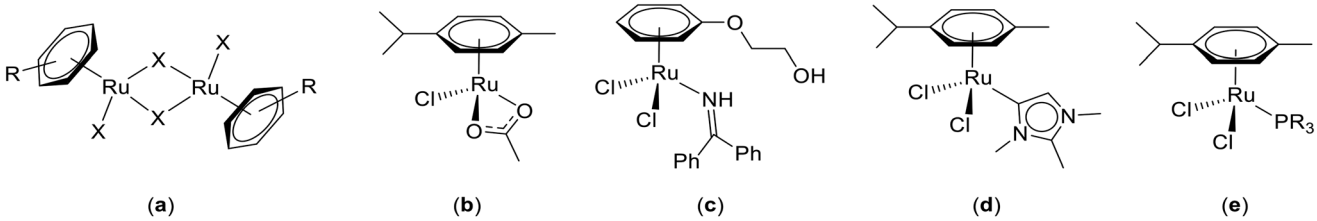

Fig. 8 Previously-investigated η^6-arene ruthenium(II) complexes for the catalytic dimerization or trimerization of alkynes: halide-bridged arene dimers (X = Cl, I; arene = C_6H_6, *p*-cymene, 1,3,5-$C_6H_3Me_3$, C_6Me_6) (a) and related mononuclear acetate as active species (b); benzophenone imine derivative with a 2-hydroxyethyl functionalized arene ligand (c); abnormal N-heterocyclic carbene complex (d); phosphane derivatives (R = Ph, Cy, ^{i}Pr, formed *in situ* from $[RuCl_2(p\text{-cymene})]_2$ + PR_3) (e).

New, effective synthetic procedures were developed for preparing the elusive benzene derivatives. Aiming to investigate the reactivity of this class of underexplored ruthenium compounds, two protocols were optimized for the preparation of rare acetylide derivatives of the type $[RuCl(CCPh)(CNR)(C_6Me_6)]$ (60% yield) and unprecedented acetonitrile complexes of the type $[RuCl_2(MeCN)_3(CNR)]$ (> 98% yield).

The bis-halide isocyanide complexes behave as effective catalytic precursors for the dimerization or trimerization of phenylacetylene. Remarkably, the selectivity of the catalytic process can be controlled by several parameters such as solvent, base, Ru loading, energy source and the arene/isocyanide combination. The crucial role played by isocyanide ligands was corroborated by control catalytic experiments with the diruthenium precursors $[RuCl_2(arene)]_2$ and the carbonyl analogues $[RuCl_2(CO)(arene)]$. The best catalytic performances for the formation of enynes were achieved using $[RuCl_2(CNCy)(p\text{-cymene})]$ as a pre-catalyst. A low catalyst loading (1 mol%) and Na_2CO_3 as a base were efficient in aqueous solution, thus providing a significant step forward in process sustainability with respect to the literature. The activation of PhCCH through coordination as an alkynyl ligand and the subsequent thermal dissociation of the arene were identified as key steps in the generation of the catalytically active species. Overall, the results reported in this work encourages further investigations on this easily available and tunable class of compounds in homogeneous catalysis.

4. Experimental section

4.1. General experimental details

All reagents and solvents were obtained from Alfa Aesar, Merck, Carlo Erba or TCI Europe and were used without further purification. Isocyanides were stored at 4 °C or −20 °C; contaminated labware was treated with HCl/EtOH. Methyl isocyanide,[57] $[RuCl_2(\eta^6\text{-arene})]_2$ (arene = *p*-cymene, C_6Me_6, C_6H_6),[7,12,13] $[RuI_2(\eta^6\text{-}p\text{-cymene})]_2$ (ref. 40) and $[RuCl_2(CNR)(\eta^6\text{-}p\text{-cymene})]$ (R = Cy, **1b**; Xyl, **1f**)[21] were prepared according to the literature. The purity of methyl isocyanide was assessed by ^1H NMR ($CDCl_3$) using Me_2SO_2 as an internal standard.[58] The synthesis of $[RuCl_2(CO)(\eta^6\text{-arene})]$ (arene = *p*-cymene, C_6Me_6)[59] and the optimized preparation of $[RuCl(\kappa^2O\text{-}O_2CCH_3)(\eta^6\text{-}p\text{-cymene})]$,[60] $[RuCl_2(Py)(\eta^6\text{-}C_6H_6)]$[61] and $[RuCl_2(SMe_2)(\eta^6\text{-}C_6H_6)]$[62] are described in the SI. All preparations were carried out under N_2 using standard Schlenk techniques. Anhydrous CH_2Cl_2 and THF were obtained from an SPS 5 solvent purifier (MBraun) and were stored over 4 Å MS; MeCN and MeOH were deaerated by bubbling Ar for 30 min. All the other operations, including work-up procedures (except for **3d** and **4b**), were carried out in air with non-anhydrous solvents. Filtrations were carried out on G3 or G4 sintered-glass filters; Celite Standard Super Cel® (Alfa Aesar) was used when indicated. All the isolated complexes are free-flowing powders relatively inert to air and moisture (except **3d**), which were kept under N_2 for long term storage as a precaution. Percent reaction yields are calculated on a molar basis with respect to the precursors $[RuX_2(\eta^6\text{-arene})]_2$ and are referred to the isolated, powdered material. Carbon, hydrogen, nitrogen and sulfur (CHNS) analyses were performed on a Vario MICRO cube instrument (Elementar). Infrared spectra of solid samples (650–4000 cm^{-1} range) were recorded on a Perkin Elmer Spectrum Two spectrometer equipped with a diamond-ATR sampling accessory. IR spectra of solutions were recorded using a CaF_2 liquid transmission cell (1500–2300 cm^{-1}) on a Perkin Elmer Spectrum 100 FT-IR spectrometer. IR spectra were processed with Spectragryph.[63] NMR spectra were recorded on a YH JNM-ECZ400S instrument (JEOL) equipped with a Royal HFX Broadband probe. $CDCl_3$ stored in the dark over Na_2CO_3 was used for NMR analysis. $^{13}C\{^1H\}$ NMR spectra were recorded with 6 or 8 s relaxation time. Chemical shifts are referenced to the residual solvent peaks (^1H, ^{13}C) or to the external standard (^{31}P to 85% H_3PO_4).[64] NMR resonances were assigned with the support of ^1H–^{13}C *gs*-HSQC and *gs*-HMBC correlation experiments. Conductivity measurements were carried using an XS COND 8 instrument (cell constant = 1.0 cm^{-1}) equipped with an NT 55 temperature probe (measurements automatically adjusted to 25 °C) and calibrated using standard KCl solutions in ultrapure water. ESI-Q/TOF flow injection analyses (FIA) were carried out using a 1200 Infinity HPLC coupled to a Jet Stream ESI interface with a quadrupole-time of flight tandem mass spectrometer 6530 Infinity Q-TOF (all from Agilent Technologies). HPLC-MS grade acetonitrile was used as the mobile phase (flow rate 0.2 mL min^{-1}, total run time 3 min). Samples were weighed, dissolved in HPLC-MS grade methanol and diluted to 10 ppm prior to injection (injection volume: 0.1 μL). ESI operating conditions: drying gas (N_2, purity >98%): 350 °C and 10 L min^{-1}; capillary voltage 4.5 kV; nozzle voltage: 1 kV; nebulizer gas 35 psig; sheath gas (N_2, purity >98%): 375 °C and 11 L min^{-1}. The fragmentor was kept at 50 V, the skimmer at 65 V and the OCT 1 RF at 750 V. High resolution MS spectra were obtained in positive mode in the range 100–1700 *m*/*z*; the mass axis was calibrated using the Agilent tuning mix HP0321 (Agilent Technologies) prepared in acetonitrile and water.

4.2. Synthesis and characterization of *p*-cymene and hexamethylbenzene isocyanide complexes

Procedure A. In a 25 mL Schlenk tube under N_2, a solution of $[RuCl_2(\eta^6\text{-arene})]_2$ (arene = *p*-cymene, C_6Me_6) (80–150 mg) in anhydrous CH_2Cl_2 (6–8 mL) was treated with the selected isocyanide (1.0–1.1 eq.). The brick red/orange mixture was stirred for 1–3 h at room temperature. The conversion was checked by IR (CH_2Cl_2) then the resulting orange-red suspension was filtered over celite. The filtrate was taken to dryness under vacuum, and the

residue was triturated with a Et_2O/hexane 1 : 1 v/v mixture (2 : 1 v/v for **1d** and **2d**) and stirred at room temperature for some time. Next, the suspension was filtered and the resulting orange (**1b–f**, **2a–d**, **2f**, **3b**, **3d**, and **3f**) or orange-brownish (**1g**) solid was washed with Et_2O/hexane 1 : 1 v/v and hexane and then dried under vacuum (40 °C). Minor variations were adopted for **1a** (specified below). The filtration step is fundamental to remove a dark brown solid (by-product); otherwise samples have a brownish shade and a lower CHN content, despite showing no impurities in ^{1}H and ^{13}C NMR spectra.

Procedure B. The reactions were carried out as described above using deaerated MeCN as a solvent (*ca.* 8–10 mL) at room temperature, unless otherwise specified.

Compounds [$RuCl_2$(CNR)(η^6-*p*-cymene)] (R = Cy, **1b**; R = Xyl, **1f**) were prepared on a 300–500 mg scale (10 mL solvent) according to both procedures, as previously reported.[21]

[$RuCl_2$(CNMe)(η^6-*p*-cymene)], 1a (Chart 1). Prepared according to procedure A using [$RuCl_2(\eta^6$-*p*-cymene)]$_2$, methyl isocyanide (1.0 eq. *vs.* Ru) and CH_2Cl_2; reaction time: 24 h. The selective formation of the title compound faces challenges related to the quinoline impurity in methyl isocyanide[58] and the consequent difficulty in adding a stoichiometric amount of the reactant. Reactions carried out with a sub-stoichiometric amount of isocyanide lead to the formation of ruthenium–quinoline by-products, while those carried out with an excess of isocyanide lead to the partial formation of *trans*-[$RuCl_2(MeNC)_4$].[15a] Only the former impurity can be effectively removed by silica chromatography, while washing the solid products with Et_2O, toluene, *etc.* is ineffective in any case. The two reaction types are described below.

Reaction #1. [$RuCl_2(\eta^6$-*p*-cymene)]$_2$ (263 mg, 0.859 mmol Ru), methyl isocyanide (60 μL, 1.00 mmol if pure) and CH_2Cl_2 (15 mL). The reaction mixture was transferred on top of a silica column (*h* 4 cm, *d* 2.3 cm). Impurities were eluted with CH_2Cl_2, and then a brown-orange band was eluted with acetone. Volatiles were removed under vacuum. The residue was dissolved in CH_2Cl_2 and filtered over celite. The filtrate was taken to dryness under vacuum, and the resulting orange-red solid was triturated with Et_2O. The suspension was filtered and the solid was washed with Et_2O and hexane and was dried under vacuum. Yield: 225 mg, 75%.

Reaction #2. [$RuCl_2(\eta^6$-*p*-cymene)]$_2$ (80 mg, 0.261 mmol Ru), methyl isocyanide (60 μL, 0.25 mmol if pure) and CH_2Cl_2 (10 mL) resulted in a bright red reaction mixture. A subsequent workup, as per procedure A, gave an orange-pink solid. Yield: 82 mg of a **1a**:*trans*-[$RuCl_2(MeNC)_4$] ≈ 15 mol mol^{-1} mixture; ^{1}H NMR ($CDCl_3$). Compound **1a** is soluble in CH_2Cl_2, insoluble in Et_2O, toluene, and hexane. X-ray quality crystals of **1a** were obtained from a CH_2Cl_2 solution layered with diethyl ether and settled aside at −20 °C. Anal. calcd. for $C_{12}H_{17}Cl_2NRu$: C: 41.51; H: 4.93; N: 4.03. Found: C: 41.58; H: 5.11; N: 4.20. IR (solid state): $\tilde{\nu}$/cm^{-1} = 3058w-sh, 3041w, 3032w, 2969w, 2962w, 2937w, 2872w, 2213s (C≡N), 1532w, 1509w-sh, 1470m, 1443m, 1414–1409m, 1385m, 1374m, 1330w, 1314w, 1299w, 1284w, 1262w, 1202w, 1164w, 1142w, 1086m, 1069m, 1058m, 1034m, 961w, 925w, 914w-sh, 872m, 853m, 802m, 787m, 698w, 671w. IR (CH_2Cl_2): $\tilde{\nu}$/cm^{-1} = 2218 s (C≡N). ^{1}H NMR ($CDCl_3$): δ/ppm = 5.61 (d, $^3J_{HH}$ = 5.9 Hz, 2H, C^4H), 5.43 (d, $^3J_{HH}$ = 5.9 Hz, 2H, C^3H), 3.62 (s, 3H, C^9H), 2.86 (hept, $^3J_{HH}$ = 6.9, C^6H), 2.28 (s, 3H, C^1H), 1.30 (d, $^3J_{HH}$ = 6.9 Hz, C^7H). ^{13}C{^{1}H} NMR ($CDCl_3$): δ/ppm = 139.2 (br., C^8); 107.5, 106.7 (C^2 + C^5); 87.8, 87.6 (C^3 + C^4); 31.3 (C^6), 30.9 (C^9), 22.6 (C^7), 19.0 (C^1).

trans-[$RuCl_2(MeNC)_4$] (impurity in **1a**). IR (solid state): $\tilde{\nu}$/cm^{-1} = 2178s-sh (C≡N). IR (CH_2Cl_2): $\tilde{\nu}$/cm^{-1} = 2186 m (C≡N). ^{1}H NMR ($CDCl_3$): δ/ppm = 3.54 (s, CH_3). ^{13}C{^{1}H} NMR ($CDCl_3$): δ/ppm = 30.2 (CH_3).

[$RuCl_2${*S*-CNCH(Me)Ph}(η^6-*p*-cymene)], 1c (Chart 2). Prepared according to procedure A using [$RuCl_2(\eta^6$-*p*-cymene)]$_2$ (149 mg, 0.480 mmol Ru) and (*S*)-(−)-α-methylbenzyl isocyanide (70 μL, 0.52 mmol); reaction time: 1 h; yield: 210 mg, 98%. The previously-reported preparation involves the use of excess isocyanide (3.1 eq.) in refluxing hexane (70 °C) for 12 h followed by recrystallization from CH_2Cl_2/petroleum ether (89% yield).[15g] Soluble in CH_2Cl_2, poorly soluble in Et_2O, and insoluble in hexane. X-ray quality crystals of **1c** were obtained from a CH_2Cl_2 solution layered with diethyl ether and settled aside at −20 °C. Anal. calcd. for $C_{19}H_{23}Cl_2NRu$: C, 52.18; H, 5.30; N, 3.20. Found: C, 51.49; H, 5.26; N, 3.16. IR (solid state): $\tilde{\nu}$/cm^{-1} = 3087w, 3060w, 3052w, 3030w, 2979w, 2966w, 2959w, 2928w, 2904w, 2867w, 2183s (C≡N), 1602w, 1538w, 1513w, 1495w, 1469m-sh, 1456m, 1449m, 1390w, 1377w, 1365w, 1350m, 1328w, 1308w, 1295w, 1281w, 1201w, 1159w, 1112w, 1093m, 1075m, 1058w-sh, 1029w, 993m, 972w, 922w, 907w, 879m, 809w, 763s, 738w, 697s, 676m-sh. IR (CH_2Cl_2): $\tilde{\nu}$/cm^{-1} = 2189s (C≡N). ^{1}H NMR ($CDCl_3$): δ/ppm = 7.44–7.38 (m, 4H, C^{12}H + C^{13}H); 7.36–7.32 (m, C^{14}H); 5.58 (d, $^3J_{HH}$ = 6.1 Hz), 5.56 (d, $^3J_{HH}$ = 6.1 Hz), 5.43

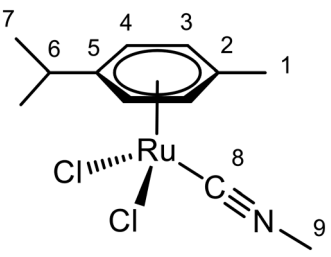

Chart 1 Structure of **1a** (numbering refers to carbon atoms).

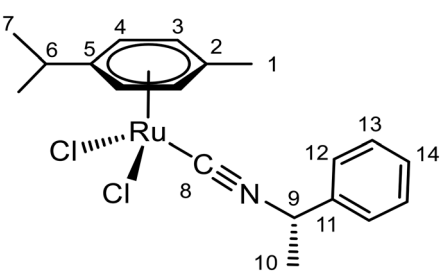

Chart 2 Structure of **1c** (numbering refers to carbon atoms).

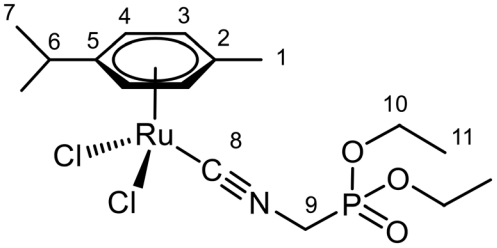

Chart 3 Structure of **1d** (numbering refers to carbon atoms).

(d, $^3J_{HH}$ = 6.0 Hz), 5.41 (d, $^3J_{HH}$ = 5.9 Hz), 5.20 (q, $^3J_{HH}$ = 6.7 Hz, C^9H), 2.77 (hept, $^3J_{HH}$ = 6.9 Hz, C^6H), 2.27 (s, 3H, C^1H), 1.77 (d, $^3J_{HH}$ = 6.8 Hz, $C^{10}H$); 1.24, 1.23 (d, $^3J_{HH}$ = 6.9 Hz, 6H, C^7H). $^{13}C\{^1H\}$ NMR ($CDCl_3$): δ/ppm = 141.2 (br, C^8), 138.1 (C^{11}), 129.3 (C^{12}), 128.8 (C^{14}), 125.7 (C^{13}), 107.7 (C^5), 107.3 (C^2); 88.1, 88.0, 87.7, 87.6 (C^3 + C^4); 57.2 (C^9), 31.4 (C^6), 25.0 (C^{10}); 22.58, 22.54 (C^7); 18.9 (C^1).

[$RuCl_2${$CNCH_2PO(OEt)_2$}(η^6-*p*-cymene)], 1d (Chart 3). Prepared according to procedure A using [$RuCl_2(\eta^6$-*p*-cymene)]$_2$ (82 mg, 0.27 mmol Ru) and diethyl isocyanomethyl phosphonate (44 μL, 0.27 mmol); reaction time: 3 h; yield: 110 mg, 85%. Alternatively prepared from [$RuCl_2(\eta^6$-*p*-cymene)]$_2$ (106 mg, 0.346 mmol Ru) and diethyl isocyanomethyl phosphonate (58 μL, 0.36 mmol) according to procedure B; reaction time: 3 h; yield: 143 mg, 86%. Soluble in CH_2Cl_2 and MeCN, poorly soluble in Et_2O, and insoluble in hexane. Anal. calcd. for $C_{16}H_{26}Cl_2NO_3PRu$: C, 39.76; H, 5.42; N, 2.90. Found: C, 38.45; H, 5.39; N, 2.86. IR (solid state): $\tilde{\nu}$/cm^{-1} = 3054w, 3033w, 2971w, 2960w, 2909w, 2872w-sh, 2207s (C≡N), 2131w-sh, 1539w, 1498w, 1469m, 1442w, 1402w, 1388m, 1326w, 1272s (P═O), 1212w, 1202w, 1162m, 1095m-sh, 1050s-sh, 1026s, 976s, 967s-sh, 880m, 845w, 784m, 706w, 693w. IR (CH_2Cl_2): $\tilde{\nu}$/cm^{-1} = 2198 (C≡N). IR (MeCN): $\tilde{\nu}$/cm^{-1} = 2199 (C≡N). ^1H NMR ($CDCl_3$): δ/ppm = 5.65 (d, $^3J_{HH}$ = 6.1 Hz, 2H, C^4H), 5.46 (d, $^3J_{HH}$ = 6.1 Hz, 2H, C^3H), 4.31–4.24 (m, 4H, $C^{10}H$), 4.22 (d, $^2J_{HP}$ = 15.1 Hz, 2H, C^9H), 2.90 (hept, $^3J_{HH}$ = 6.8 Hz, 1H, C^6H), 2.28 (s, 3H, C^1H), 1.39 (t, $^3J_{HH}$ = 7.0 Hz, $C^{11}H$), 1.29 (d, $^3J_{HH}$ = 6.9 Hz, C^7H). $^{13}C\{^1H\}$ NMR ($CDCl_3$): δ/ppm = 144.6 (br., C^8), 108.6 (C^5), 107.6 (C^2), 88.5 (C^4), 88.3 (C^3), 64.5 (d, $^2J_{CP}$ = 6.6 Hz, C^{10}), 40.7 (d, $^1J_{CP}$ = 153.7 Hz, C^9), 31.3 (C^6), 22.6 (C^7), 18.9 (C^1), 16.6 (d, $^3J_{CP}$ = 5.7 Hz, C^{11}). $^{31}P\{^1H\}$ NMR ($CDCl_3$): δ/ppm = 13.8.

[$RuCl_2${$CNCH_2CO_2Et$}(η^6-*p*-cymene)], 1e (Chart 4). Prepared according to procedure A using [$RuCl_2(\eta^6$-*p*-cymene)]$_2$ (83 mg, 0.27 mmol Ru) and ethyl isocyanoacetate (32 μL, 0.29 mmol); reaction time: 1 h; yield: 104 mg, 91%. Alternatively prepared from [$RuCl_2(\eta^6$-*p*-cymene)]$_2$ (104 mg, 0.340 mmol Ru) and ethyl isocyanoacetate (38 μL, 0.35 mmol) according to procedure B; reaction time: 3 h; yield: 124 mg, 87%. The previously-reported preparation involves a prolonged reaction time (20 h) and purification *via* silica gel chromatography followed by crystallization (28% yield).[15b] Soluble in CH_2Cl_2 and MeCN and insoluble in Et_2O and hexane. X-ray quality crystals of **1e**·CH_2Cl_2 were obtained from a CH_2Cl_2 solution layered with hexane and settled aside at −20 °C. Anal. calcd. for $C_{15}H_{21}Cl_2NO_2Ru$: C: 42.97; H: 5.05; N: 3.34. Found: C: 42.05; H: 4.99; N: 3.30. IR (solid state): $\tilde{\nu}$/cm^{-1} = 3057w, 2066w, 2893w, 2831w, 2196s (C≡N), 1753s (C═O), 1472m-sh, 1500w, 1467w, 1444w, 1427w, 1388w-sh, 1376m, 1351w, 1295w, 1280w, 1253w, 1206s-br, 1166m-sh, 1118w, 1096w, 1060w, 1041m, 1003w, 948w, 928w, 895w, 957m, 795w, 704w. IR (CH_2Cl_2): $\tilde{\nu}$/cm^{-1} = 2205 (C≡N); 1759s, 1750sh (C═O). IR (MeCN): $\tilde{\nu}$/cm^{-1} = 2206 (C≡N); 1761s, 1750s (C═O). ^1H NMR ($CDCl_3$): δ/ppm = 5.68 (d, $^3J_{HH}$ = 6.1 Hz, 2H, C^4H), 5.48 (d, $^3J_{HH}$ = 6.0 Hz, 2H, C^3H), 4.63 (s, 2H, C^9H), 4.32 (q, $^3J_{HH}$ = 7.2 Hz, 2H, $C^{11}H$), 2.96 (hept, $^3J_{HH}$ = 6.9 Hz, 1H, C^6H), 2.32 (s, 3H, C^1H), 1.35 (t, $^3J_{HH}$ = 7.2 Hz, 3H, $C^{12}H$), 1.31 (d, $^3J_{HH}$ = 6.9 Hz, 6H, C^7H). $^{13}C\{^1H\}$ NMR ($CDCl_3$): δ/ppm = 164.3 (C^{10}), 146.4 (br, C^8), 109.1 (C^5), 107.7 (C^2); 88.7, 88.3 (C^3 + C^4); 63.3 (C^{11}), 46.6 (C^9), 31.3 (C^6), 22.6 (C^7), 19.0 (C^1), 14.2 (C^{12}).

[$RuCl_2${$CN(4\text{-}C_6H_4OMe)$}(η^6-*p*-cymene)], 1g (Chart 5). Prepared according to procedure A using [$RuCl_2(\eta^6$-*p*-cymene)]$_2$ (73 mg, 0.24 mmol Ru) and 4-methoxyphenyl isocyanide (33 mg, 0.25 mmol); reaction time: 1 h; yield: 95 mg, 91%. Soluble in CH_2Cl_2, poorly soluble in Et_2O, and insoluble in hexane. Anal. calcd. for $C_{18}H_{21}Cl_2NORu$: C, 49.21; H, 4.82; N, 3.19. Found: C, 49.08; H, 4.80; N, 3.11. X-ray quality crystals of **1g**·$CHCl_3$ were obtained from a $CHCl_3$ solution layered with hexane and settled aside at −20 °C. IR (solid state): $\tilde{\nu}$/cm^{-1} = 3068w, 3037w, 3006w, 2959s, 2926w, 2872w, 2840w, 2167s (C≡N), 1601s, 1581w, 1503s, 1465m, 1443m, 1242w, 1405w, 1386m, 1377m, 1323w, 1302m, 1253s, 1201m, 1182m, 1161m, 1117w, 1107m, 1090m, 1058m, 1028s, 922w, 878w, 849m, 831s, 810m, 798m-sh, 726w, 706w, 694w, 670w.

IR (CH_2Cl_2): $\tilde{\nu}$/cm^{-1} = 2168 (C≡N). ^1H NMR ($CDCl_3$): δ/ppm = 7.38 (d, $^3J_{HH}$ = 8.9 Hz, 1H), 6.88 (d, $^3J_{HH}$ =

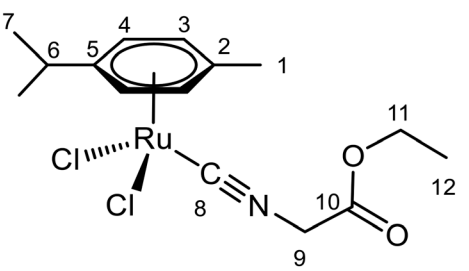

Chart 4 Structure of **1e** (numbering refers to carbon atoms).

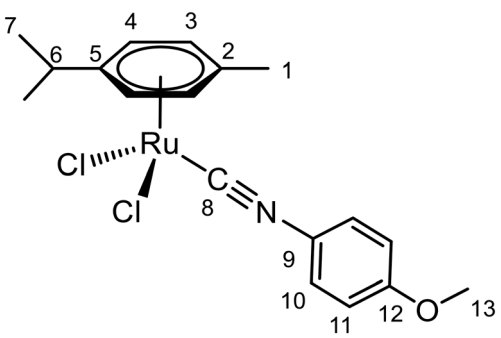

Chart 5 Structure of **1g** (numbering refers to carbon atoms).

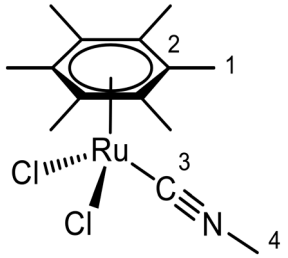

Chart 6 Structure of **2a** (numbering refers to carbon atoms).

8.9 Hz, 1H), 5.69 (d, $^3J_{HH}$ = 6.0 Hz, 1H), 5.51 (d, $^3J_{HH}$ = 6.0 Hz, 1H), 3.83 (s, 3H), 2.91 (hept, $^3J_{HH}$ = 7.1 Hz, 1H), 2.35 (s, 3H), 1.34 (d, $^3J_{HH}$ = 6.9 Hz, 6H). $^{13}C\{^1H\}$ NMR ($CDCl_3$): δ/ppm = 160.5 ($C^{12}O$), 147.4 (br, C^8N), 128.3 (C^{10}), 120.3 (C^9), 114.8 (C^{11}), 108.6 (C^5), 108.0 (C^2); 88.53, 88.49 (C^3 + C^4); 55.8 ($C^{13}O$), 31.5 (C^6), 22.7 (C^7), 19.1 (C^1).

[$RuCl_2$(CNMe)(η^6-C_6Me_6)], 2a (Chart 6). Prepared according to procedure A using [$RuCl_2(\eta^6$-$C_6Me_6)]_2$ (87 mg, 0.26 mmol Ru) and methyl isocyanide (70 μL, *ca.* 0.3 mmol);[58] reaction time: 1 h; yield: 92 mg, 94%. Differently from **1a**, a reaction carried out with a slight excess of isocyanide in refluxing CH_2Cl_2 selectively afforded **2a**, without any [$RuCl_2(MeNC)_4$] by-product. Soluble in CH_2Cl_2 and insoluble in Et_2O/hexane mixtures and hexane. Anal. calcd. for $C_{18}H_{21}Cl_2NORu$: C, 44.80; H, 5.64; N, 3.73. Found: C, 43.10; H, 5.43; N, 3.72. IR (solid state): $\tilde{\nu}$/cm^{-1} = 3033–2993w, 2939w, 2198s (C≡N), 1446m, 1416m, 1386m, 1066m, 1014m, 960w, 817w, 785w. IR (CH_2Cl_2): $\tilde{\nu}$/cm^{-1} = 2200 s (C≡N). ^1H NMR ($CDCl_3$): δ/ppm = 3.61 (s, 3H, C^4H), 2.14 (s, 18H, C^1H). $^{13}C\{^1H\}$ NMR ($CDCl_3$): δ/ppm = 144.3 (C^3), 98.1 (C^2), 30.9 (C^4), 16.1 (C^1).

[$RuCl_2$(CNCy)(η^6-C_6Me_6)], 2b (Chart 7). Prepared according to procedure A using [$RuCl_2(\eta^6$-$C_6Me_6)]_2$ (82 mg, 0.25 mmol Ru) and cyclohexyl isocyanide (33 μL, 0.27 mmol); reaction time: 2 h; yield: 99 mg, 91%. Alternatively prepared from [$RuCl_2(\eta^6$-$C_6Me_6)]_2$ (275 mg, 0.822 mmol Ru) and cyclohexyl isocyanide (102 μL, 0.820 mmol) according to procedure B; reaction time: 3 h; yield: 326 mg, 90%. The previously-reported preparation involves excess isocyanide (10 eq.), prolonged reaction time (20 h) and purification *via* silica gel chromatography (59% yield).[15b] Compound **2b** is soluble in CH_2Cl_2 and insoluble in hexane. Anal. calcd. for $C_{19}H_{29}Cl_2NRu$: C, 51.47; H, 6.59; N, 3.16. Found: C, 50.75; H, 6.62; N, 3.12. IR (solid state): $\tilde{\nu}$/cm^{-1} = 2960w, 2939w, 2917m, 2857m, 2159s (C≡N), 1523w, 1540m, 1437m, 1379m, 1360m-sh, 1353m, 1314m, 1269w, 1240w, 1154w, 1128w, 1067m, 1025m, 1007m, 933w, 866w, 658m. IR (CH_2Cl_2): $\tilde{\nu}$/cm^{-1} = 2175 (C≡N). ^1H NMR ($CDCl_3$): δ/ppm = 3.94 (td, $^3J_{HH}$ = 8.5, 4.0 Hz, 1H, C^4H); 2.12 (s, 18H, C^1H); 2.06–1.97 (m, 2H), 1.84–1.70 (m, 4H), 1.58–1.46 (m, 1H), 1.44–1.32 (m, 3H) (C^5H + C^6H + C^7H); no changes were observed in the ^1H NMR spectrum after several days at −20 °C. $^{13}C\{^1H\}$ NMR ($CDCl_3$): δ/ppm = 143.4 (br., C^3), 97.8 (C^2), 55.2 (C^4), 33.3 (C^5), 24.9 (C^7), 23.3 (C^6), 16.0 (C^1).

[$RuCl_2${*S*-CNCH(Me)Ph}(η^6-C_6Me_6)], 2c (Chart 8). Prepared according to procedure A using [$RuCl_2(\eta^6$-$C_6Me_6)]_2$ (81 mg, 0.24 mmol Ru) and (*S*)-(−)-α-methylbenzyl isocyanide (35 μL, 0.26 mmol); reaction time: 1.5 h; yield: 98 mg, 86%. Soluble in CH_2Cl_2 and insoluble in Et_2O and hexane. Needle-shaped X-ray quality crystals of **2c**·H_2O were obtained from a CH_2Cl_2 solution layered with hexane and settled aside at −20 °C. The water molecule in the crystal structure probably originates from the residual water content of the organic solvents used for crystallization since the isolated powder of **2c** does not contain water (CHN analyses) and is not hygroscopic. Anal. calcd. for $C_{21}H_{27}Cl_2NRu$: C, 54.19; H, 5.85; N, 3.01. Found: C, 53.77; H, 5.75; N, 2.94. IR (solid state): $\tilde{\nu}$/cm^{-1} = 3056w, 2997w, 2985w, 2935w, 2890w, 2872w, 2167s (C≡N), 1601w, 1496w, 1449m, 1380m, 1338m, 1315w-sh, 1228w, 1195w, 1156w, 1097w-sh, 1068m, 1031m, 1009m, 917w, 850w, 778s, 740s, 700s. IR (CH_2Cl_2): $\tilde{\nu}$/cm^{-1} = 2169 s (C≡N). ^1H NMR ($CDCl_3$): δ/ppm = 7.47–7.32 (m, 5H, Ph), 5.17 (q, $^3J_{HH}$ = 6.7 Hz, 1H, C^4H), 2.06 (s, 18H, C^1H), 1.77 (d, $^3J_{HH}$ = 6.8 Hz, 3H, C^5H). $^{13}C\{^1H\}$ NMR ($CDCl_3$): δ/ppm = 146.3 (br. C^3), 138.9 (C^6), 129.2 (C^7), 128.8 (C^9), 125.9 (C^8), 98.3 (C^2), 56.9 (C^4), 24.7 (C^5), 16.0 (C^1).

[$RuCl_2${$CNCH_2PO(OEt)_2$}(η^6-C_6Me_6)], 2d (Chart 9). Prepared according to procedure A using [$RuCl_2(\eta^6$-$C_6Me_6)]_2$ (52 mg, 0.16 mmol Ru) and diethyl isocyanomethyl phosphonate (30 μL, 0.19 mmol); reaction time: 3 h; yield: 70 mg, 88%. Alternatively prepared from [$RuCl_2(\eta^6$-$C_6Me_6)]_2$ (81 mg, 0.24 mmol Ru) and diethyl isocyanomethyl phosphonate (46 μL, 0.29 mmol) according to procedure B; reaction time: 2.5 h; yield: 109 mg, 88%. Soluble in CH_2Cl_2 and MeCN and insoluble in Et_2O and hexane. Anal. calcd.

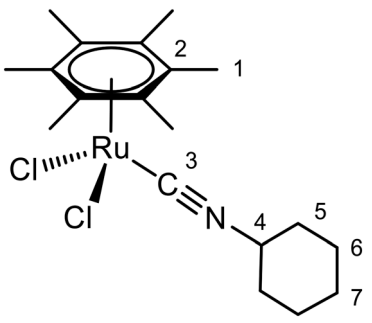

Chart 7 Structure of **2b** (numbering refers to carbon atoms).

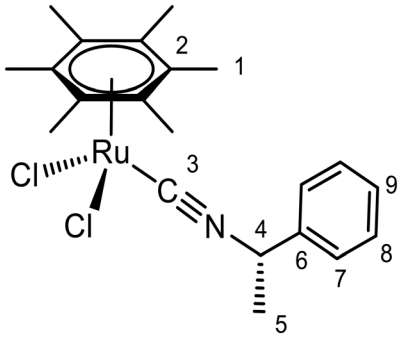

Chart 8 Structure of **2c** (numbering refers to carbon atoms).

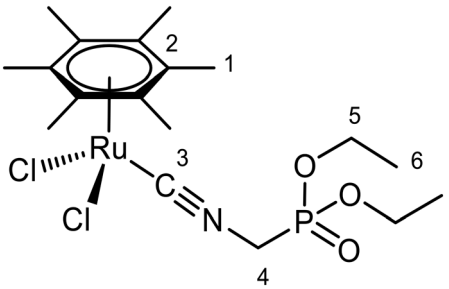

Chart 9 Structure of **2d** (numbering refers to carbon atoms).

for $C_{18}H_{30}Cl_2NO_3PRu$: C, 42.28; H, 5.91; N, 2.74. Found: C, 41.56; H, 5.86; N, 2.69. IR (solid state): $\tilde{\nu}/cm^{-1}$ = 2995w, 2983w, 2974w, 2954w, 2934w, 2920w, 2182s (C≡N), 1484w, 1456w, 1441w, 1398m, 1390m, 1371m-sh, 1291m-sh, 1271s (P═O), 1247w-sh, 1216w, 1160w, 1150w, 1102w, 1070w-sh, 1042s-sh, 1020s, 982s, 964s, 852m, 820w-sh, 792s, 774m, 719w. IR (CH_2Cl_2): $\tilde{\nu}/cm^{-1}$ = 2180s (C≡N). IR (MeCN): $\tilde{\nu}/cm^{-1}$ = 2181 s (C≡N). ^1H NMR ($CDCl_3$): δ/ppm = 4.31–4.22 (m, 4H, C^5H), 4.16 (d, $^1J_{HP}$ = 15 Hz, 2H, C^4H), 2.14 (s, 18H, C^1H), 1.39 (t, $^3J_{HH}$ = 7.1 Hz, C^6H). $^{13}C\{^1H\}$ NMR ($CDCl_3$): δ/ppm = 149.6 (br, C^3), 99.1 (s, C^2), 64.3 (d, $^2J_{CP}$ = 7 Hz, C^5), 40.6 (d, $^1J_{CP}$ = 154 Hz, C^4), 16.6 (d, $^3J_{CP}$ = 6 Hz, C^6), 16.0 (s, C^1). $^{31}P\{^1H\}$ NMR ($CDCl_3$): δ/ppm = 14.7.

[$RuCl_2$(CNXyl)(η^6-C_6Me_6)], 2f (Chart 10). Prepared according to procedure A using $[RuCl_2(\eta^6\text{-}C_6Me_6)]_2$ (62 mg, 0.19 mmol Ru) and xylyl isocyanide (25 mg, 0.19 mmol); reaction time: 3 h; yield: 73 mg, 84%. Alternatively prepared according to procedure B using $[RuCl_2(\eta^6\text{-}C_6Me_6)]_2$ (105 mg, 0.314 mmol Ru) and xylyl isocyanide (43 mg, 0.32 mmol); reaction temperature/time: 45 °C, 3.5 h. Yield: 124 mg, 85%. The reaction in MeCN at room temperature is very slow. Compound **2f** is soluble in CH_2Cl_2 and insoluble in Et_2O and hexane. Anal. calcd. for $C_{21}H_{27}Cl_2NRu$: C, 54.19; H, 5.85; N, 3.01. Found: C, 53.65; H, 5.54; N, 3.01. IR (solid state): $\tilde{\nu}/cm^{-1}$ = 2981w, 2914w, 2128s (C≡N), 1526-1488w, 1462m, 1438m, 1377m, 1264w, 1185w, 1162w, 1091w, 1067m, 1029w, 1007m, 975w, 921w, 897w, 814w, 777s, 738m, 718m, 667m. IR (CH_2Cl_2): $\tilde{\nu}/cm^{-1}$ = 2141 (C≡N). ^1H NMR ($CDCl_3$): δ/ppm = 7.14 (dd, $^3J_{HH}$ = 8.6, 6.4 Hz, 1H, C^8H); 7.07 (d, $^3J_{HH}$ = 7.4 Hz, 2H, C^7H); 2.45 (s, 6H, C^6H); 2.19 (s, 18H, C^1H). $^{13}C\{^1H\}$ NMR ($CDCl_3$): δ/ppm = 157.3 (br., C^3), 135.6 (C^5), 128.7 (C^8), 127.9 (C^7), 127.8 (sh., C^4), 99.2 (C^2), 19.3 (C^1), 16.2 (C^6).

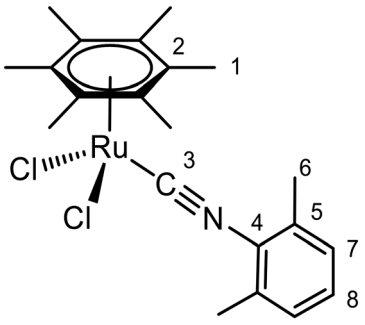

Chart 10 Structure of **2f** (numbering refers to carbon atoms).

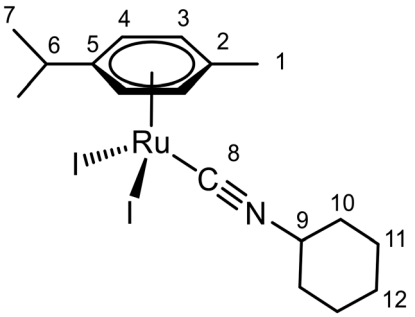

Chart 11 Structure of **1b-I** (numbering refers to carbon atoms).

[RuI_2{CN(C_6H_{11})}(η^6-*p*-cymene)], 1b-I (Chart 11). In a 25 mL Schlenk tube under N_2, a violet-red solution of $[RuI_2(\eta^6\text{-}p\text{-cymene})]_2$ (102 mg, 0.209 mmol Ru) and cyclohexyl isocyanide (28 μL, 0.23 mmol) in anhydrous CH_2Cl_2 (4 mL) was stirred for 1 h at reflux temperature. The conversion was checked by IR (CH_2Cl_2) and then the resulting violet-red suspension was filtered over celite. The filtrate was taken to dryness under vacuum and the residue was triturated in hexane and stirred at room temperature for some time. Next, the suspension was filtered and the resulting purple red-violet solid was washed with hexane and dried under vacuum (40 °C). Yield: 114 mg, 91%. Soluble in MeCN and CH_2Cl_2, poorly soluble in Et_2O, and insoluble in hexane. X-ray quality crystals of **1b-I** were obtained from an acetone solution layered with a diethyl ether/hexane mixture and settled aside at −20 °C. Anal. calcd. for $C_{17}H_{25}I_2NRu$: C, 34.19; H, 4.21; N, 2.34. Found: C, 33.97; H, 4.18; N, 2.31. IR (solid state): $\tilde{\nu}/cm^{-1}$ = 3056w, 3036w, 2959w, 2933m, 2922m, 2855w, 2184s (C≡N), 1536w, 1495w, 1467w, 1444w, 1434w, 1381m, 1363m, 1352m, 1324s, 1276w, 1262w, 1241w, 1201w, 1153w, 1140w, 1128w, 1115w, 1088w, 1055m, 1021m, 998w-sh, 931w-sh, 921w, 897w, 886w, 863m, 822w, 799w, 671w, 659m. IR (CH_2Cl_2): $\tilde{\nu}/cm^{-1}$ = 2177s (C≡N). IR (MeCN): $\tilde{\nu}/cm^{-1}$ = 2177 s (C≡N). ^1H NMR ($CDCl_3$): δ/ppm = 5.61 (d, $^3J_{HH}$ = 6.1 Hz, 2H, C^4H), 5.49 (d, $^3J_{HH}$ = 6.0 Hz, 2H, C^3H), 4.09 (m, $^3J_{HH}$ = 7.3, 3.6 Hz, C^9H), 2.97 (hept, $^3J_{HH}$ = 6.9 Hz, C^6H), 2.55 (s, 3H, C^1H), 1.95–1.73 (m, 6H), 1.47–1.36 (m, 4H) ($C^{10}H$ + $C^{11}H$ + $C^{12}H$); 1.31 (d, $^3J_{HH}$ = 6.9 Hz, 6H, C^7H); no changes were observed in the ^1H NMR spectrum after several weeks at −20 °C. $^{13}C\{^1H\}$ NMR ($CDCl_3$): δ/ppm = 136.3 (br, C^8), 110.0 (C^5), 105.9 (C^2); 89.1, 87.8 (C^3 + C^4); 55.2 (C^9); 32.9, 32.1 (C^6 + C^{10}); 25.0 (C^{12}); 23.1, 22.8 (C^7 + C^{11}); 20.6 (C^1).

4.3. Synthesis and characterization of benzene isocyanide complexes

Procedure C. In a 25 mL Schlenk tube under N_2, an orange-brown suspension of $[RuCl_2(SMe_2)(\eta^6\text{-}C_6H_6)]$ (90–200 mg) in anhydrous CH_2Cl_2 (8–10 mL) was treated with the appropriate isocyanide (1.0–1.1 eq.) and was stirred at reflux for 1–2.5 h. The conversion was checked by IR (CH_2Cl_2) and

then the resulting mixture (red solution + orange solid) was cooled to room temperature and filtered over a celite pad (3–4 cm), to remove a dark brown residue. The red/brick orange filtrate was taken to dryness under vacuum and the residue was triturated with a Et_2O/THF 1 : 1 v/v mixture under stirring at room temperature for a few hours. Next, the resulting suspension (orange solid + pale yellow-greenish solution) was filtered. The orange solid was washed with Et_2O/THF 1 : 1 v/v, Et_2O, and hexane and then dried under vacuum (40 °C). The workup procedure for **3d** is slightly different (described below).

The filtration step is fundamental to remove a dark brown solid (by-product). The final solid/liquid extraction with the Et_2O/THF mixture is crucial to remove several minor by-products; in this respect, toluene, Et_2O or their mixtures with hexane are ineffective.

Procedure D. The procedure was carried out as described above, using $[RuCl_2(Py)(\eta^6\text{-}C_6H_6)]$ as a precursor and running the reaction at room temperature for 2 h.

Procedure E. In a 25 mL Schlenk tube under N_2, a brick-red suspension of $[RuCl_2(\eta^6\text{-}C_6H_6)]$ (75 mg, 0.30 mmol Ru) in anhydrous CH_2Cl_2 (6 mL) was treated with the appropriate isocyanide (1.0 eq.) and stirred at reflux for 4 h. The conversion was checked by IR (CH_2Cl_2) and then the resulting mixture (red solution + a small amount of an orange-red solid) was cooled to room temperature and filtered over celite. The filtrate was taken to dryness under vacuum. The resulting orange solid was washed with a Et_2O/hexane 2 : 1 v/v mixture and hexane and dried under vacuum (40 °C).

$[RuCl_2(CNCy)(\eta^6\text{-}C_6H_6)]$, 3b (Chart 12). The title compound was previously isolated as a 'salmon pink' solid in unknown yield from the reaction of $[RuCl_2(\eta^6\text{-}C_6H_6)]_2$ and cyclohexyl isocyanide (10 eq.) in refluxing benzene; elemental analyses (CHNCl) and partial ^{1}H NMR ($CDCl_3$) and IR (solid state) data were given.[15a]

Prepared according to procedure C using $[RuCl_2(SMe_2)(\eta^6\text{-}C_6H_6)]$ (189 mg, 0.604 mmol) and cyclohexyl isocyanide (75 μL, 0.60 mmol); reaction time: 1 h, yield: 199 mg, 91%. Alternatively prepared from $[RuCl_2(Py)(\eta^6\text{-}C_6H_6)]$ (104 mg, 0.32 mmol) and cyclohexyl isocyanide (40 μL, 0.32 mmol) according to procedure D; yield: 93 mg, 82%. Soluble in CH_2Cl_2, poorly soluble in THF and acetone, and insoluble in toluene, Et_2O, hexane, and ^{i}PrOH. Anal. calcd. for $C_{13}H_{17}Cl_2NRu$: C, 43.46; H, 4.77; N, 3.90. Found: C, 42.0; H, 4.51; N, 3.81. IR (solid state): $\tilde{\nu}$/cm^{-1} = 3077w, 3051w, 2957w-sh, 2937m, 2858w, 2219s (C≡N), 2115w, 1460w, 1445m-sh, 1429s, 1364w, 1354w, 1326m, 1272w, 1237w, 1152m, 1137w, 1127w, 1114w, 1032w, 1012w, 980w, 964s-sh, 927w, 863w, 824s, 796-761w, 732w, 697w, 663m. IR (CH_2Cl_2): $\tilde{\nu}$/cm^{-1} = 2203 s (C≡N). ^{1}H NMR ($CDCl_3$): δ/ppm = 5.81 (s, 6H, C_6H_6), 4.10–3.99 (m, 1H, C^2H); 2.02–1.89 (m, 2H, C^3H), 1.89–1.73 (m, 4H, C^3H + C^4H), 1.53–1.34 (m, 4H, C^4H + C^5H). $^{13}C\{^1H\}$ NMR ($CDCl_3$): δ/ppm = 136.1 (br., C^1), 89.3 (C_6H_6), 55.6 (C^2), 32.6 (C^3), 24.9 (C^5), 22.8 (C^4). Release of benzene is observed in the $CDCl_3$ solution of **3b** stored at room temperature (*ca.* 6% after 14 h). ^{1}H NMR (CH_3OD): δ/ppm = 5.87 (s, 6H, C_6H_6), 4.22–4.14 (m, 1H, C^2H); 1.98–1.88, 1.86–1.75, 1.52–1.39 (m, 10H, C^3H + C^4H + C^5H).

The reaction of $[RuCl_2(\eta^6\text{-}C_6H_6)]_2$ and cyclohexyl isocyanide, according to procedure E, gave a peach orange solid (94 mg) consisting of **3b** [IR (CH_2Cl_2): $\tilde{\nu}$ = 2203 cm^{-1}], *trans*-$[RuCl_2(CNCy)_4]$ [IR (CH_2Cl_2): $\tilde{\nu}$ = 2154 cm^{-1}][15a] and unknown isocyanide complexes [IR (CH_2Cl_2): $\tilde{\nu}$/cm^{-1} = 2114, 2061].

$[RuCl_2\{CNCH_2PO(OEt)_2\}(\eta^6\text{-}C_6H_6)]$, 3d (Chart 13). Prepared according to procedure C using $[RuCl_2(SMe_2)(\eta^6\text{-}C_6H_6)]$ (94 mg, 0.30 mmol) and diethyl isocyanomethyl phosphonate (54 μL, 0.34 mmol); reaction time: 2.5 h. The resulting dark red turbid solution was taken to dryness under vacuum. All the subsequent operations were carried out under N_2 using anhydrous solvents. The residue was triturated with Et_2O (20 mL) and the solution was discarded. Next, the solid was washed twice with a Et_2O/THF 4 : 1 v/v mixture (20 mL), as described above, and then suspended in Et_2O. The mixture was filtered (G4) and the resulting orange solid was washed with Et_2O and hexane, dried under vacuum (room temperature) and stored under N_2. Yield: 110 mg, 85%. A workup in air using non-anhydrous solvents led to extensive decomposition of the compound. Soluble in CH_2Cl_2 and $CHCl_3$, scarcely soluble in Et_2O and Et_2O/THF 5 : 1 v/v, and insoluble in hexane. IR (solid state): $\tilde{\nu}$/cm^{-1} = 3074w, 3049w, 2976w, 2958w, 2905w; 2215s, 2191s, 2127m-sh (C≡N); 1430w, 1395w, 1368w, 1280w, 1250s (P═O), 1221w, 1160w, 1098w, 1046s-sh, 1012s, 978s, 948s-sh, 857w, 823m, 794m, 776m, 715w. IR (CH_2Cl_2): $\tilde{\nu}$/cm^{-1} = 2208 s (C≡N). ^{1}H NMR ($CDCl_3$): δ/ppm = 5.87 (s, 6H, C_6H_6); 4.33–4.25 (m, 4H, C^3H), 4.21 (d, $^2J_{HP}$ = 15.2 Hz, 2H, C^2H), 1.41 (t, $^3J_{HH}$ = 7.04 Hz, 6H, C^4H). $^{13}C\{^1H\}$ NMR ($CDCl_3$): δ/ppm = 142.2 (C^1), 90.8 (+ sh.*, C_6H_6),

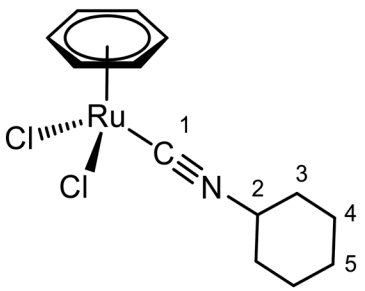

Chart 12 Structure of **3b** (numbering refers to carbon atoms).

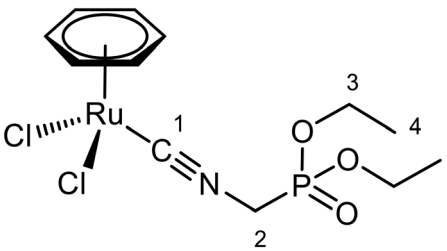

Chart 13 Structure of **3d** (numbering refers to carbon atoms).

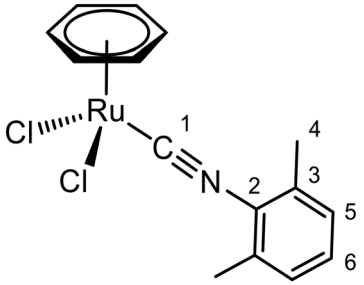

Chart 14 Structure of **3f** (numbering refers to carbon atoms).

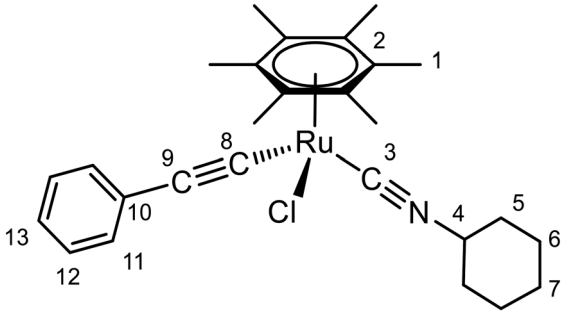

Chart 15 Structure of **4b** (numbering refers to carbon atoms).

65.1 (+ sh.*, C^3), 42.8 (br.*, C^2), 16.6 (C^4); *C_6H_6 and C^3 resonances show line broadening and a shoulder peak, the C^2 resonance is very broad and almost hidden over the baseline. $^{31}P\{^1H\}$ NMR ($CDCl_3$): δ/ppm = 13.6. Release of benzene (*ca.* 35% after 14 h) and the formation of $Ru(C_6H_6)$ by-product(s) (δ_H = 5.69 ppm, δ_C = 81.2, 64.7 ppm, δ_P = 14.9 ppm) are observed in the $CDCl_3$ solution of **3d** stored at room temperature.

[$RuCl_2$(CNXyl)(η^6-C_6H_6)], 3f (Chart 14). Prepared according to procedure C using [$RuCl_2(SMe_2)(\eta^6$-$C_6H_6)$] (204 mg, 0.653 mmol) and xylyl isocyanide (87 mg, 0.66 mmol); reaction time: 1 h, yield: 203 mg, 82%. Alternatively prepared from [$RuCl_2$(Py)(η^6-C_6H_6)] (54 mg, 0.16 mmol) and xylyl isocyanide (28 mg, 0.18 mmol) according to procedure **D**; yield: 56 mg, 90%. Soluble in CH_2Cl_2, less soluble in $CHCl_3$ and acetone, scarcely soluble in THF, and insoluble in Et_2O and hexane. Anal. calcd. for $C_{15}H_{15}Cl_2NRu$: C, 47.25; H, 3.97; N, 3.67. Found: C, 46.3; H, 3.65; N, 3.62. IR (solid state): $\tilde{\nu}$/cm^{-1} = 3070w, 3058w-sh, 2980w, 2947w, 2158s (C≡N), 1600w, 1590w, 1471m, 1435m, 1382m, 1370w-sh, 1264w, 1237w, 1214w, 1180w, 1158w, 1084w, 1067w, 1036w, 1016w, 1006w, 990w, 971w, 900w, 829m-sh, 815s, 786s, 762w-sh, 718w, 692w, 665m. IR (CH_2Cl_2): $\tilde{\nu}$/cm^{-1} = 2172s (C≡N). ^1H NMR ($CDCl_3$): δ/ppm = 7.22–7.17 (m, 1H, C^6H), 7.11 (d, $^3J_{HH}$ = 7.6 Hz, 2H, C^5H), 5.93 (s, 6H, C_6H_6), 2.48 (s, 6H, C^4H). $^{13}C\{^1H\}$ NMR ($CDCl_3$): δ/ppm = 149.5 (br., C^1), 135.9 (C^3), 129.6 (C^6), 128.1 (C^5), 126.9 (br., C^2), 90.2 (C_6H_6), 19.0 (C^4). Release of benzene is observed in the $CDCl_3$ solution of **3f** stored at room temperature (*ca.* 14% after 14 h).

The reaction of [$RuCl_2(\eta^6$-$C_6H_6)]_2$ and xylyl isocyanide, according to procedure E, gave an orange solid consisting of **3f** [IR (CH_2Cl_2): $\tilde{\nu}$ = 2172 cm^{-1}], presumably *trans*-[$RuCl_2$(CNXyl)$_4$] [IR (CH_2Cl_2): $\tilde{\nu}$ = 2135 cm^{-1}][26] and unknown isocyanide complexes [IR (CH_2Cl_2): $\tilde{\nu}$/cm^{-1} = 2082, 2020].

4.4. Synthesis and characterization of acetylide–isocyanide and acetonitrile–isocyanide complexes

[RuCl(CCPh)(CNCy)(η^6-C_6Me_6)], 4b (Chart 15). In a 25 mL Schlenk tube under N_2, a solution of [$RuCl_2(\eta^6$-$C_6Me_6)]_2$ (60 mg, 0.18 mmol Ru) in anhydrous CH_2Cl_2 (3 mL) was treated with CyNC (22 μL, 0.18 mmol) and was stirred at room temperature for 1 h. IR analysis of the bright orange-red solution confirmed the quantitative formation of **2b**. Volatiles were removed under vacuum; all the subsequent operations (including the workup) were carried out under N_2 using deaerated solvents. The residue was re-dissolved with MeOH (3 mL) and treated with PhCCH (22 μL, 0.20 mmol, 1.1 eq.) and NaOH (1.56 mol L^{-1} solution in MeOH; 0.13 mL, 0.20 mmol, 1.1 eq.). The orange solution was stirred at room temperature for *ca.* 2.5 h, affording an orange-amber solution. The formation of **4b** was checked by IR. The MeOH solution was extracted with hexane (2 × 5 mL), and then dried under vacuum. The residue was triturated with hexane/CH_2Cl_2 2 : 1 v/v. The suspension was moved into a column and filtered over a celite pad. The procedure was repeated until complete extraction (colorless solution) of the title product from the yellow residue of sodium salts. The orange-amber filtrate solution was taken to dryness under vacuum. The residue was triturated with cold (−20 °C) pentane and the mixture was rapidly filtered in air (the pale-yellow filtrate rapidly darkened in air). The resulting ochre solid was washed further with pentane, dried under vacuum (RT) and stored under N_2. Yield: 58 mg, 64%. The formation of **4b** is quite selective, as shown by IR analysis, but solutions/suspensions of **4b** in Et_2O or hexane are unstable when exposed to air. A progressive browning is observed when the workup is carried out in air, together with the appearance of carbonyl stretching bands in the IR spectrum; eventually, an impure brown **4b** is obtained in a low yield (down to *ca.* 25%). However, solid **4b** stored under N_2 is stable for months (IR analysis).

Soluble in CH_2Cl_2 and $CHCl_3$, less soluble in Et_2O and Et_2O/hexane mixtures, and poorly soluble in hexane and pentane. X-ray quality crystals of **4b** were obtained from a CH_2Cl_2 solution layered with hexane and settled aside at −20 °C. Anal. calcd. for $C_{27}H_{34}ClNRu$: C, 63.70; H, 6.73; N, 2.75. Found: C, 59.8; H, 6.39; N, 2.71. IR (solid state): $\tilde{\nu}$/cm^{-1} = 2928 m, 2855w, 2144 s (C≡N), 2088s (C≡C), 1939w, 1902w-sh, 1591m, 1482m, 1447m, 1382m, 1363m, 1351m, 1325m, 1260w, 1240w, 1208w, 1171w, 1155w, 1129w, 1067m, 1024m, 1012m, 933w, 891w, 863w, 765s, 753s-sh, 696s, 659m. IR (CH_2Cl_2): $\tilde{\nu}$/cm^{-1} = 2161s (C≡N), 2098s (C≡C), 1594w, 1485w, 1451w, 1441w, 1421w. ^1H NMR ($CDCl_3$): δ/ppm = 7.36 (d, $^3J_{HH}$ = 7.6 Hz, 2H, $C^{11}H$), 7.14 (t, $^3J_{HH}$ = 7.6 Hz, 2H, $C^{12}H$), 7.02 (t, $^3J_{HH}$ = 7.4 Hz, 1H,$C^{13}H$), 3.91 (tt, $^3J_{HH}$ = 7.5, 3.6 Hz,

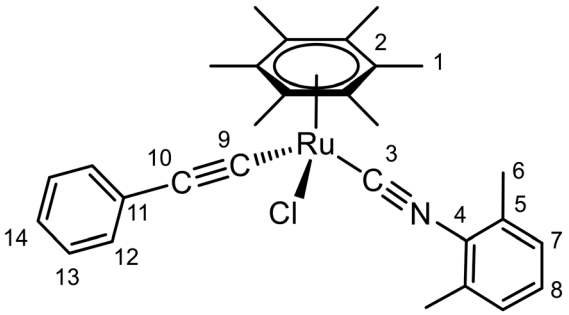

Chart 16 Structure of **4f** (numbering refers to carbon atoms).

1H, C^4H), 2.17 (s, 18H, C^1H), 1.99–1.90 (m, 2H), 1.87–1.69 (m, 4H), 1.51–1.43 (m, 4H), (C^5H + C^6H + C^7H); no changes were observed in the ^1H NMR spectrum after 24 h at room temperature. $^{13}C\{^1H\}$ NMR ($CDCl_3$): δ/ppm = 147.8 (br., C^3), 131.7 (C^{11}), 129.4 (C^{10}), 127.6 (C^{12}), 124.4 (C^{13}); 110.6 (C^8); 104.1 (C^9); 101.9 (C^2), 54.9 (C^4); 33.5, 33.4 (C^5); 25.1, 23.0 (C^6); 16.2 (C^1).

[RuCl(CCPh)(CNXyl)(η⁶-C₆Me₆)], 4f (Chart 16). The synthetic procedure was optimized with respect to the literature,[15c] wherein the reaction of **2f**, PhCCH (≈12 eq.) and KOH (1 eq.) in MeOH at room temperature for 4 h resulted in 43% yield of **4f**. A comprehensive characterization of the title compound is also provided, while only ^1H NMR, UV-vis and a few IR data were given in the literature.[15c]

In a 25 mL Schlenk tube under N_2, a solution of $[RuCl_2(\eta^6\text{-}C_6Me_6)]_2$ (61 mg, 0.18 mmol Ru) and XylNC (24 mg, 0.19 mmol) in anhydrous CH_2Cl_2 (5 mL) was stirred at room temperature for 1 h. An IR analysis of the bright red solution confirmed the quantitative formation of **2f**. Volatiles were removed under vacuum, and the residue was re-dissolved with deaerated MeOH (6 mL) under N_2 and treated with PhCCH (24 μL, 0.22 mmol, 1.2 eq.) and NaOH (1.48 mol L^{-1} solution in MeOH; 0.15 mL, 0.22 mmol, 1.2 eq.). The red solution was stirred at 45 °C for 3 h, affording a yellow-ochre solid and a red-brown solution. The mixture was cooled to −20 °C and filtered. The filtrate, containing a mixture of unidentified Ru complexes, hexamethylbenzene and only a trace amount of **4f**, was discarded. The resulting yellow-ochre solid was washed with cold MeOH (−20 °C, *ca.* 2 mL) Et_2O, and hexane and was dried under vacuum (RT) and stored under N_2. Yield: 55 mg, 57%. A procedure in which the second step was carried out in air led to the isolation of **4f** in lower yield (43%) while, contrary to the expectations,[15c] no reaction occurred in another test carried out at room temperature. Soluble in CH_2Cl_2 and $CHCl_3$, poorly soluble in MeOH, Et_2O and their mixtures, and insoluble in hexane. X-ray quality crystals of **4f** were obtained from a CH_2Cl_2 solution layered with hexane and settled aside at −20 °C. Anal. calcd for $C_{29}H_{32}ClNRu$: C, 65.58; H, 6.07; N, 2.64. Found: C, 62.20; H, 6.02; N, 2.48. IR (solid state): $\tilde{\nu}/cm^{-1}$ = 3065w, 3015w, 2975w, 2944w, 2915w, 2110s (C≡N); 2091s (C≡C); 1594w, 1554w, 1483m, 1465w, 1437w, 1377w, 1210w, 1193w, 1171w, 1162w, 1138w, 1066w, 1025w, 1006w, 904w, 842w, 818w, 773s, 762s, 719m, 695s, 673m. IR (CH_2Cl_2): $\tilde{\nu}/cm^{-1}$ = 2127 s (C≡N); 2099s (C≡C); 1594w, 1485w, 1467w, 1385w. ^1H NMR ($CDCl_3$): δ/ppm = 7.34 (d, 2H, $^3J_{HH}$ = 7.2 Hz, $C^{12}H$), 7.15 (t, $^3J_{HH}$ = 7.6 Hz, 2H, $C^{13}H$), 7.12–6.99 (m, 4H, $C^{14}H$ + C^7H + C^8H), 2.49 (s, 6H, C^6H), 2.24 (s, 18H, C^1H); no changes were observed in the ^1H NMR spectrum after 14 h at room temperature. $^{13}C\{^1H\}$ NMR ($CDCl_3$): δ/ppm = 161.4 (br., C^3), 135.3 (C^5), 131.6 (C^{12}), 129.2 (C^{11}), 128.7 (C^4), 128.0 (C^8), 127.8 (C^{13}), 127.7 (C^7), 124.6 (C^{14}), 109.5 (C^9), 104.3 (C^{10}), 103.3, 19.3, 16.4 (C^6).

Attempts to synthesize [RuCl(CCPh)(CNR)(η⁶-*p*-cymene)] (R = Cy, Xyl). All reactions of **1b** and PhCCH with various bases/solvents (Et_3N/EtOH; ^{t}BuOK/THF; Na_2CO_3/MeCN) gave brown solutions, which did not contain the expected acetylide compound. Likewise, a reaction of **1f**, PhCCH and NaOH/MeOH carried out as described for **4f** gave a brown solution after 1.5 h at room temperature, which contained a mixture of unidentified Ru complexes and a minor amount of unreacted **1f** (IR and ^1H NMR). In each case, the IR band for the isocyanide stretching of the title compounds (estimated at *ca.* 2180 cm^{-1} for R = Cy and 2150 cm^{-1} for R = Xyl) was not detected. A typical IR profile of the products obtained by these reactions is given as follows. IR (CH_2Cl_2): $\tilde{\nu}/cm^{-1}$ = 2165s, 2146s, 2081m-w for R = Cy; 2096s, 2070s, 2013m for R = Xyl.

[RuCl₂(MeCN)₃(CNCy)], 5b (Chart 17).[35] In a 50 mL Schlenk tube under N_2, a solution of $[RuCl_2(\eta^6\text{-}p\text{-cymene})]_2$ (205 mg, 0.672 mmol Ru) and CyNC (84 μL, 0.68 mmol) in deaerated MeCN (10 mL) was stirred at room temperature for 3 h. An IR analysis of the red solution confirmed the quantitative formation of **1b**. The mixture was heated at reflux (T_{bath} = 90 °C) for 24 h, affording a light-yellow solution. The quantitative formation of **5b** was checked by IR. The solution was cooled to room temperature and was extracted with hexane (15 mL × 4). The acetonitrile solution was taken to dryness under vacuum. The yellow residue was triturated in a Et_2O/hexane 1 : 2 v/v mixture and the suspension was filtered. The resulting sand yellow solid was thoroughly washed with Et_2O/hexane 1 : 1 v/v and hexane and was dried under vacuum (room temperature). Yield: 270 mg, 99%. A long reaction time is essential to ensure quantitative conversion of **1b**; after 14 h a bright yellow solution is obtained, which contains traces of unreacted **1b**. The

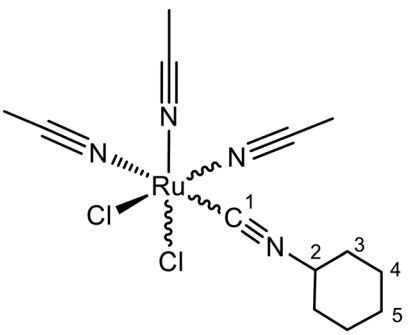

Chart 17 Structure of **5b** (numbering refers to carbon atoms; wavy bonds represent *fac*, *mer*,*cis* and *mer*,*trans* isomers).

MeCN/hexane extraction is fundamental to remove *p*-cymene (normal boiling point 177 °C); otherwise a sticky yellow solid is obtained. Soluble in MeCN, CH_2Cl_2, and $CHCl_3$, moderately soluble in acetone, and insoluble in Et_2O and hexane. Anal. calcd. for $[RuCl_2(MeCN)_3(CNCy)]$ = $C_{13}H_{20}Cl_2N_4Ru$: C, 38.62; H, 4.99; N, 13.86; anal. calcd. for $[RuCl_2(MeCN)_{2.5}(CNCy)(H_2O)_{0.5}]$[65] = $C_{12}H_{19.5}Cl_2N_{3.5}O_{0.5}Ru$: C, 36.69; H, 5.00; N, 12.48. Found: C, 36.64; H, 5.28; N, 12.45. IR (solid state): $\tilde{\nu}/cm^{-1}$ = 3460m-br (H_2O),[65] 2926m, 2855w-sh; 2281w (MeC≡N); 2154m-sh, 2118s, 2059m-sh (C≡NCy); 1363w, 1449m, 1420m, 1364m, 1351m-sh, 1321m, 1268w, 1239w, 1150w, 1127w, 1032m, 1026m, 944m, 930w, 892w, 862w, 657s. Λ_m (MeCN, 5.7 × 10^{-3} mol L^{-1}) = 24 S cm^2 mol^{-1}. IR (CH_2Cl_2): $\tilde{\nu}/cm^{-1}$ = 2288w (MeC≡N); 2165m-br, 2137s (C≡NCy); 1452w, 1365w, 1325w. IR (MeCN): $\tilde{\nu}/cm^{-1}$ = 2161m-sh, 2132s (C≡NCy). ^1H NMR ($CDCl_3$): δ/ppm = 4.24, 4.02 (m, 1H, C^2H); 2.58, 2.40 (s, 9H, CH_3CN) 1.96 (s, MeCN) (9H); 2.15–1.97 (m, 2H), 1.93–1.71 (m, 4H), 1.59–1.29 (m, 4H) (C^3H + C^4H + C^5H). ^1H NMR (CD_3CN): δ/ppm = 4.17, 4.10 (m, 1H, C^2H); 2.44, 2.44, 2.43, 2.40, 2.39 (s, 8.1H, Ru–NCMe), 1.96 (s, 0.9H, free MeCN) (tot. 9H); 1.95–1.88 (m, 2H), 1.87–1.66 (m, 4H), 1.56–1.40 (m, 4H) (C^3H + C^4H + C^5H). $^{13}C\{^1H\}$ NMR (CD_3CN): δ/ppm = 149.4 (br., C^1), 125.5, 125.1, 124.9, 123.8, 123.4, 123.3, 121.8 (Ru–NCMe); 118.2* (free MeCN); 56.1, 55.9, 55.7, 55.5 (C^2); 34.3, 34.2, 33.6, 33.5 (C^3); *25.89*, *25.86*, *25.69*, *25.66* (C^5); 23.1, 23.0 (br., C^4); 4.38, 4.31, 4.27, 4.25 (MeCN–Ru); *from ^1H–^{13}C HMBC; relative intensity of the four sets of signals 38 : 30 : 19 : 13. A change in the relative intensity of C^2H and CH_3CN signals in the ^1H NMR spectrum occurred over 14 h at room temperature, accompanied by an increase of the peak due to free CH_3CN (corresponding to *ca.* 0.07 eq. after 30 min; 0.3 eq. after 14 h); no further changes occurred over the next 10 days. Complete CH_3CN/CD_3CN exchange, except for the signal at 2.44 ppm (residual relative integral 1.9H *vs.* CyNC), occurred after heating the solution at 50 °C for 24 h (Fig. S68). IR (solid from CD_3CN solution, differences with respect to the original sample): $\tilde{\nu}/cm^{-1}$ = 3494m-br, 3410m-br (H_2O); 2299w ($CD_3C{\equiv}N$); 2226w (CD_3 + C–C); 2121s-sh, 2095s, 2017w-sh (C≡NCy); 1633m (H_2O).

[$RuCl_2(MeCN)_3$(CNXyl)], 5f (Chart 18).[35] In a 50 mL Schlenk tube under N_2, a solution of $[RuCl_2(\eta^6\text{-}p\text{-cymene})]_2$ (200 mg, 0.654 mmol Ru) and XylNC (86 mg, 0.66 mmol) in deaerated MeCN (10 mL) was stirred at room temperature for 3 h, affording an orange suspension (**1f** is poorly soluble in MeCN). An aliquot of the solution was analyzed by IR and then the mixture was heated at reflux (T_{bath} = 90 °C). After 14 h, a yellow solution was obtained. IR (MeCN) and ^1H NMR (CD_3CN) spectra indicated the quantitative formation of **5f** and the release of *p*-cymene.‡ The solution was cooled to room temperature and was extracted with hexane (4 × 15 mL). Next, the acetonitrile solution was taken to dryness under vacuum. The yellow residue was triturated in a Et_2O/hexane 1 : 1 v/v mixture and the suspension was filtered. The resulting sand yellow solid was thoroughly washed with Et_2O/hexane 1 : 1 v/v and hexane and was dried under vacuum (room temperature). Yield: 270 mg, 97%. Soluble in MeCN and CH_2Cl_2, moderately soluble in acetone, and insoluble in Et_2O/hexane 1 : 1 v/v and hexane. Anal. calcd for $[RuCl_2(MeCN)_3(CNXyl)]$ = $C_{15}H_{18}Cl_2N_4Ru$: C, 42.26; H, 4.26; N, 13.14; anal. calcd for $[RuCl_2(MeCN)_{2.5}(CNXyl)(H_2O)_{0.5}]$[65] = $C_{14}H_{17.5}Cl_2N_{3.5}O_{0.5}Ru$: C, 40.54; H, 4.25; N, 11.82. Found: C, 40.21; H, 4.46; N, 11.98. IR (solid state): $\tilde{\nu}/cm^{-1}$ = 3460w-br (H_2O),[65] 2958w, 2908w; 2283w (MeC≡N); 2072s, 2016s-sh (C≡NXyl); 1589w, 1466m, 1420m, 1375w, 1261w, 1193w, 1165w, 1091w, 1032m, 944w, 820w, 771m, 721m, 674m. Λ_m (MeCN, 3.4 × 10^{-3} mol L^{-1}) = 17 S cm^2 mol^{-1}. IR (CH_2Cl_2): $\tilde{\nu}/cm^{-1}$ = 2290w (MeC≡N); 2133m-sh, 2104s, 2018w (C≡NXyl); 1606w, 1469w, 1416w. IR (MeCN): $\tilde{\nu}/cm^{-1}$ = 2130m-sh; 2100s, 2015w (C≡NXyl). ^1H NMR ($CDCl_3$): δ/ppm = 7.16, 7.08, 7.06 (m, 3H, C^5H + C^6H); 2.62 (s-br, 1.6H, Ru–NCMe); 2.52, 2.51, 2.48 (s, 6H, C^4H); 2.43, 2.42, 2.41 (s, 6H, Ru–NCMe), 2.12 (s-br, 1.4H, Ru–NCMe). ^1H NMR (CD_3CN): $\tilde{\nu}/cm^{-1}$ = 7.26–7.11 (m, 3H, C^5H + C^6H), 2.49 (s, 6H, C^4H); 2.45, 2.446, 2.442, 2.43, 2.42, 2.40 (s, 7.6H, Ru–NCMe), 1.96 (s, 1.4H, free MeCN) (tot. 9H). $^{13}C\{^1H\}$ NMR (CD_3CN): δ/ppm = 167.7, 163.4 (C^1), 136.13, 136.08, 135.6, 135.6 (C^3); 130.64, 130.56 (C^2); 129.5, 129.4, 129.0, 128.9, 128.73, 128.67, 128.2, 128.0 (C^5 + C^6); 125.7, 125.4, 125.3, 123.8 (Ru–NCMe); 118.2* (free MeCN); 19.1, 19.0, 18.9, 18.8 (C^4); 4.36, 4.29, 4.27, 4.24 (MeCN–Ru); *from ^1H–^{13}C HMBC; relative intensity of the four sets of signals: 45 : 23 : 18 : 14.

Exchange with the deuterated solvent lowered the relative integral of Ru–NCMe in the ^1H NMR spectrum from 7.6H (freshly prepared solution) to 7.2H (14 h at room temperature) to 7.0H after several days. Complete CH_3CN/CD_3CN exchange, except for the signal at 2.446 ppm (residual relative integral 1.3H *vs.* CNXyl), occurred after heating the solution at 50 °C for 24 h (Fig. S73). IR (solid from CD_3CN solution, differences with respect to the original sample): $\tilde{\nu}/cm^{-1}$ = 3494m-br, 3395m-br (H_2O); 2298w ($CD_3C{\equiv}N$); 2226w (CD_3 + C–C); 2140s, 2097m-sh (C≡NCy); 1627m (H_2O).

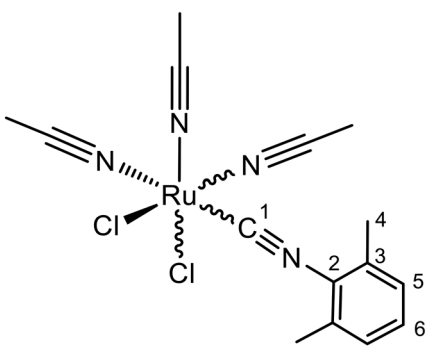

Chart 18 Structure of **5f** (numbering refers to carbon atoms; wavy bonds represent *fac*, *mer,cis* and *mer,trans* isomers).

4.5. X-ray crystallography

Crystal data and collection details for **1a**, **1c**, **1e**·½CH_2Cl_2, **1g**·$CHCl_3$, **1e**, **2c**·H_2O, **1b-I**, **4b** and **4f** are reported in Table 7.

‡ *p*-cymene. ^1H NMR (CD_3CN): $\tilde{\nu}/cm^{-1}$ = 7.11 (app. q, $^3J_{HH}$ = 8.3 Hz, 4H), 2.86 (hept, $^3J_{HH}$ = 6.8 Hz), 2.43 (s, 3H), 1.20 (d, $^3J_{HH}$ = 6.9 Hz, 6H).

Table 7 Crystal data and measurement details for **1a**, **1c**, **1e**·½CH_2Cl_2, **1g**·$CHCl_3$, **1e**, **2c**·H_2O, **1b-I**, **4b** and **4f**

Compound	**1a**	**1c**	**1e**·½CH_2Cl_2	**1g**·$CHCl_3$	**2c**·H_2O	**1b-I**	**4b**	**4f**
Formula	$C_{12}H_{17}Cl_2NRu$	$C_{19}H_{23}Cl_2NRu$	$C_{15.5}H_{22}Cl_3NO_2Ru$	$C_{19}H_{22}Cl_5NORu$	$C_{21}H_{29}Cl_2NORu$	$C_{17}H_{25}I_2NRu$	$C_{27}H_{34}ClNRu$	$C_{29}H_{32}ClNRu$
FW	347.23	437.35	461.76	558.69	483.42	598.25	509.07	531.07
T, K	100(2)	100(2)	100(2)	100(2)	100(2)	100(2)	100(2)	100(2)
λ, Å	0.71073	0.71073	0.71073	0.71073	0.71073	0.71073	0.71073	0.71073
Crystal system	Monoclinic	Orthorhombic	Monoclinic	Triclinic	Orthorhombic	Monoclinic	Monoclinic	Monoclinic
Space group	$P2_1/c$	$P2_12_12_1$	$C2/c$	$P\bar{1}$	$P2_12_12_1$	$P2_1/c$	$P2_1/n$	$P2_1/c$
a, Å	9.745(2)	9.1021(6)	25.2987(9)	10.3192(14)	7.3074(4)	9.7509(6)	7.5945(4)	8.2888(9)
b, Å	10.958(3)	11.0511(8)	17.9124(6)	12.9409(19)	12.8439(7)	16.0618(10)	12.2445(6)	12.6570(13)
c, Å	12.730(3)	18.3886(13)	8.3465(3)	18.335(2)	22.1781(13)	12.8319(8)	25.2295(12)	23.549(3)
α, °	90	90	90	71.028(4)	90	90	90	90
β, °	98.973(5)	90	94.2520(10)	89.935(4)	90	99.133(2)	91.324(2)	98.116(4)
γ, °	90	90	90	78.471(3)	90	90	90	90
Cell volume, Å^3	1342.7(5)	1849.7(2)	3771.9(2)	2263.4(5)	2081.5(2)	1984.2(2)	2345.5(2)	2445.8(4)
Z	4	4	8	4	4	4	4	4
D_c, g cm^{-3}	1.718	1.571	1.626	1.640	1.543	2.003	1.442	1.442
μ, mm^{-1}	1.538	1.135	1.262	1.293	1.020	3.897	0.796	0.767
F(000)	696	888	1864	1120	991	1136	1056	1096
Crystal size, mm	0.12 × 0.10 × 0.06	0.13 × 0.11 × 0.08	0.18 × 0.15 × 0.12	0.24 × 0.21 × 0.18	0.19 × 0.17 × 0.13	0.21 × 0.18 × 0.11	0.15 × 0.13 × 0.10	0.14 × 0.11 × 0.08
θ limits, °	2.116–25.090	2.150–26.995	1.614–25.680	1.702–26.024	1.832–27.997	2.047–27.000	1.615–27.996	1.747–27.000
Reflections collected	11 631	22 191	25 475	24 777	32 825	27 260	28 581	35 819
Independent reflections	2353 [R_{int} = 0.0732]	4024 [R_{int} = 0.0537]	3563 [R_{int} = 0.0296]	8611 [R_{int} = 0.0761]	5026 [R_{int} = 0.0286]	4310 [R_{int} = 0.0418]	5623 [R_{int} = 0.0482]	5346 [R_{int} = 0.0554]
Data/restraints/parameters	23 536/202/197	4024/0/212	3563/169/248	8611/198/496	5026/4/248	4310/12/193	5623/3/277	5346/0/297
Goodness on fit on F^{2a}	1.200	1.240	1.274	1.216	1.145	1.303	1.113	1.193
R_1 ($I > 2\sigma(I)$)^b	0.0692	0.0426	0.0459	0.0669	0.0206	0.0300	0.0430	0.0535
wR_2 (all data)^c	0.1681	0.0979	0.1137	0.1665	0.0531	0.0677	0.0955	0.1069
Largest diff. peak and hole, e Å^{-3}	2.127/−1.416	1.247/−1.127	1.221/−0.984	1.593/−1.183	0.512/−0.621	1.185/−0.625	1.319/−1.238	1.034/−1.626

^{a} Goodness on fit on $F^2 = [\sum w(F_O^2 - F_C^2)^2/(N_{ref} - N_{param})]^{1/2}$, where $w = 1/[\sigma^2(F_O^2) + (aP)^2 + bP]$, where $P = (F_O^2 + 2F_C^2)/3$; N_{ref} = number of reflections used in the refinement; N_{param} = number of refined parameters. ^{b} $R_1 = \sum||F_O| - |F_C||/\sum|F_O|$. ^{c} w$R_2 = [\sum w(F_O^2 - F_C^2)^2/\sum w(F_O^2)^2]^{1/2}$, where $w = 1/[\sigma^2(F_O^2) + (aP)^2 + bP]$, where $P = (F_O^2 + 2F_C^2)/3$.

Data were recorded on a Bruker APEX II diffractometer equipped with a PHOTON2 detector using Mo-Kα radiation. The structures were solved by direct methods and refined by full-matrix least-squares based on all data using F^2.[66] C-bonded hydrogen atoms were fixed at calculated positions and refined using a riding model. O-bonded hydrogen atoms of **2c**·H_2O were located in the Fourier difference map and refined isotropically using a riding model.

4.6. Catalytic studies

Catalytic experiments were performed in a reaction station (electrothermal STEM) glass tube where 3 mL of the desired solvent, one mmol of the terminal alkyne, one mmol of mesitylene as an internal standard, the base and the Ru pre-catalyst (1 to 2.5 mol%) were added. The reaction was then heated to the desired temperature and left to react for up to 24 hours. All reactions were performed in closed vessels with a cooling coil of water. An extraction was performed with ethyl acetate to a final organic volume of 4 mL. Samples were centrifuged and analyzed by GC–MS (Shimadzu QP201OSE) using mesitylene as an internal standard. Conversion and selectivity were calculated using a calibration curve using the internal standard method. The alternative energy methods were performed using the mono-waver CEM Discovery, ball-mill PM100, and ultrasonic bath ATU series ATM.

4.7. Reactivity with phenylacetylene and Na_2CO_3 under catalytically relevant conditions

In MeCN with a higher Ru load and concentration. The selected Ru compound (**1b**, **1f**, **2b**, **2f**, **3b**, or **3f**; 7–8 mg, 0.018 mmol, 1 eq.) was added to a 5 mL test tube together with Na_2CO_3 (20 mg, 0.19 mmol, 1 eq.), MeCN (2.0 mL) and PhCCH (20 μL, 0.18 mmol, 10 eq.). The mixture (orange solution + colorless solid; $c^0_{Ru} = 9 \times 10^{-3}$ mol L^{-1}) was stirred while immersed into a pre-heated oil bath at 80 °C. After 2 h, the brown (**1b**, **1f**, **3b**, and **3f**) or orange (**2b** and **f**) suspension was cooled to room temperature and was analyzed by IR (MeCN). Next, volatiles were removed under vacuum, and the residue was analyzed by ^{1}H NMR ($CDCl_3$) and IR (CH_2Cl_2). In each case, both *Z* and *E* diphenyl-but-3-en-1-yne were identified from the characteristic doublets,[67] with prevalence of the latter. IR spectra are shown in Fig. S76–S81 while results of the IR/NMR analyses are compiled in Table S4.

In EtOH or MeCN. The selected Ru compound (**1b**, **2b** or **2f**; 10 mg, 0.021–0.024 mmol) was added to a 50 mL test tube together with Na_2CO_3 (22–25 mg, 0.21–0.24 mmol, 10 eq.), the desired solvent (MeCN or EtOH; 10 mL) and PhCCH (231–264 μL, 2.10–2.40 mmol, 100 eq.). The mixture (yellow solution + colorless solid; c^0_{Ru} = 2.1–2.4 × 10^{-3} mol L^{-1}) was stirred while immersed into a pre-heated oil bath at 55, 60 or 80 °C for 4–24 h and progressively turned to dark brown over time. At different reaction times, an aliquot (0.50 mL) of the solution was taken to dryness under vacuum, re-dissolved in a small volume of CH_2Cl_2 and analyzed by IR [note: direct IR or Raman analyses of the reaction mixture were not suitable due to the low Ru concentration and the overwhelming absorptions of phenylacetylene and organic products]. Subsequently, CH_2Cl_2 was removed under vacuum, and the residue was dissolved in MeCN (0.50 mL) and then re-added to the reaction mixture. The final reaction mixture was filtered over a celite pad to remove most of the sodium salts and then volatiles were removed under vacuum. The residue was re-dissolved in CH_2Cl_2, filtered over a celite pad and taken to dryness under vacuum. The oily residue was triturated in hexane or hexane/Et_2O mixtures to solubilize the remaining PhCCH and the related organic products. The suspension was filtered and the resulting brown solid was washed with hexane, dried under vacuum and analyzed by ^{1}H, ^{1}H–^{13}C HMBC NMR ($CDCl_3$), ESI-MS and MS/MS (MeOH). Control experiments without PhCCH in MeCN were carried out as described above and samples were analyzed by IR (CH_2Cl_2). Experimental details, IR spectra and spectroscopic/spectrometric data are reported in the SI (Tables S5–S10 and Fig. S82–S90).

In water/mesitylene. The selected Ru compound (**1b** or **2f**; 10 mg, 0.021–0.024 mmol) was added to a 50 mL test tube together with Na_2CO_3 (22–25 mg, 0.21–0.24 mmol, 10 eq.), H_2O (10 mL), mesitylene (3.4 mL) and PhCCH (231–264 μL, 2.10–2.40 mmol, 100 eq.). The biphasic mixture (colorless aqueous phase/orange organic phase) was stirred while immersed into a pre-heated oil bath at the desired temperature (≈25, 55 or 80 °C) for 1–4 h. Both phases progressively turned brown over time. Afterwards, the organic phase was separated, taken to dryness under vacuum (40 °C) and analyzed by IR (CH_2Cl_2). The aqueous phase was extracted with CH_2Cl_2 and the organic solution was taken to dryness under vacuum. The brown residue was analyzed by IR (CH_2Cl_2). Experimental details, IR spectra and data are reported in the SI (Table S11, Fig. S91–S92).

Conflicts of interest

The authors declare no competing financial interest.

Data availability

Supplementary information (SI): preparation and characterization of $[RuCl_2(L)(\eta^6\text{-}C_6H_6)]$ (L = Py, SMe_2) and $[RuCl_2(CO)(\eta^6\text{-arene})]$ (arene = *p*-cymene, C_6Me_6); IR and NMR spectra of ruthenium bis-halide–isocyanide, acetylide–isocyanide and acetonitrile–isocyanide complexes; comparison of selected spectroscopic data for isocyanide ligands; catalytic studies: GC-MS spectra reactivity with phenylacetylene and Na_2CO_3 under catalytically relevant conditions.

CCDC 2504593 (**1a**), 2504594 (**1c**), 2504595 (**1e**·½CH_2Cl_2), 2504596 (**1g**·$CHCl_3$), 2504597 (**2c**·H_2O), 2504598 (**1b-I**), 2504599 (**4b**) and 2504600 (**4f**) contain the supplementary crystallographic data for the X-ray studies reported in this paper.[68a–h]

Acknowledgements

L. B. and F. M. thank the University of Pisa for financial support under the "PRA 2022-2023 – *Progetti di Ricerca di Ateneo*" (Institutional Research Grants) – Project no. PRA_2022_12 "*New challenges of transition metal and lanthanide complexes in the perspective of green chemistry*". This research was funded in whole or in part by the Fundação para a Ciência e a Tecnologia, I. P. (FCT, https://ror.org/00snfqn58 [1]) under the projects UIDB/00100/2020 (https://doi.org/10.54499/UIDB/00100/2020) and UIDP/00100/2020 (https://doi.org/10.54499/UIDP/00100/2020) of Centro de Química Estrutural, LA/P/0056/2020 (https://doi.org/10.54499/LA/P/0056/2020) of Institute of Molecular Sciences, and 2021.04926.BD, (https://doi.org/10.54499/2021.04926.BD) Ph. D. grant of H. M. L., and by the Instituto Politécnico de Lisboa through the IPL/IDI&CA2023/SMARTCAT_ISEL project. For the purpose of Open Access, the author applied a CC BY public copyright license to any Author Accepted Manuscript (AAM) version arising from this submission. L. B. thanks Prof. Ilaria Degano (University of Pisa) for ESI-MS analyses.

Notes and references

1 (*a*) G. C. Vougioukalakis and R. H. Grubbs, Ruthenium-Based Heterocyclic Carbene-Coordinated Olefin Metathesis Catalysts, *Chem. Rev.*, 2010, **110**, 1746–1787; (*b*) A. Fürstner, trans-Hydrogenation, gem-Hydrogenation, and trans-Hydrometalation of Alkynes: An Interim Report on an Unorthodox Reactivity Paradigm, *J. Am. Chem. Soc.*, 2019, **141**, 11–24; (*c*) T. Koike and M. Akita, Visible-light radical reaction designed by Ru- and Ir-based photoredox catalysis, *Inorg. Chem. Front.*, 2014, **1**, 562–576; (*d*) C. Gunanathan and D. Milstein, Bond Activation and Catalysis by Ruthenium Pincer Complexes, *Chem. Rev.*, 2014, **114**, 12024–12087.

2 (*a*) R. Noyori and S. Hashiguchi, Asymmetric Transfer Hydrogenation Catalyzed by Chiral Ruthenium Complexes, *Acc. Chem. Res.*, 1997, **30**, 97–102; (*b*) T. Ikariya and J. Blacker, Asymmetric Transfer Hydrogenation of Ketones with Bifunctional Transition Metal-Based Molecular Catalysts, *Acc. Chem. Res.*, 2007, **40**, 1300–1308; (*c*) A. M. R. Hall, D. B. G. Berry, J. N. Crossley, A. Codina, I. Clegg, J. P. Lowe, A. Buchard and U. Hintermair, Does the Configuration at the Metal Matter in Noyori–Ikariya Type Asymmetric Transfer Hydrogenation Catalysts?, *ACS Catal.*, 2021, **11**, 13649–13659.

3 (*a*) G. S. Caleffi, J. d. O. C. Brum, A. T. Costa, J. L. O. Domingos and P. R. R. Costa, Asymmetric Transfer Hydrogenation of Arylidene-Substituted Chromanones and Tetralones Catalyzed by Noyori–Ikariya Ru(II) Complexes: One-Pot Reduction of C═C and C═O bonds, *J. Org. Chem.*, 2021, **86**, 4849–4858; (*b*) T. Touge, M. Kuwana, Y. Komatsuki, S. Tanaka, H. Nara, K. Matsumura, N. Sayo, Y. Kashibuchi and T. Saito, Development of Asymmetric Transfer Hydrogenation with a Bifunctional Oxo-Tethered Ruthenium Catalyst in Flow for the Synthesis of a Ceramide (d-erythro-CER[NDS]), *Org. Process Res. Dev.*, 2019, **23**, 452–461; (*c*) K. Gupta, D. Tyagi, A. D. Dwivedi, S. M. Mobina and S. K. Singh, Catalytic transformation of bio-derived furans to valuable ketoacids and diketones by water-soluble ruthenium catalysts, *Green Chem.*, 2015, **17**, 4618–4627; (*d*) V. S. Shende, A. B. Raut, P. Raghav, A. A. Kelkar and B. M. Bhanage, Room-Temperature Asymmetric Transfer Hydrogenation of Biomass-Derived Levulinic Acid to Optically Pure γ-Valerolactone Using a Ruthenium Catalyst, *ACS Omega*, 2019, **4**, 19491–19498; (*e*) Z. Wang, Z. Zhao, Y. Li, Y. Zhong, Q. Zhang, Q. Liu, G. A. Solan, Y. Ma and W.-H. Sun, Ruthenium-catalyzed hydrogenation of CO2 as a route to methyl esters for use as biofuels or fine chemicals, *Chem. Sci.*, 2020, **11**, 6766.

4 (*a*) R. Ghosh, N. Ch. Jana, S. Panda and B. Bagh, Transfer Hydrogenation of Aldehydes and Ketones in Air with Methanol and Ethanol by an Air-Stable Ruthenium–Triazole Complex, *ACS Sustainable Chem. Eng.*, 2021, **9**, 4903–4914; (*b*) M. Ruiz-Castañeda, L. Santos, B. R. Manzano, G. Espino and F. A. Jalón, A Water/Toluene Biphasic Medium Improves Yields and Deuterium Incorporation into Alcohols in the Transfer Hydrogenation of Aldehydes, *Eur. J. Inorg. Chem.*, 2021, 1358–1372; (*c*) M. N. A. Fetzer, G. Tavakoli, A. Klein and M. H. G. Prechtl, Ruthenium-Catalyzed E-Selective Partial Hydrogenation of Alkynes under Transfer-Hydrogenation Conditions using Paraformaldehyde as Hydrogen Source, *ChemCatChem*, 2021, **13**, 1317–1325.

5 (*a*) H. G. Nedden, A. Zanotti-Gerosa and M. Wills, The Development of Phosphine-Free "Tethered" Ruthenium(II) Catalysts for the Asymmetric Reduction of Ketones and Imines, *Chem. Rec.*, 2016, **16**, 2623–2643; (*b*) DENEB® and TS-DPEN® series in the Merck or Strem catalogues.

6 Selected references: (*a*) A. S. Phearman, J. M. Moore, D. D. Bhagwandin, J. M. Goldberg, D. M. Heinekey and K. I. Goldberg, (Hexamethylbenzene)Ru catalysts for the Aldehyde-Water Shift reaction, *Green Chem.*, 2021, **23**, 1609; (*b*) Z. Wu, Z.-Q. Wang, H. Cheng, Z.-H. Zheng, Y. Yuan, C. Chen and F. Verpoort, Gram-scale synthesis of carboxylic acids via catalytic acceptorless dehydrogenative coupling of alcohols and hydroxides at an ultralow Ru loading, *Appl. Catal., A*, 2022, **630**, 118443; (*c*) P. Liu, N. Thanh Tung, X. Xu, J. Yang and F. Li, N-Methylation of Amines with Methanol in the Presence of Carbonate Salt Catalyzed by a Metal–Ligand Bifunctional Ruthenium Catalyst [(p-cymene)Ru(2,2′-bpyO)(H2O)], *J. Org. Chem.*, 2021, **86**, 2621–2631; (*d*) A. Verma, S. Hazra, P. Dolui and A. J. Elias, Ruthenium-Catalyzed Synthesis of α-Alkylated Ketones and Quinolines in an Aqueous Medium via a Hydrogen-Borrowing Strategy Using Ketones and Alcohols, *Asian J. Org. Chem.*, 2021, **10**, 626–633; (*e*) K. Kalita, S. Kushwahaa and S. K. Singh, Ligand-tuned catalytic activity of ruthenium-imidazolyl amine complexes for reversible formic acid dehydrogenation and CO2 hydrogenation to formic acid, *Inorg. Chem. Front.*, 2025, **12**, 6847–6860; (*f*) L. Biancalana, S. Fulignati, C. Antonetti, S. Zacchini, G. Provinciali, G. Pampaloni, A. M. Raspolli Galletti and F. Marchetti, Ruthenium p-cymene complexes with a-diimine ligands as catalytic precursors for the transfer hydrogenation of ethyl levulinate to γ-valerolactone, *New J. Chem.*, 2018, **42**, 17574–17586.

7 R. Colaiezzi, C. Saviozzi, N. di Nicola, S. Zacchini, G. Pampaloni, M. Crucianelli, F. Marchetti, A. Di Giuseppe and L. Biancalana, Ruthenium(II) arene complexes bearing simple dioxime ligands: effective catalysts for the one-pot transfer hydrogenation/N-methylation of nitroarenes with methanol, *Catal. Sci. Technol.*, 2023, **13**, 2160–2183.

8 R. Gonzalez-Fernandez, P. Crochet and V. Cadierno, Arene-ruthenium (II) and osmium (II) complexes as catalysts for nitrile hydration and aldoxime rearrangement reactions, *Inorg. Chim. Acta*, 2020, **517**, 120180 and references therein.

9 (*a*) P. B. Arockiam, C. Bruneau and P. H. Dixneuf, Ruthenium (II)-catalyzed C–H bond activation and functionalization, *Chem. Rev.*, 2012, **112**, 5879–5918; (*b*) C. Binnani, D. Tyagi, R. K. Rai, S. M. Mobin and S. K. Singh, C-H Bond Activation/ Arylation Catalyzed by Arene–Ruthenium–Aniline Complexes in Water, *Chem. – Asian J.*, 2016, **11**, 3022–3031; (*c*) T. Rogge and L. Ackermann, Arene-Free Ruthenium(II/IV)-Catalyzed Bifurcated Arylation for Oxidative C-H/C-H Functionalizations, *Angew. Chem., Int. Ed.*, 2019, **58**, 15640–15645.

10 (*a*) C. S. Day and D. E. Fogg, High-Yield Synthesis of a Long-Sought, Labile Ru-NHC Complex and Its Application to the Concise Synthesis of Second-Generation Olefin Metathesis Catalysts, *Organometallics*, 2018, **37**, 4551–4555; (*b*) M. Bassetti, F. Centola, D. Sémeril, C. Bruneau and P. H. Dixneuf, Rate Studies and Mechanism of Ring-Closing Olefin Metathesis Catalyzed by Cationic Ruthenium Allenylidene Arene Complexes, *Organometallics*, 2003, **22**, 4459–4466.

11 (*a*) P. Kumar, R. K. Gupta and D. S. Pandey, Half-sandwich arene ruthenium complexes: synthetic strategies and relevance in catalysis, *Chem. Soc. Rev.*, 2014, **43**, 707–733; (*b*) G. Süss-Fink, Water-soluble arene ruthenium complexes: From serendipity to catalysis and drug design, *J. Organomet. Chem.*, 2014, **751**, 2–19.

12 M. A. Bennett and A. K. Smith, Arene ruthenium(II) complexes formed by dehydrogenation of cyclohexadienes with ruthenium(III) trichloride, *J. Chem. Soc., Dalton Trans.*, 1974, 233–241.

13 M. A. Bennett, T.-N. Huang, T. W. Matheson and A. K. Smith, 16. (η_6-Hexamethylbenzene)Ruthenium Complexes, *Inorg. Synth.*, 1982, **21**, 72–78.

14 *Ca.* 45 [RuX_2(CNR)(η^6-arene)] derivatives among *ca.* 4000 [RuX_2(L)(η^6-arene)] complexes (X = halide; L = generic monodentate ligand except halides and hydride). Reaxys, 27/11/2025.

15 (*a*) F. Faraone and V. Marsala, (η_6-C_6H_6)Ru(CNC_6H_{11})Cl_2. A mixed arene-isocyanide complex, *Inorg. Chim. Acta*, 1978, **27**, L109–L110; (*b*) R. Dussel, D. Pilette, P. H. Dixneuf and W. P. Fehlhammer, Isocyanide arene-ruthenium(II) complexes and activation of alkenylacetylenes: synthesis and characterization of isocyanide carbene- and mixed carbene-ruthenium compounds, *Organometallics*, 1991, **10**, 3287–3291; (*c*) Y. Yamamoto, R. Satoh and T. Tanase, Preparation of [Ru(η_6-C_6Me_6)Cl(C≡CPh)(RNC)] (R = C_8H_9 (2,6-xylyl) or C6H2Me3-2,4,6) and its reaction with tetracyanoethylene. Crystal structures of [Ru(η_6-C_6Me_6)Cl{C[=C(CN)2]CPh=C(CN)2} (C8H9NC)] and cis-[$RuCl_2$(C_8H_9NC)$_2$], *J. Chem. Soc., Dalton Trans.*, 1995, 307–311, [*Synthetic procedure and characterization data are missing*]; (*d*) S. Krawielitzki and W. Beck, Metal complexes of biologically important ligands. Part 94. Hexanuclear isocyanide and carbene metal complexes from neomycin B, *Chem. Ber.*, 1997, **130**, 1659–1662; (*e*) F. Simal, S. Sebille, L. Hallet, A. Demonceau and A. F. Noels, Evaluation of ruthenium-based catalytic systems for the controlled atom transfer radical polymerization of vinyl monomers, *Macromol. Symp.*, 2000, **161**, 73–85, [*Synthetic procedure and characterization data are missing*]; (*f*) Y. Yamamoto, H. Nakamura and J.-F. Ma, Preparation and characterization of ruthenium(II), rhodium(III) and iridium(III) complexes of isocyanide bearing the azo group, *J. Organomet. Chem.*, 2001, **640**, 10–20; (*g*) E. Hodson and S. J. Simpson, Synthesis and characterization of [(η_6-cymene)Ru(L)X_2] compounds: single crystal X-ray structure of [(η6-cymene)Ru(P{OPh}3)Cl2] at 203 K, *Polyhedron*, 2004, **23**, 2695–2707; (*h*) O. Kaufhold, A. Flores-Figueroa, T. Pape and F. E. Hahn, Template synthesis of ruthenium complexes with saturated and benzannulated NH,NH-stabilized N-heterocyclic carbene ligands, *Organometallics*, 2009, **28**, 896–901; (*i*) G. Albertin, S. Antoniutti, J. Castro and S. Paganelli, Preparation and reactivity of p-cymene complexes of ruthenium and osmium incorporating 1,3-triazenide ligands, *J. Organomet. Chem.*, 2010, **695**, 2142–2152; (*j*) A. P. Walsh, W. W. Brennessel and J. D. Jones, Synthesis and characterization of a series of rhodium, iridium, and ruthenium isocyanide complexes, *Inorg. Chim. Acta*, 2013, **407**, 131–138; (*k*) C. Hubbert, M. C. Dietl, D. Zahner, F. Rominger, M. Rudolph and A. S. K. Hashmi, Modular Approach toward Protic N-Heterocyclic Carbene Complexes from Tosylated Benzyl Isocyanide Metal Complexes and Imines, *Organometallics*, 2023, **42**, 2762–2770.

16 (*a*) E. Singleton and H. E. Oosthuizen, Metal Isocyanide Complexes, *Adv. Organomet. Chem.*, 1983, **22**, 209–310; (*b*) W. Sattler, L. M. Henling, J. R. Winkler and H. B. Gray, Bespoke Photoreductants: Tungsten Arylisocyanides, *J. Am. Chem. Soc.*, 2015, **137**, 1198–1205; (*c*) S. Mukhopadhyay, A. G. Patro, R. S. Vadavi and S. Nembenna, Coordination Chemistry of Main Group Metals with Organic Isocyanides, *Eur. J. Inorg. Chem.*, 2022, **31**, e202200469.

17 (*a*) K. A. Waibel, R. Nickisch, N. Möhl, R. Seimb and M. A. R. Meier, A more sustainable and highly practicable synthesis of aliphatic isocyanides, *Green Chem.*, 2020, **22**, 933–941; (*b*) P. Patil, M. Ahmadian-Moghaddam and A. Dömling, Isocyanides 2.0, *Green Chem.*, 2020, **22**, 6902–6911.

18 (*a*) A. J. L. Pombeiro, M. F. C. Guedes Da Silva and R. A. Michelin, Aminocarbyne complexes derived from isocyanides activated towards electrophilic addition, *Coord. Chem. Rev.*, 2001, **218**, 43–74; (*b*) H. W. Fruhauf, Organotransition metal [3+2] cycloaddition reactions, *Coord. Chem. Rev.*, 2002, **230**, 79–96; (*c*) L. M. Slaughter, Acyclic Aminocarbenes in Catalysis, *ACS Catal.*, 2012, **2**, 1802–1816; (*d*) R. M. Kirk and A. F. Hill, Phosphinoisocyanide/Alkyne Cycloaddition: Generation of Azaphospholylidene (NPHC) Ligands, *Angew. Chem., Int. Ed.*, 2025, **64**, e202504620; (*e*) V. G. Albano, S.

Bordoni, L. Busetto, F. Marchetti, M. Monari and V. Zanotti, C-N coupling between μ-aminocarbyne and nitrile ligands promoted by tolylacetylide addition to [Fe2{μ-CN(Me)(Xyl)}(μ-CO)(CO)(NCCMe3)(Cp)2][SO3CF3]: Formation of a novel bridging η1:η2 allene-diaminocarbene ligand, *J. Organomet. Chem.*, 2003, **684**, 37–43; (*f*) F. Marchetti, S. Zacchini and V. Zanotti, Carbon monoxide–isocyanide coupling promoted by acetylide addition to a diiron complex, *Chem. Commun.*, 2015, **51**, 8101–8104.

19 (*a*) M. Knorn, E. Lutskera and O. Reiser, Isonitriles as supporting and non-innocent ligands in metal catalysis, *Chem. Soc. Rev.*, 2020, **49**, 7730–7752; (*b*) K. T. Mahmudov, V. Yu. Kukushkin, A. V. Gurbanov, M. A. Kinzhalov, V. P. Boyarskiy, M. F. C. Guedes da Silva and A. J. L. Pombeiro, Isocyanide metal complexes in catalysis, *Coord. Chem. Rev.*, 2019, **384**, 65–89.

20 (*a*) A. Naik, T. Maji and O. Reiser, Iron(II)–bis(isonitrile) complexes: novel catalysts in asymmetric transfer hydrogenations of aromatic and heteroaromatic ketones, *Chem. Commun.*, 2010, **46**, 4475–4477; (*b*) D. Cahard, V. Bizet, X. Dai, S. Gaillard and J.-L. Renaud, Iron(II) complexes are suitable catalysts for the isomerization of trifluoromethylated allylic alcohols. Synthesis of trifluoromethylated dihydrochalcones, *J. Fluorine Chem.*, 2013, **155**, 78–82; (*c*) R. Bigler, R. Huber and A. Mezzetti, Highly Enantioselective Transfer Hydrogenation of Ketones with Chiral (NH)2P2 Macrocyclic Iron(II) Complexes, *Angew. Chem., Int. Ed.*, 2015, **54**, 5171–5174; (*d*) J. B. Curley, N. E. Smith, W. H. Bernskoetter, N. Hazari and B. Q. Mercado, Catalytic Formic Acid Dehydrogenation and CO_2 Hydrogenation Using Iron PNRP Pincer Complexes with Isonitrile Ligands, *Organometallics*, 2018, **37**, 3846–3853; (*e*) D. H. Nguyen, D. Merel, N. Merle, X. Trivelli, F. Capeta and R. M. Gauvin, Isonitrile ruthenium and iron PNP complexes: synthesis, characterization and catalytic assessment for base-free dehydrogenative coupling of alcohols, *Dalton Trans.*, 2021, **50**, 10067–10081.

21 L. Biancalana, N. Di Fidio, D. Licursi, S. Zacchini, A. Cinci, A. M. Raspolli Galletti, F. Marchetti and C. Antonetti, New ruthenium(II) isocyanide complexes as transfer hydrogenation catalysts for the sustainable production of γ-valerolactone from ethyl levulinate in the presence of C_2-C_6 alcohols, *J. Catal.*, 2024, **439**, 115761.

22 (*a*) J. Magano and J. R. Dunetz, Large-Scale Applications of Transition Metal-Catalyzed Couplings for the Synthesis of Pharmaceuticals, *Chem. Rev.*, 2011, **111**, 2177–2250; (*b*) L. M. D. R. S. Martins, A. M. F. Phillips and A. J. L. Pombeiro, in *Sustainable Synthesis of Pharmaceuticals: Using Transition Metal Complexes as Catalysts*, ed. M. M. Pereira and M. J. F. Calvete, The Royal Society of Chemistry, 2018, ch. 8, pp. 193–229; (*c*) A. M. Trzeciak and A. W. Augustyniak, The role of palladium nanoparticles in catalytic C–C cross-coupling reactions, *Coord. Chem. Rev.*, 2019, **384**, 1–20.

23 (*a*) J.-F. Chen and C. Li, Cobalt-Catalyzed gem-Cross-Dimerization of Terminal Alkynes, *ACS Catal.*, 2020, **10**, 3881–3889; (*b*) M. Galiana-Cameo, A. Urriolabeitia, E. Barrenas, V. Passarelli, J. J. Pérez-Torrente, A. Di Giuseppe, V. Polo and R. Castarlenas, Metal–Ligand Cooperative Proton Transfer as an Efficient Trigger for Rhodium-NHC-Pyridonato Catalyzed gem-Specific Alkyne Dimerization, *ACS Catal.*, 2021, **11**, 7553–7567.

24 L. K. G. Ackerman-Biegasiewicz, S. K. Kariofillis and D. J. Weix, Multimetallic-Catalyzed C–C Bond-Forming Reactions: From Serendipity to Strategy, *J. Am. Chem. Soc.*, 2023, **145**, 6596–6614.

25 (*a*) S. M. Weber and G. Hilt, Late 3d Metal-Catalyzed (Cross-) Dimerization of Terminal and Internal Alkynes, *Front. Chem.*, 2021, **9**, 635826; (*b*) L. Cui, K. Yang, Y. Yang, D. Ma, X. Ren and G. Wang, Nickel(II)-Catalyzed Oxidative Homocoupling of Terminal Alkynes, *Eur. J. Org. Chem.*, 2025, **28**, e202500207; (*c*) O. N. Temkin, "Golden Age" of Homogeneous Catalysis Chemistry of Alkynes: Dimerization and Oligomerization of Alkynes, *Kinet. Catal.*, 2019, **60**, 689–732; (*d*) C. Slugovc, D. Doberer and C. Gemel, Ruthenium Catalyzed Homocoupling of Terminal Alkynes, *Monatsh. Chem.*, 1998, **129**, 221–233; (*e*) S. S. Gawali and C. Gunanathan, Iron-catalyzed regioselective cyclotrimerization of alkynes to benzenes, *J. Organomet. Chem.*, 2019, **881**, 139–149; (*f*) S. E. García-Garrido, Catalytic Dimerization of Alkynes, in *Modern Alkyne Chemistry*, 2014, ed. B. M. Trost and C.-J. Li, DOI: 10.1002/9783527677894.ch11; (*g*) Q. Liang, K. Hayashi and D. Song, Catalytic Alkyne Dimerization without Noble Metals, *ACS Catal.*, 2020, **10**, 4895–4905.

26 M. E. G. Mosquera, I. Egido, C. Hortelano, M. López-Lópeza and P. Gómez-Sal, Comparison of halogen bonding networks with Ru(ii) complexes and analysis of the influence of the XB interactions on their reactivity, *Faraday Discuss.*, 2017, **203**, 257–283.

27 D. E. Fogg and B. R. James, Chiral phosphine complexes of ruthenium(I1) arenes, *J. Organomet. Chem.*, 1993, **462**, C21–C23.

28 Aside from **3b**, only the carbonyl and a 3,5-dihexyl-1-methyl-1H-1,2,3-triazolydene derivatives were reported. (*a*) H. Werner, G. Brauers and O. Nurnberg, Reaktionen der Aren(carbonyl)ruthenium-Komplexe $[C_6Me_6Ru(CO)Cl_2]$ und $[(Mes)Ru(CO)Cl_2]$ mit Alkyl- und Allyl-Grignardreagenzien. Die Kristall- und Molekülstruktur von {[η_5-$C_6Me_6(CH_2$-$CH=CH_2)$]Ru(exo-η_3-C_3H_5)(CO)}, *J. Organomet. Chem.*, 1993, **454**, 247–255; (*b*) D. Canseco-Gonzalez and M. Albrecht, Wingtip substituents tailor the catalytic activity of ruthenium triazolylidene complexes in base-free alcohol oxidation, *Dalton Trans.*, 2013, **42**, 7424–7432.

29 S. Stampatori, I. Tolbatov, S. Zacchini, G. Pampaloni, F. Marchetti, N. Re and L. Biancalana, Elucidating the ruthenium-mediated conversion of aryl alkynes to alkoxy(benzyl)carbene and benzyl carbonyl complexes, *Inorg. Chem. Commun.*, 2025, **171**, 113547.

30 (*a*) Y. Yamamoto, T. Tanase, C. Sudoh and T. Turuta, Reactions of (η6-C6Me6)RuCl(MDMPP-P,O) and (η6-C6Me6) RuCl(BDMPP-P,O,O) complexes with Lewis bases or alkynes, where MDMPP-P,O-P(2-O-6-MeOC6H3)Ph2 and BDMPP-P,O,O-P(2-O-6-MeOC6H3)2{2,6-(MeO)2C6H3}, *J. Organomet. Chem.*,

1998, **569**, 29–37; (*b*) C. Menéndez, D. Morales, J. Pérez, V. Riera and D. Miguel, New Types of (Arene)ruthenium Alkynyl Complexes, *Organometallics*, 2001, **20**, 2775–2781; (*c*) A. Romero, D. Peron and P. H. Dixneuf, Metallacumulenes: preparation of novel alkenyl–allenylidene– and diynyl–ruthenium complexes. Crystal structure of a Ru–C≡C–C≡C–C(OSiMe3)Ph2 derivative, *J. Chem. Soc., Chem. Commun.*, 1990, 1410–1412.

31 Reaxys, 27/11/2025: 20 substances containing the {Ru(CNR)(CCR)} fragment. Selected references: (*a*) G. Albertin, S. Autoniutti, E. Bordignon, F. Cazzaro, S. Ianelli and G. Pelizzi, Preparation, Structure, and Reactivity of New Bis(acetylide) and Acetylide-Vinylidene Ruthenium(II) Complexes Stabilized by Phosphite Ligands, *Organometallics*, 1995, **14**, 4114–4125; (*b*) D. Touchard, S. Guesmi, L. Le Pichon, A. Daridor and P. H. Dixneuf, Ammonia ruthenium complexes for the access to new hydrido, carbonyl and isocyanide ruthenium-alkynyl derivatives, *Inorg. Chim. Acta*, 1998, **280**, 118–124; (*c*) J. Montoya, A. Santos, J. López, A. M. Echavarren, J. Ros and A. Romero, Reactions of alkenyl and alkynyl ruthenium(II) complexes with isocyanides: Synthesis of α, β-unsaturated η1-acylruthenium(II) complexes and X-ray structure of [Ru(C≡CPh)(CNtBu)3(PPh3)2]PF6, *J. Organomet. Chem.*, 1992, **426**, 383–398.

32 *Spectral Database for Organic Compounds, SDBS, National Institute of Advanced Industrial Science and Technology (AIST)*, National Institute of Advanced Industrial Science and Technology, 2025, https://sdbs.db.aist.go.jp.

33 J. P. al Dulaimi, R. J. H. Clark, S. M. Saavedra and Md. A. Salam, Spectroelectrochemical studies on some new ruthenium(II) complexes containing both cyanide and isocyanide ligands, *Inorg. Chim. Acta*, 2002, **300–302**, 175–180.

34 (*a*) R. D. Foust and P. C. Ford, The Preparation and Spectral Properties of Some Organonitrile Complexes of pentaamminerhodium(III), *Inorg. Chem.*, 1972, **11**, 899; (*b*) B. N. Storhoff and H. C. Lewis, Organonitrile complexes of transition metals, *Coord. Chem. Rev.*, 1977, **23**, 1–29.

35 CHN and IR data suggest that a minor amount of coordinated water could be present in solid **5b**, **f**. However, for simplicity, the products are treated as pure $[RuCl_2(CNR)(MeCN)_3]$ (mixtures of isomers).

36 I. Bratsos and E. Alessio, Ruthenium(II) Chloro Complexes of dimethylsulfoxide, *Inorg. Synth.*, 2010, **35**, 148–152.

37 R. K. Henderson, A. P. Hill, A. M. Redman and H. F. Sneddon, Development of GSK's acid and base selection guides, *Green Chem.*, 2015, **17**, 945–949.

38 P. J. Dyson and P. G. Jessop, Solvent effects in catalysis: rational improvements of catalysts via manipulation of solvent interactions, *Catal. Sci. Technol.*, 2016, **6**, 3302–3316.

39 (*a*) A. Toledo, I. Funes-Ardoiz, F. Maseras and A. C. Albéniz, Palladium-Catalyzed Aerobic Homocoupling of Alkynes: Full Mechanistic Characterization of a More Complex Oxidase-Type Behavior, *ACS Catal.*, 2018, **8**, 7495–7506; (*b*) K. Kikuchi-Igarashi, Y. Tahara, H. Hirano, C. Ambe, H. Kinoshita and K. Miura, Platinum-Catalyzed Hydrative Dimerization of Alkynylsilanes to α,β-Unsaturated Ketones, *Org. Lett.*, 2024, **26**, 5689–5694; (*c*) I. Kageyuki, J. Lia and H. Yoshida, Platinum–P(BFPy)3-catalyzed regioselective diboration of terminal alkynes with (pin)B–B(aam), *Org. Chem. Front.*, 2022, **9**, 1370–1374.

40 L. Biancalana, E. Zanda, M. Hadiji, S. Zacchini, A. Pratesi, G. Pampaloni, P. J. Dyson and F. Marchetti, Role of the (pseudo) halido ligand in ruthenium(ii) p-cymene α-amino acid complexes in speciation, protein reactivity and cytotoxicity, *Dalton Trans.*, 2021, **50**, 15760–15777 and references therein.

41 R. Salvio, F. Julia-Hernandez, Ĺ. Pisciottani, R. Mendoza-Meroño, S. García-Granda and M. Bassetti, Kinetics and Mechanistic Insights into the Acetate-Assisted Dimerization of Terminal Alkynes under Ruthenium- and Acid Promoted (RAP) Catalysis, *Organometallics*, 2017, **36**, 3830–3840.

42 (*a*) N. W. Alcock, A. F. Hill and R. P. Melling, Polyazolyl chelate chemistry. 3. (σ-Organyl)[tris(pyrazol-1-yl)borato] ruthenium complexes, *Organometallics*, 1991, **10**, 3898–3903; (*b*) N. W. Alcock, A. F. Hill, R. P. Melling and A. R. Thompsett, Diyne coordination chemistry. 4. Synthesis, molecular structure, and protonation reactions of the zerovalent complex [Ru(.eta.2-PhC.tplbond.CC.tplbond.CPh)(CO)2(PPh3)2], *Organometallics*, 1993, **12**, 641–648.

43 F. Faraone, P. Piraino, V. Marsala and S. Sergi, Tricarbonyldichloro(thiocarbonyl)ruthenium(II) and related complexes: synthesis and réactions to give aminomercaptocarbene and isocyanide complexes, *J. Chem. Soc., Dalton Trans.*, 1977, 859–861.

44 Selected examples in the following references. (*a*) M. I. Bruce, B. G. Ellis, B. W. Skelton and A. H. White, Further reactions of some bis(vinylidene)diruthenium complexes, *J. Organomet. Chem.*, 2005, **690**, 792–801; (*b*) K. Ogata, J. Seta, K. Sugawara, N. Tsutsumi, Y. Yamamoto, K. Kuge and K. Tatsumi, Metal-assisted preparation of the alkenyl ketone and carbonyl complexes from 1-alkyne and H2O: C–C triple bond cleavage of terminal alkyne, *Inorg. Chim. Acta*, 2006, **359**, 1549–1558; (*c*) G. Albertin, S. Antoniutti, M. Bortoluzzi, J. Castro and M. Trevisan, Ruthenium(II) pentamethylcyclopentadienyl half-sandwich carbene complexes with polypyridyl ligands, *J. Organomet. Chem.*, 2017, **848**, 1–9; (*d*) Y. Borguet, X. Sauvage, G. Zaragoza, A. Demonceau and L. Delaude, Synthesis and Catalytic Evaluation in Olefin Metathesis of a Second-Generation Homobimetallic RutheniumArene Complex Bearing a Vinylidene Ligand, *Organometallics*, 2011, **30**, 2730–2738.

45 K. Nakamoto, *Infrared and Raman Spectra of Inorganic and Coordination Compounds*, John Wiley & Sons, Inc., 4th edn, 1986.

46 K. Salzmann, C. Segarra and M. Albrecht, Donor-Flexible Bis(pyridylidene amide) Ligands for Highly Efficient Ruthenium-Catalyzed Olefin Oxidation, *Angew. Chem., Int. Ed.*, 2020, **59**, 8932–8936.

47 (*a*) G. Albertin, S. Antoniutti, E. Bordignon, F. Cazzaro, S. Ianelli and G. Pelizzi, Preparation, Structure,and Reactivity of New Bis(acety1ide)and Acetylide-Vinylidene Ruthenium(I1) Complexes Stabilized by Phosphite Ligands, *Organometallics*, 1996, **14**, 4114–4125; (*b*) J. M. Lynam, T. D. Nixon and A. C.

Whitwood, Solvent and phosphine dependency in the reaction of cis-RuCl2(P–P)2 (P–P = dppm or dppe) with terminal alkynes, *J. Organomet. Chem.*, 2008, **693**, 3103–3110; (*c*) J.-H. Lee and K. G. Caulton, Coupling of terminal alkynes by RuHXL2 (X = Cl or N(SiMe3)2, L = PiPr3), *J. Organomet. Chem.*, 2008, **693**, 1664–1673.

48 I. Czeluśniak, A. Jezierska and M. Siczek, Dimerization of aryl alkynes by Grubbs-Hoveyda complex: investigation of factors affecting the efficiency of the process based on experimental and theoretical approaches, *Polyhedron*, 2022, **225**, 116067.

49 M. Gierada, I. Czeluśniak and J. Handzlik, Dimerization and cyclotrimerization of terminal arylalkynes initiated by a phosphine-free ruthenium alkylidene complex, *Mol. Catal.*, 2019, **469**, 18–26.

50 (*a*) M. Bassetti, C. Pasquini, A. Raneri and D. Rosato, Selective Dimerization of Arylalkynes to(E)-1,4-Diaryl Enynes Catalyzed by the[Ru(p-cymene)Cl2]2/Acetic Acid System under Phosphine-Free Conditions, *J. Org. Chem.*, 2007, **72**, 4558–4561; (*b*) C. Pasquini and M. Bassetti, One-Pot Desilylation/Dimerization of Terminal Alkynes by Ruthenium and Acid-Promoted (RAP) Catalysis, *Adv. Synth. Catal.*, 2010, **352**, 2405–2410; (*c*) R. Iona and M. Bassetti, Dimerization of Aromatic Terminal Alkynes Featuring Hydrophilic Functional Groups under Ruthenium and Acid Promoted Catalysis: Competitive Alkyne Hydration upon Substituent Effect, *ChemistrySelect*, 2020, **5**, 6666–6669.

51 A. Coniglio, M. Bassetti, S. E. García-Garrido and J. Gimeno, Dimerization of Terminal Arylalkynes in Aqueous Medium by Ruthenium and Acid Promoted (RAP) Catalysis: Acetate-Assisted (sp)C-(sp2)C Bond Formation, *Adv. Synth. Catal.*, 2012, **354**, 148–158.

52 K. Melis, P. Samulkiewicz, J. Rynkowski and F. Verpoort, Ruthenium-catalyzed selective anti-Markovnikov trans addition of carboxylic acids and tail-to-tail dimerization of terminal alkynes, *Tetrahedron Lett.*, 2002, **43**, 2713–2716.

53 A. Prades, M. Viciano, M. Sanau and E. Peris, Preparation of a Series of "Ru(p-cymene)" Complexes with Different N-Heterocyclic Carbene Ligands for the Catalytic â-Alkylation of Secondary Alcohols and Dimerization of Phenylacetylene, *Organometallics*, 2008, **27**, 4254–4259.

54 B. Özgün Öztürk, S. Karabulut and Y. Imamoglu, A practical ruthenium based catalytic system bearing a switchable selectivity, between the dimerization and cyclotrimerization reactions of alkynes, *Appl. Catal., A*, 2012, **433–434**, 214–222.

55 T. Matsuda, K. Kato, T. Goya, S. Shimada and M. Murakami, Ruthenium-Catalyzed Cycloisomerization of 2,2′-Diethynylbiphenyls Involving Cleavage of a Carbon–Carbon Triple Bond, *Chem. – Eur. J.*, 2016, **22**, 1941–1943.

56 W.-L. Huang, G.-J. Hung, S.-T. He, G.-R. Chiang and Y.-H. Lo, Synthesis and reactivity of water-soluble areneeruthenium(II) complexes and dimerization of terminal alkynes in organic and aqueous media, *J. Organomet. Chem.*, 2015, **775**, 1–5.

57 R. E. Schuster, J. E. Scott and J. Casanova Jr., Methyl Isocyanide, *Org. Synth.*, 1966, **46**, 75.

58 Methyl isocyanide is prepared from tosyl chloride, *N*-methyl formamide and quinoline and is isolated by distillation under reduced pressure. The resulting liquid is not pure methyl isocyanide mainly due to the presence of quinoline. Aged samples, stored at −20 °C under N_2, show increased amount of quinoline due to isocyanide decomposition. ^{1}H NMR ($CDCl_3$) δ/ppm = 3.13 (t, $^3J_{NH}$ = 2.2 Hz, MeNC), 2.97 (s, Me_2SO_2).

59 H. Werner and R. Werner, Die Vorstufen zur Synthese der Metall-Basen, ArM(PR3)2 und ArM(PR3)L (M = Ru, Os), *Chem. Ber.*, 1982, **115**, 3766–3780.

60 D. A. Tocher, R. O. Gould, T. A. Stephenson, M. A. Bennett, J. P. Ennett, T. W. Matheson, L. Sawyer and V. K. Shah, Areneruthenium(II) carboxylates: reactions with ligands and the X-ray structure of the p-cymene pyrazine complex [Ru(η-p-MeC6H4CHMe2)Cl(pyz)2]PF6, *J. Chem. Soc., Dalton Trans.*, 1983, 1571–1581.

61 T. Arthur and T. A. Stephenson, Synthesis of triple halide-bridged arene complexes of ruthenium(II) and osmium(II), *J. Organomet. Chem.*, 1981, **208**, 369–387.

62 M. Gaye, B. Demerseman and P. H. Dixneuf, (Dialkylsulfide) (arene) ruthenium(II) derivatives, *J. Organomet. Chem.*, 1991, **411**, 263–270.

63 F. Menges, "Spectragryph – optical spectroscopy software", Version 1.2.16d, @ 2016–2020, https://www.effemm2.de/spectragryph.

64 (*a*) R. K. Harris, E. D. Becker, S. M. Cabral De Menezes, R. Goodfellow and P. Granger, NMR nomenclature. Nuclear spin properties and conventions for chemical shifts (IUPAC Recommendations 2001), *Pure Appl. Chem.*, 2001, **73**, 1795–1818; (*b*) G. R. Fulmer, A. J. M. Miller, N. H. Sherden, H. E. Gottlieb, A. Nudelman, B. M. Stoltz, J. E. Bercaw and K. I. Goldberg, NMR Chemical Shifts of Trace Impurities: Common Laboratory Solvents, Organics, and Gases in Deuterated Solvents Relevant to the Organometallic Chemist, *Organometallics*, 2010, **29**, 2176–2179.

65 CHNS analyses and IR spectra suggest that some water is present also in the solid state. Various combinations of coordinated water and residual water (wet solid) could explain the results (for instance, the theoretical CHN content of $[RuCl_2(CH_3CN)_{2.7}(CNR)(H_2O)_{1.0}]$ fits well the experimental one). Therefore, for the sake of simplicity, compounds **5b**, **f** are best viewed as mixtures of *fac*-, *mer*,*cis*- and *mer*,*trans*-isomers of $[RuCl_2(MeCN)_3(CNR)]$.

66 G. M. Sheldrick, Crystal structure refinement with SHELXL, *Acta Crystallogr., Sect. C: Struct. Chem.*, 2015, **71**, 3–8.

67 C. S. Yi, N. Liu, A. L. Rheingold and L. M. Liable-Sands, Ruthenium-Acetylide-Mediated Catalytic Dimerization of RC≡CH (R = Ph, CO2Me) and the Formation of the New Ruthenium η_3-Butadienyl Complex C5Me5Ru(PPh3)[η_3-PhCHCHC=C(Ph)C≡CCPh], *Organometallics*, 1997, **16**, 3910–3913.

68 (*a*) CCDC 2504593: Experimental Crystal Structure Determination, 2025, DOI: 10.5517/ccdc.csd.cc2q27bd; (*b*) CCDC 2504594: Experimental Crystal Structure Determination, 2025, DOI: 10.5517/ccdc.csd.cc2q27cf; (*c*)

CCDC 2504595: Experimental Crystal Structure Determination, 2025, DOI: 10.5517/ccdc.csd.cc2q27dg; (*d*) CCDC 2504596: Experimental Crystal Structure Determination, 2025, DOI: 10.5517/ccdc.csd.cc2q27fh; (*e*) CCDC 2504597: Experimental Crystal Structure Determination, 2025, DOI: 10.5517/ccdc.csd.cc2q27gj; (*f*) CCDC 2504598: Experimental Crystal Structure Determination, 2025, DOI: 10.5517/ccdc.csd.cc2q27hk; (*g*) CCDC 2504599: Experimental Crystal Structure Determination, 2025, DOI: 10.5517/ccdc.csd.cc2q27jl; (*h*) CCDC 2504600: Experimental Crystal Structure Determination, 2025, DOI: 10.5517/ccdc.csd.cc2q27km.